Time-Dependent Behaviour of Reinforced Concrete Beams under Sustained and Repeated Loads

Sultan Ahmed Daud

Submitted in accordance with the requirements for the degree of Doctor of Philosophy

The University of Leeds

School of Civil Engineering

June 2017

Declaration

The candidate confirms that the work submitted is his own, except where work which has formed part of jointly-authored publications has been included. The contribution of the candidate and the other authors to this work has been explicitly indicated below. The candidate confirms that appropriate credit has been given within the thesis where reference has been made to the work of others.

Parts of the work in chapters 4,5 and 6 have appeared in the following publications:

1. DAUD, S., FORTH, J. P. & NIKITAS, N. Time-Dependent Behaviour of Reinforced concrete Beams under Sustained and Repeated Loading. World Academy of Science, Engineering and Technology, 2015.

2. DAUD, S., FORTH, J. P., & NIKOLAOS NIKITAS 2016. Time-Dependent Behavior of Reinforced Concrete Beams under Sustained Loading. In: Environment, Efficiency and Economic Challenges for Concrete, Proceedings of the international Conference, Dundee, Scotland 4-6th July.

3. DAUD, S., FORTH, J. P., & NIKOLAOS NIKITAS 2016.Time-Dependent Behaviour of Fully Cracked Unbonded Reinforced Concrete Beams under Repeated and Sustained Loading. Submitted for publication in Engineering Structure.

Acknowledgements

I would like to express my sincere appreciation and gratitude to my supervisors **Prof. John P. Forth and Dr Nicolas Nikitas** for their continuous and invaluable guidance, advice, encouragement and support throughout this work.

I would like to recognize the dedicated efforts put in by the George Earl Laboratory staff (**Norman Harmon, Peter Flatt, Stephen Holmes, Marvin Wilman and Robert Clarke**) in accomplishment of my experimental work throughout the studies.

My deepest appreciation goes to the School of Civil Engineering staff, students and all of my friends students particularly **Muhammad Kashif Shehzad** who supported me in all respects during my PhD research.

Most importantly, the efforts of **my late father** (who died on 25 June 2007) and **my beloved mother** in inculcating such virtues in me which enabled me to progress upto this stage of my life. Their unwavering encouragement in all my academic endeavours and in pursuit of my PhD has always been of great value. Lastly, I would like to acknowledge the support and encouragement of my sisters and my brothers

Abstract

This thesis primarily aims to explore the flexural behaviour of reinforced concrete beams subjected to different loading types. Both bonded and partially debonded (in the maximum moment zone) reinforced concrete beams under static sustained and repeated loading were investigated. Information relating to surface strains and mid-span deflection were continuously recorded for a period of 90 days so that meaningful comparisons could be made between the structural displacements of the beams tested under different load levels. The range of the sustained load applied varied from that corresponding to the first cracking moment to that required to produce a stabilised crack pattern. The experimental outcomes show that the long-term mid-span deflection of the reinforced concrete beams where the reinforcement was artificially debonded from the concrete is substantially higher than that of bonded reinforced concrete beams under sustained loading. For beams subjected to repeated loading, the amplitude of the repeated loading was deemed to be around one eighth of the sustained load. The bond between concrete and steel in reinforced concrete beams subjected to a repeating load can be significantly damaged due to the loading even though the frequency is relatively low (i.e. 0.2 H_z). On the other hand, and more unexpectedly, for the cyclically applied loading there was no substantial difference between the observed ultimate deformations of the bonded and debonded beams. Moreover, there is a linear relationship between the number of cracks and the shrinkage deflection. Beams having a higher number of cracks develop more deflection due to shrinkage.

Nonlinear finite element software (Midas FEA) was used to simulate the experimental tests. It was found that a numerical-experimental match could only be achieved after applying necessary modifications to the shrinkage strain distribution along the beam section. In addition, the capacity of the software to separate the shrinkage and creep deflection clearly allows the relationship between number of cracks and shrinkage to be observed, and confirms what was observed in the experimental investigation.

Table of Contents

List of Tables

List of Figures

Glossary and Abbreviations

A_c	Cross Sectional area of the concrete, [mm^2].
A_{SC}	Area of the steel compressive reinforcement, [mm^2].
A_{ST}	Area of the steel tensile reinforcement, [mm^2].
d	Distance from the extreme compression fibre to the centroid of the tension reinforcement, [mm].
d_b	Diameter of the reinforcement, [mm].
E_{t_0}	Modulus of elasticity of the concrete at time t_0, [GPa].
$E_{eff(t,t_0)}$	Effective modulus of elasticity of the concrete at time t, [GPa].
E_s	Elastic modulus of the steel reinforcement, [GPa].
f_{cm}	Mean compressive strength of concrete. [MPa].
$f_{ct,eff}$	Effective tensile strength of the concrete allowing for the effect of shrinkage, [MPa].
f_{ct}	Direct tensile strength of the concrete, [MPa].
h_s	Notational size of member, [mm].
I_{cr}	Moment of inertia of the cracked section, [mm^4].
I_{eff}	Effective moment of inertia, [mm^4].
I_{uc}	Moment of inertia of the uncracked section, [mm^4].
k	The ratio of the neutral axis depth to the beam effective depth
k_t	The ratio of the neutral axis depth at time t to the beam effective depth
k_s	Constant depends on the support conditions.
L	Span length, [mm].
l_b	Embedded length, [mm].
M	Design moment, [N.mm].
M_a	Applied moment, [N.mm].
M_{cr}	Cracking moment, [N.mm].
M	The ratio of the creep to instantaneous strain.
n	Modular ratio between the reinforcement and the concrete.
n_t	Modular ratio between the reinforcement and the concrete at time t

P	Pull-out load on the bar, [kN].
RH	Relative humidity.
S	First moment of area of the reinforcement about the centroid of the section.
$t - t_0$	Time under loading [days].
U	Perimeter in contact with atmosphere, [mm].
$(E_c I_e)_i$	Short-term flexural rigidity, [N/mm^2].
$(E_c I_e)_t$	Long-term flexural rigidity, [N/mm^2].
$\emptyset_{(t,t_0)}$	Creep coefficient at time t.
$\emptyset'_{ct}$	Creep coefficient prevailing to the compression fibre.
$\Delta_{(t,t_0)}$	Deflection at any time [mm].
Δ_c	Creep deflection, [mm].
Δ_i	Initial deflection, [mm].
Δ_{long}	Long-term deflection, [mm].
Δ_{sh}	Shrinkage deflection [mm].
$x_{(t,t_0)}$	Reduction factor taking into account the age of the concrete.
x_{id}	Initial neutral depth, [mm].
$x_t d$	Effective depth, [mm].
α_{eff}	Modular ratio, taking account of an effective modulus of elasticity of the concrete allowing for creep.
β_H	Coefficient depending on the relative humidity and the notional member size.
$\varepsilon_{cr\,(t_0)}$	Strain of the concrete at time t_0.
ε_c	Elastic concrete strain in the extreme fibre in the compression zone.
$\varepsilon_{cr(t,t_0)}$	Strain of the concrete at time t.
ε'_{crp}	Creep strain on the extreme compression fibre
ε_s	Tensile reinforcement strain.
ε_{sh}	Free Shrinkage strain.
μ_m	Material modifier.
μ_s	Section modifier.
ρ'	Compression reinforcement ration.

$\sigma_{ct,sh}$	Tensile stress developed in the concrete due to restraint of shrinkage by the reinforcement, [MPa].
φ_0	Notional creep.
κ	Average curvature, [mm^{-1}].
κ_{cr}	Curvature calculated for the cracked section, [mm^{-1}].
κ_{crp}	Creep curvature, [mm^{-1}].
κ_i	Instantaneous curvature, [mm^{-1}].
κ_{sh}	Shrinkage curvature, [mm^{-1}].
κ_{mid}	Curvatures at the middle section, [mm^{-1}].
κ_{uc}	Curvature calculated for the uncracked section, [mm^{-1}].
β	Coefficient taking account the duration of loading (0.5 for sustained or cyclic loading and 1 for single short-term load).
$\beta(t_0)$	Factor to allow for the effect of concrete age at loading on the notional creep coefficient.
Z	Coefficient dependent on the time under load.
M	Factor which is a function of the compressive strength.
ξ	Distributed coefficient allowing for tension stiffening.
P	Reinforcement ratio related to the area of concrete immediately surrounding the reinforcement
τ	Bond strength.
Ψ	Empirical factor (called the creep modification factor) which accounts for the cracking and reinforcement effect on creep.
φRH	Factor to allow for the effect of relative humidity on the notional creep coefficient.

Chapter 1 Introduction

1.1 Background

Two forms of guidance are provided in Eurocode 2 (2004) to assist designers with the estimation of the long-term deflections of reinforced concrete spanning elements. The span to effective depth ratios derived by Beeby and Scott (2004b) estimate deflection in terms of a pass / fail check and have previously been shown to be adequate (Vollum, 2009). However, with the trend for longer spans / shallower depths, more accuracy is required and guidance is provided in the form of a prediction method which considers the estimation of the elastic, creep and shrinkage (incorporating tension stiffening and its loss) curvature to try and achieve this greater accuracy. Previous work (Forth et al., 2014) investigating the accuracy of this prediction method has suggested certain shortcomings in the theory (i.e. the fact that the approach is based on the theory of uncracked sections but uses cracked section properties and the fact that the method uses a fixed tension stiffening factor for either short or long-term loading). Further questions of the prediction theory were also raised by Higgins et al. (2013) and Daud et al. (2015) relating to the use of a single factor for loss of tension stiffening to represent both a sustained and repeating long-term load. Here, the definition of a repeating load is one which can cycle about the design maximum sustained load - Higgins et al. (2013) and Daud et al. (2015) have shown that a repeating or cyclic load will produce a significantly higher deflection than the deflection of a beam subjected to a sustained load representing the average of the repeating load. They attributed the extra deflection found in the repeated or cyclic load tests to the loss of tension stiffening in the early stages.

In the Eurocode 2 (2004) prediction method, the factor β, which represents the loss of tension stiffening correctly suggests a reduction in tension stiffening with

time under sustained loading – this has been adequately shown by (Beeby and Scott, 2004a). However, very rarely in practice is the load constant and sustained; Vollum (2009) has shown that the applied load can frequently exceed the design load and that it is reasonable to consider a 10 to 15 % exceedance.

In the 1970's, the Concrete in the Oceans (CiO) research program assigned the long-term deterioration technique focusing on the reinforced concrete section capacity rather than load types (Higgins et al., 2013). The loss of tension stiffening is incorporated in both the calculation of the creep and shrinkage curvature. Scott and Beeby (2005) illustrated that under sustained load, up to 50% of tension stiffening is lost over the first 20 to 30 days, at which point the loss stabilised. This finding was achieved when a stabilised crack pattern was present within the test samples; the losses were allegedly due to the development of internal cracking (Goto, 1971).

However, it must be accepted that many elements do not exhibit a stabilised crack pattern and in these cases tension stiffening is higher and the loss is lower. Conversely, where a stabilised crack pattern does exist and a repeating load occurs there could be a greater loss in tension stiffening from the 'overload' leading to increased internal cracking and loss of bond and, hence, greater long-term deflections are possible. This again undermines the validity of a single value for β in the long-term. Higgins et al. (2013) reported that the additional deformations caused by repeated load types occurred primarily within the initial loading period (0-10 days). Moreover Zanuy et al. (2010) presented an experimental study on a lightly reinforced concrete bridge deck subjected to fatigue loading. As the number of load cycles increased there was a progressive loss in tension stiffening. Vakhshouri and Nejadi (2014a) also indicated that load types (i.e. cyclic or a combination of different loading) might affect the deflection behaviour of reinforced concrete beams.

All of this assumes that any bond deterioration is caused purely by stress induced cracking and curvature. However, another important long-term factor in all of this which is coupled with the potential further loss of bond due to repeated loading (and hence additional deflection) is the effect of corrosion on the loss of bond.

Corrosion - either general corrosion, or pitting corrosion at a crack that is yet to develop into general corrosion - will also contribute to the loss of bond as it will remove the ability for the rebar and the concrete to act compositely (Eyre and Nokhasteh, 1992, Sharaf and Soudki, 2002). These authors also commented on the fact that the ultimate moment capacity provided by the codes will be impaired as corrosion promoted debonding will reduce the composite behaviour between the reinforcement and concrete (Jnaid and Aboutaha, 2014).

1.2 Aims and Objectives

This research aims to highlight how the loading characteristics impact on the long-term deformation of reinforced concrete beams. Attention is focussed on how creep, shrinkage, and tension stiffening develop and effect the behaviour of fully cracked cross section reinforced concrete beams. In particular the effect of debonding of the reinforcement in the constant moment zone on the long-term behaviour of the reinforced concrete beams under static sustained and cyclic repeated loading will be investigated experimentally to study the effect of the loss of tension stiffening with time.

To further understand the effect of these parameters on the long-term behaviour of reinforced concrete beams, a nonlinear finite element software Midas FEA will be used to simulate the experimental results. It will be shown in Chapter 6 that, in order to use Midas FEA, a modification to the way software distributes the shrinkage strain over the cross section of a cracked section needs to be introduced.

In order to achieve these aims, the following objectives will require investigation:

1.2.1 First Phase

- In addition to the compressive strength, tensile strength and the modulus of elasticity tests, creep and shrinkage tests for the concrete were conducted to provide sufficient data for the theoretical analysis and the modelling.

- Pull-out tests on prisms with bonded and debonded reinforcement were performed to assess the method of debonding the reinforcement used in the beam tests and to get a better understanding of the long-term behaviour of debonded reinforced concrete members.

1.2.2 Second Phase

- To investigate experimentally the long-term mid-span deflection of concrete beams reinforced with different types of steel reinforcement bars (i.e. bonded, debonded and symmetrical reinforcement).
- To investigate experimentally the long-term mid-span deflection of reinforced concrete beams with different loading conditions (i.e. sustained and repeated loadings).
- To gain a better understanding of the effect of the number of cracks on the long-term deflection.
- To validate the Eurocode 2 (2004) suggested equation to predict the long-term deflection under both sustained and repeated loading conditions.
- To enhance current nonlinear finite element models to better predict the long-term deflection of reinforced concrete beams.

1.3 Layout of the Thesis

This thesis contains seven chapters. In addition to this chapter, a review of the literature already produced by researchers aiming to develop the long-term behaviour of reinforced concrete beams was presented in ***Chapter 2***. Also in this chapter, the fundamental concepts related to the time-dependent behaviour of the concrete are presented. The experimental programme performed in this study is detailed in ***Chapter 3***. Material properties, mix design, and instrumentation used are described in detail. Moreover, main parameters and beams identification are presented here. Test setup procedure are summarised in this chapter, and finally, the short and long-term properties (i.e. concrete compressive strength, tensile strength, modulus of elasticity, creep and shrinkage strain) of the concrete used in this study are presented. ***Chapter 4*** begins with the results obtained from the pull-out tests of the bonded and debonded samples to assist the degree of debonding the reinforcement. Then the long-term beam deflection and surface strain development of the reinforced concretes were presented and discussed. The long-term properties of the concrete used in this study i.e. creep coefficient and shrinkage were presented against those predicted by the Eurocode 2 (2004) and Model Code (2010) then discussed in ***Chapter 5***. The accuracy of the theoretical approach proposed by the Eurocode 2 (2004) to predict the long-term deflection was investigated here***.*** In this chapter also, the 90 days deflection results of the reinforced concrete beams are extrapolated to find the ultimate deflection. The finite element analyses of the long-term behaviour, using the finite element commercial package Midas FEA are presented in ***Chapter 6***. The analyses were conducted after developing a modification to the way shrinkage strain is distributed along the beam section. The results of the finite element analyses were also discussed in this chapter. Moreover, the modification applied to the software was verified with a previous work. Finally, the conclusions drawn from this study are presented in ***Chapter 7****,* along with a summary of the outcomes and recommendations for future research.

Chapter 2 Literature Review

2.1 Introduction

Concrete is a brittle material with little capacity to carry loads in flexure without cracking. To support concrete structures subjected to some form of tension and increase ductility, steel reinforcement is added to resist tensile force. Globally, reinforced concrete structures have been successfully used in all types of infrastructure, such as bridges, houses, airports, etc. for over a century in their current form. With time and as a result of overloading the structures or due to the environmental conditions (hot in summer and cold in winter), the deformation in reinforced concrete beams increases as the material properties change i.e. concrete will inherently creep and shrink.

In addition, there is an extra deflection due to the softening effect from the loss of tension stiffening which develops as more cracks (internal/external) are produced. In flexural members, however, when the load is applied, primary cracks occur below the neutral axis (i.e. for sagging members) when the concrete reaches its tensile strength. Simplistically, tension stiffening designates the interaction between the concrete and reinforcement below the neutral axis and between the cracks, which typically reduces by development of more cracks with time due to creep and shrinkage effects.

Several design codes such as Eurocode 2 (2004), ACI 318, and Model Code (2010) have suggested equations to predict the long-term deflection of reinforced concrete spanning elements.

This chapter starts with the description of the bond between the reinforcement and concrete, as bond between them is one of the factors which effects the long term deflection. Section 2.3 provides a review of the previous experimental work investigating the long-term proprieties of the concrete (i.e. creep, shrinkage and tension stiffening). Section 2.4 describes the methods that are used to predict the

long-term deflection focusing on that suggested by the Eurocode 2 (2004) and the ACI 318 codes. Section 2.5 discusses literature related to the behaviour of cracked reinforced concrete beams subjected to different types of loading and time-dependent parameters that might increase deflection with time. Finally Section 2.6 draws a conclusion from the previous literature.

2.2 Bond Between Concrete and Steel

In reinforced concrete flexural members, when the load is applied, it is transferred from the concrete to the reinforcement through the bond between the concrete and steel. At low levels of loading (i.e. $M_a \leq M_{cr}$) both the concrete and reinforcement act elastically where M_a and M_{cr} are the applied and cracking moment, respectively. As the load increases (i.e. $M_a \geq M_{cr}$), primary cracks are produced as the concrete reaches its tensile strength at the weakest point. When $M_a >> M_{cr}$ and the stabilized cracking stage is achieved, the bond between the two materials enhances the transmission of the load and this load transition will be most effective when there is a perfect bonding. In 1971, there was an attempt by Goto (1971) to study the mechanism of the bond between the deformed reinforcement and the surrounding concrete by injecting red ink inside tension specimens. He found that internal cracks, which formed at each rib on the bar, had a great influence on the bond mechanism between the reinforcement and the concrete. Moreover, secondary cracks were formed near the primary cracks rather than in the middle third between two adjacent primary cracks. Finally, Goto (1971) found that, when the primary crack spacing is close to the maximum crack spacing, secondary cracks are more likely to be visible.

There are many factors affecting the bond strength such as the strength of concrete and the yield strength, diameter and surface geometry of the steel reinforcement; there is also the embedded length of the reinforcement inside the concrete to consider (Kim et al., 2012, Krishnakumar et al., 2013). The basic behaviour of reinforced concrete members depends on the bond between the concrete and reinforcement; this composite interaction is reflected by the bond stress (Chong et al., 2008).

Crack width and spacing in reinforced concrete members have been studied by different researchers (Gergely and Lutz, 1968, Bazant and Oh, 1983, Chen and Baker, 2003).

Bazant and Oh (1983) suggested that the energy required to produce a crack should be considered in the equation which predicts crack spacing since cracking is theoretically described as a fracture.

An extensive analysis was carried out by Forth and Beeby (2014) to give a better understanding of the relationship between reinforcement and concrete in tension. They found that crack width increases nonlinearly with the increase in cover as shown in Figure 2-1.
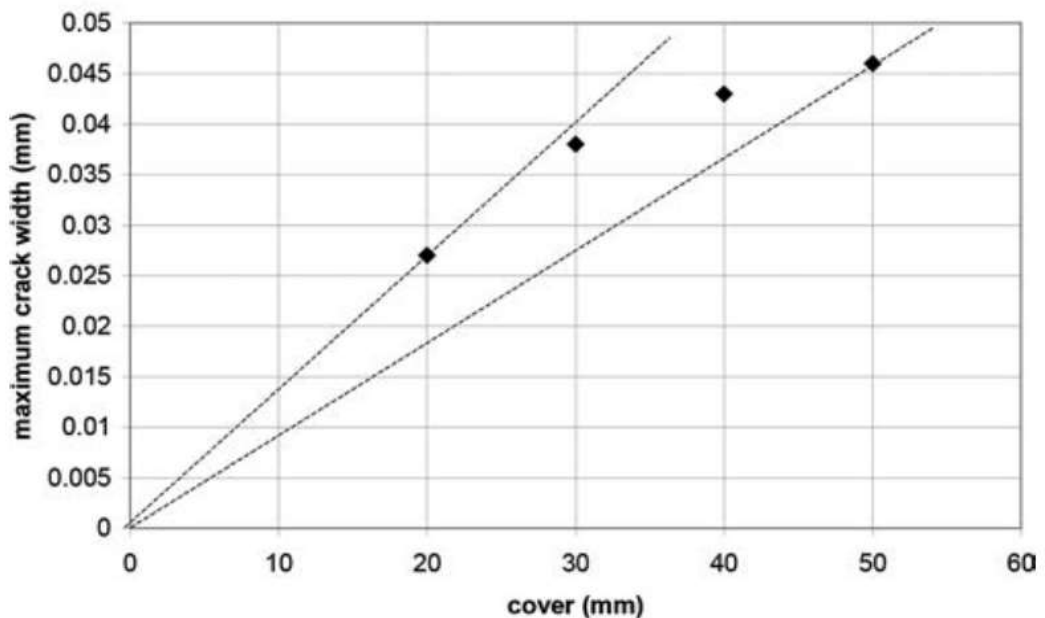
Figure 2-1: Variation in maximum surface crack width with the cover (Forth and Beeby, 2014)

Chen and Baker (2003) found that the crack spacing in reinforced concrete members is influenced by bond slip. Generally cracked beams with plain reinforcement have less surface and internal cracks than beams with deformed reinforcement.

Moreover the crack spacing in the case of beams with deformed reinforcement is less than that of beams with plain reinforcement (Mohammed et al., 2001).

According to Kimura and Jirsa (1992), deformed reinforcement geometry has a great influence on the bond between the steel reinforcement and surrounding concrete. Where bond stress increases, the height of the ribs increase and the ribs spacing decrease.

Previous work showed that corrosion influences the bond capacity between the reinforcement and the surrounding concrete (Mangat and Elgarf, 1999, Fang et al., 2004, Zhou et al., 2015). Cabrera and Ghoddoussi (1992) noticed that after a certain amount of corrosion (between 1% and 3 %) bond strength decreases with an increase in the corrosion. Moreover, Demis et al. (2010) showed experimentally that bond deterioration due to corrosion is more than compensated by the increase in the compressive strength due to time.

Load type (i.e. sustained or cyclic) is another factor which influences the bond between the concrete and the reinforcement. Comprehensive studies were conducted on the behaviour of reinforced concrete beams under short-term cyclic loading, focusing on the bond between the steel and the concrete (Neild et al., 2002). According to Neild et al. (2002), under monotonic or low cyclic loading, at a certain stress level, the adhesive component of bond between the reinforcement and concrete deteriorates and only the frictional component will remain.

According to the CEB-FIP Model Code (1990) the increasing part of the bond stress-slip curve slope will be affected due to the creep effect or loading types (repeated loading), whereas slip will increases due to a permeant load or repeated loading, as shown in Figure 2-2. Where t is the duration of loading and n is the number of cycles in case of repeated loading.
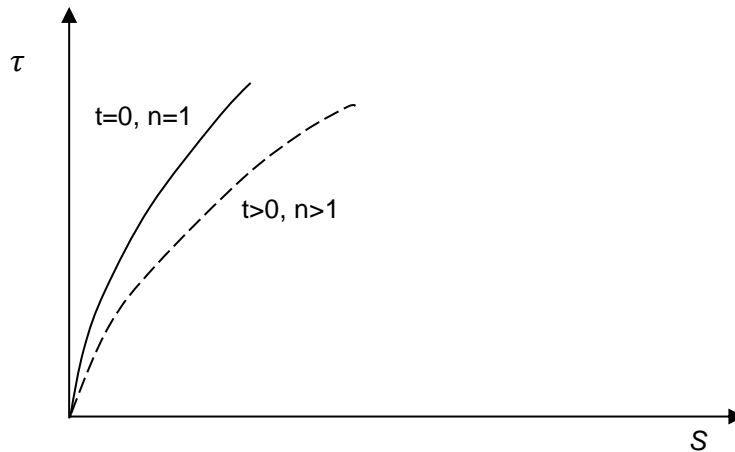
Figure 2-2: Creep effects on the τ-s curve. (CEB-FIP, 1990)

Rehm and Eligehausen (1979) conducted pull-out tests of 308 specimens under cyclic/repeated loading. They noticed that if fatigue failure does not occur, repeated loading only has an influence on the bond under service loading. Also, the bond strength was 5% higher in the preloaded specimens than in the statically loaded specimens.

Hawkins et al. (1982) showed experimentally that the bond stress-slip envelope is similar up to the maximum capacity for both cyclic loading and monotonic loading. In the descending part of the bond stress-slip curves, the bond stress for a given slip is always less in cyclic loading than monotonic loading.

Daud et al. (2015) showed experimentally on full scale beams, i.e. 4.2 m span, that the interaction between concrete and reinforcement depends on the type of load applied, i.e. sustained or cyclic load. They found that overall the deflection is substantially higher in the case of repeated cyclic loads than in the case of equivalent sustained loads.

2.3 Long-Term Properties of Concrete

Concrete exhibits creep and shrinkage and this behaviour is affected by the environment (i.e. temperature and relative humidity). Therefore, in design, these two long-term effects are the main parameters incorporated within code prediction methods which estimate the long-term deflection.

2.3.1 Creep

Creep can be defined as a time-dependent distortion of concrete under sustained loading (Tamtsia and Beaudoin, 2000, Zhang et al., 2014). Once stress is applied, concrete will undergo an elastic deformation, which depends on the amount of applied stress and the age of concrete. If the stress is sustained, creep develops in the concrete. If the stress is removed from concrete, it will exhibit a hysteresis effect (Buettner and Hollrah, 1968), known as elastic recovery, which is always less than the elastic strain after loading. The effect of hysteresis is to produce a nonlinear stress-strain curve for unloaded concrete different from the loading stress-strain curve.

Although many investigations on creep recovery after unloading have been recorded (Counto, 1964, Tang et al., 2014), our knowledge of this phenomenon i.e. creep recovery, is limited to the changing in the material composite during loading of the concrete. After applying stress to the concrete, it will undergo physical changes due to the load and chemical changes over time. These physical and chemical changes will affect the modules of elasticity after unloading concrete. Typical creep and creep recovery is shown in Figure 2-3.
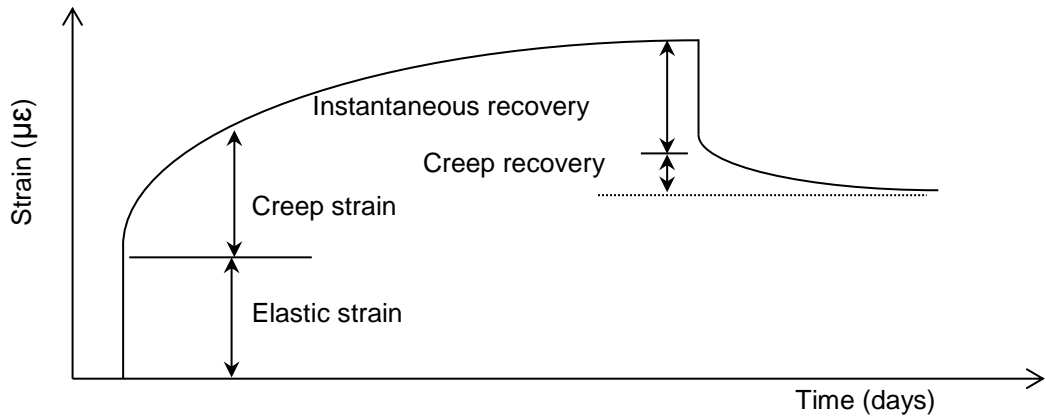
Figure 2-3: Combined curve of elastic and creep strains showing amount of recovery

Compressive creep is often calculated experimentally by subtracting the elastic strain and the shrinkage of unloaded samples from the total time-dependent deformation of loaded samples as shown in Figure 2-4. Creep was first noticed by Hatt in 1907 when he applied sustained loads to a number of reinforced concrete beams and checked the deflection (Bazant, 1975).
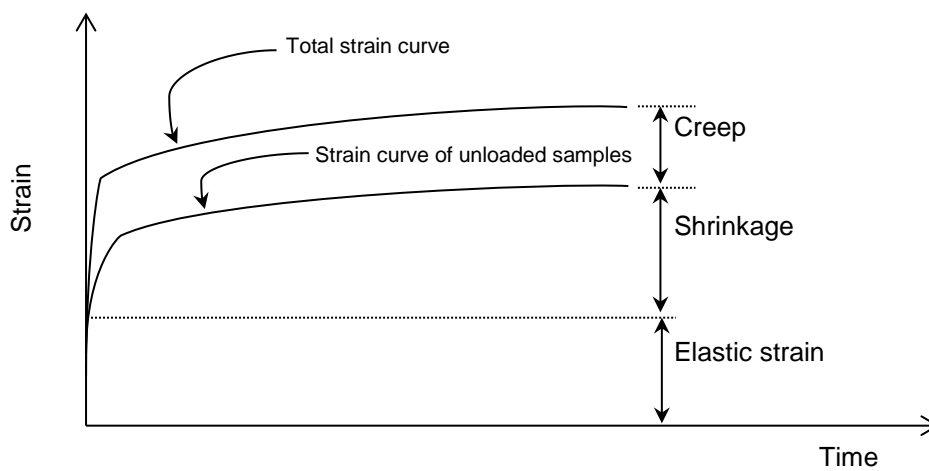
Figure 2-4: Concrete strain under load

During the last century, several methods were produced to analyse the effects of creep on the long-term deflection of reinforced concrete members based on the calculation of the creep coefficient. The simplest and oldest analytical method is the Effective Modulus Method (EMM). The other models are the Age-adjusted Effective Modulus Method (AEMM), which is more complicated, the Rate of Creep Method (RCM), the Rate of Flow Method (RFM) and the Step by Step Model (SSM). SSM enables a more accurate prediction of the changes in the concrete stresses occurring over time (Savoia, 2011).

According to Gilbert (1988), the EMM was first suggested by Faber (1928). The basic idea of this model is to modify the concrete modulus of elasticity to account for creep, where the reduced or effective modulus of elasticity for the concrete can be defined as:

$$E_{eff(t,t_0)} = \frac{E_{t_0}}{1+\emptyset_{(t,t_0)}}$$
(2-1)

Where:

E_{t_0} is the modulus of elasticity of concrete at time t_0,

t_0 is the age of concrete at the time of application of loading

$\emptyset_{(t,t_0)}$ is the creep coefficient at time t.

A reduction factor $\chi_{(t,t_0)}$ to take into account the age of concrete was introduced to the EMM to produce the AEMM. It was first suggested by Trost (1967) and later developed by Bazant (1972) and cited by (Dezi et al., 1993). The value of $E_{c(t,t_0)}$ used in the AEMM can be calculated using the following formula (Bazant, 1972).

$$\mathbf{E}_{\mathbf{eff(t,t_0)}} = \frac{E_{t_0}}{1+\chi_{(t,t_0)}\emptyset_{(t,t_0)}}$$

(2-2)

The above equation has been applied by many researchers, including Bazant (1972), Nie and Cai (2000) and Forth et al. (2003) to predict the long-term deflection.

The values of the *ageing coefficient* $\chi_{(t,t_0)}$ generally range from 0.4 to 1.0, depending on the rate of application of the gradually applied stress in the period after t_0. For practical situations where the final deflection is required, a typical value of $\chi_{(t,t_0)}$ could be 0.65 for normal concrete (Gilbert and Ranzi, 2010). This value of $\chi_{(t,t_0)}$ is relatively low, where both Forth et al. (2003) and Nie and Cai (2000) used the age adjusted coefficient for creep factor, chi ($\chi_{(t,t_0)}$ =0.8).

However, in design, there are numerous analytical methods developed to take into account the creep effects on the long-term deflection. Most of these methods are based on the calculation of the creep coefficient. The creep characteristics of a construction material are usually defined by the creep coefficient, which is the ratio of the creep strain to elastic strain as follows:

$$\emptyset_{(t,t_0)} = \frac{\varepsilon_{cr(t,t_0)}}{\varepsilon_{t_0}}$$

(2-3)

It has been shown that 18 to 38% of the 20 year creep of concrete takes place in the first 15 days after loadings and up to 70% within the first 90 days; about 83% of the total creep occurs in the first year (Troxell et al., 1958). A more recent study showed that up to 50% of the final creep takes place in the first three months and about 90% of the final creep occurs within two to three years (Gilbert, 2002). There are many factors affecting creep, including the magnitude of the applied stress, the age of concrete, properties of the raw materials, ambient environment, volume to surface ratio and the amount of steel reinforcement in the reinforced concrete (Liu, 2007, Haranki, 2009). In addition, when the concrete strength

increases, the creep capacity decreases. The concrete's capacity to creep also decreases as either the maximum size of aggregate or aggregate content increases and/or the water/cement ratio decreases (Gilbert and Ranzi, 2010). In terms of the age of concrete mentioned above, creep obtained when $t_0 = 300$ days is about 40% of that when $t_0 = 7$ days (Neville and Brooks, 2010). However, there are many design codes that predict creep; in Chapter 4 the creep predicted by Eurocode 2 (2004) and Model Code (2010) will be reviewed briefly.

Creep and shrinkage are closely related to each other and both connected to the hydrated cement paste and aggregate content. Generally, concrete that is resistant to shrinkage also has a low creep potential (Gambhir, 2013).

2.3.2 Shrinkage

Shrinkage is usually defined as a reduction in the volume of the unstressed concrete specimen. In general, there are four kinds of shrinkage in concrete; carbonation, autogenous, plastic, and drying (Lam, 2002, Jayasinghe, 2011).

The first type of shrinkage occurs as a chemical reaction, i.e. calcium hydroxide $Ca(OH)_2$ reacts with the carbon dioxide present in the air. Carbonation shrinkage is a relatively small part of the long-term drying shrinkage. Autogenous shrinkage can be described as the shrinkage of cementitious materials without any loss of weight or transfer of moisture to the exterior environment at a constant temperature (Li et al., 2010). It was shown that autogenous shrinkage increases with the decrease of water-cement ratio (Tazawa and Miyazawa, 1995b). Thus, normal concrete with high water-cement ratio, autogenous shrinkage is expected to be low, as there is enough water to complete the hydration.

Plastic shrinkage is a problem with the construction and not a true shrinkage phenomena. It occurs due to the evaporation of the water from the surface of the concrete when it is still in the plastic state. In such cases, the fresh concrete top surface cannot resist the shrinkage strain, and plastic cracks could be developed (Soroushian and Ravanbakhsh, 1998). This kind of shrinkage can be avoided by keeping the surface of the concrete wet.

Drying shrinkage is the most notable phenomenon. It can be defined as the reduction in concrete volume following the evaporation of the water as the concrete has achieved the final set (Gilbert, 2001). Drying shrinkage is dependent on the internal pore space (Holt, 2001). This kind of shrinkage is rapid during early stages of drying and slows during the later stages, depending on the environmental conditions. In reinforced concrete structures, shrinkage induces tensile stresses, which leads to new cracks, an increase in the deflection and an increase in the width of the existing cracks. Therefore, drying shrinkage should be considered as a major factor which affects the long-term behaviour of the reinforced concrete members. Like creep, there are many factors that affect shrinkage. According to Pickett (1956) and Carlson (1937), aggregates help to reinforce the concrete against shrinkage; Carlson (1937) showed that the shrinkage strain decreased as the aggregate content increased. More studies were carried out to investigate the effect of using different types of aggregates on shrinkage (Tazawa and Miyazawa, 1995a, Kohno et al., 1999, Bentur et al., 2001). They found that concrete made from a lightweight aggregate has less autogenous shrinkage, while autogenous shrinkage does not occur at all in the lightweight aggregate concretes with saturated-surface-dry. However, that autogenous shrinkage does not occur in the lightweight aggregate is controversial, where in perfect conditions there still some parts of the cement that do not hydrate.

Likewise, the water-cement ratio is another important factor which affects shrinkage. Normally, shrinkage is proportional to water-cement ratio, i.e. concrete with a higher water-cement ratio has a higher drying shrinkage. Additional factors that affect the magnitude of shrinkage strain are volume/surface ratio, relative humidity, and the temperature of the ambient environment.

Member size is an important factor in shrinkage since dry shrinkage results from the evaporation of water from the surface (Brooks, 2003), where the dry shrinkage decreases with the increase of volume/surface ratio, as shown in Figure 2-5.
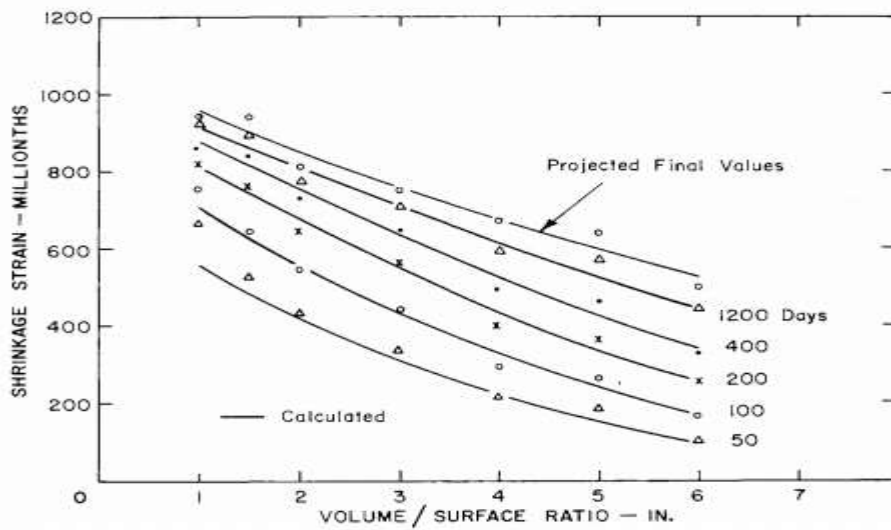
Figure 2-5: Influence of volume/surface ratio on shrinkage of concrete (Hansen and Mattock, 1966)

Similar to volume/surface ratio effect on shrinkage, relative humidity affects dry shrinkage of the concrete, where the shrinkage increases with the decrease in the relative humidity as shown in (Brooks, 2003, Troxell et al., 1958).
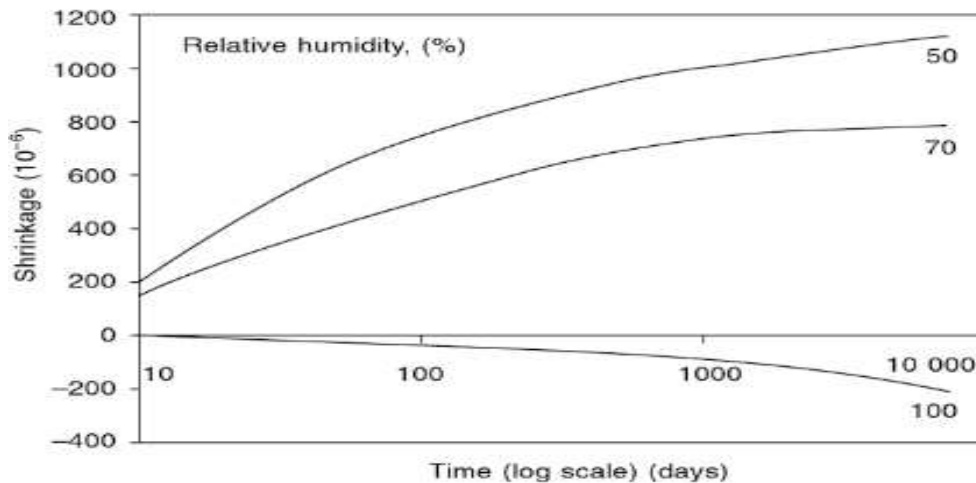
Figure 2-6: Shrinkage as a function of time for concrete sorted at different relative humidity; time is from the age of 28 days after wet curing cited by (Brooks, 2003)

2.3.3 Tension Stiffening

Tension stiffening is the ability of the concrete to resist tension stresses even after cracking has taken place; this effectively further increases the stiffness of reinforced concrete.

Bischoff (2001) carried out tests to investigate the effect of shrinkage on cracking behaviour and tension stiffening in reinforced concrete members. The author presented his results through axially loaded reinforced concrete members with dimensions of 2000 mm length and 250 mm x 250 mm cross section. The steel reinforcement ratio (1.2% and 1.9%) and the shrinkage (i.e. either 153 $\mu\varepsilon$ or 250 $\mu\varepsilon$) were the parameters that this research focused on. The experimental results showed that tension stiffening is affected by shrinkage which leads to the underestimation of tension stiffening, where measured results can be half the true results when the shrinkage is not taken into account. Moreover, he showed that there is still a loss of tension stiffening with time even after the stabilized crack pattern has been achieved. However the author found that the cracking load was reduced due to shrinkage while crack width was not affected. Scott and Beeby (2005) studied experimentally the long-term tension stiffening effects in concrete tension specimens. These specimens had dimensions of 1200 mm long and 120 x 120 mm cross section and were reinforced axially by a single reinforcement bar (i.e. 12mm Ø, 16mm Ø or 20mm Ø). The authors' test ran for three to four months and they found that, after approximately 20 days of sustained loading, the tension stiffening value was half the initial tension stiffening value as shown in Figure 2-7.
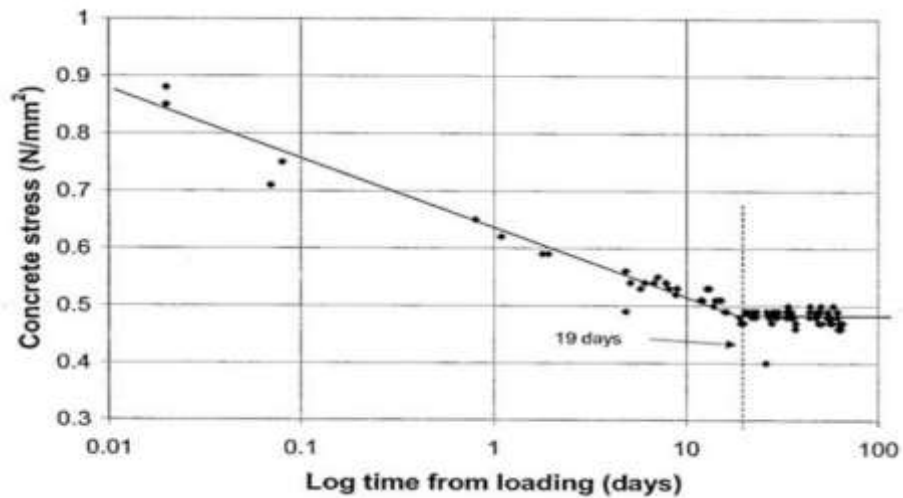
Figure 2-7: Loss of tension stiffening with time. (Scott and Beeby, 2005)

Beeby and Scott (2006) studied experimentally the mechanism of loss in tension stiffening with time. Authors attributed the reduction of tension stiffening with time to cumulative damage since the concrete under long-term loading is going to reduce in its tensile strength. The authors considered that tensile stresses will increase when the concrete around the reinforcement shrinks. The following equation was suggested to consider the effect of shrinkage on the tensile strength:

$$f_{ct,eff} = f_{ct} - \sigma_{ct,sh} = f_{ct} - \frac{E_s \rho \varepsilon_{sh}}{1 + \alpha_e \rho} \tag{2-4}$$

Where:

E_s is the elastic modulus of the steel reinforcement

$f_{ct,eff}$ is the effective tensile strength of the concrete allowing for the effect of shrinkage.

f_{ct}	is the direct tensile strength of the concrete.
$\sigma_{ct,sh}$	is the tensile stress developed in the concrete due to restraint of shrinkage by the reinforcement.
ε_{sh}	is the free shrinkage strain prior to cracking.
ρ	is the reinforcement ratio related to the area of concrete immediately surrounding the reinforcement.
α_e	is the modular ratio, taking account of the effective modulus of elasticity of concrete (i.e. allowing for creep).

Gilbert (2007) carried out tests to study the tension stiffening in lightly reinforced concrete slabs. Gilbert tested eleven one-way slabs with reinforcement ratios (ρ) ranging from 0.0018 to 0.01. Different approaches (ACI 318, Eurocode2, and BS 8110) were used to design lightly reinforced slabs to study tension stiffening effects. It was found that the effect of tension stiffening on deflection was comparatively higher than that in heavily reinforced members. The Eurocode 2 (2004) approach was considered the most suitable approach to represent the load deflection relationship.

Kaklauskas and Gribniak (2011) studied the effect of shrinkage on moment curvature and tension stiffening relationships. At early stages of loading, it was found that concrete members may undergo shrinkage strain, which is more than the cracking strain. The authors carried out their tests on three rectangular reinforced concrete beams (3000 mm length, 300 mm height and 280 mm width) and they studied the effect of shrinkage on tension stiffening under short-term loading. The shrinkage effect was subtracted from the moment–curvature and tension stiffening by a numerical procedure, as shown in Figure 2-8.
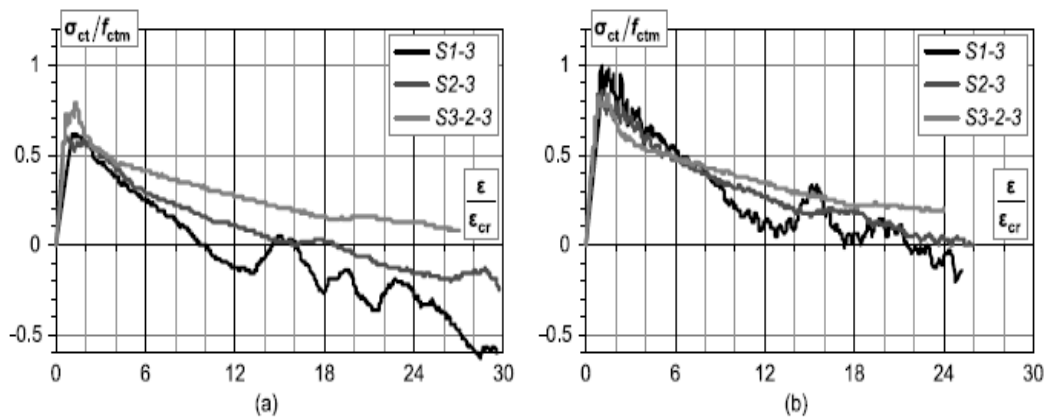
Figure 2-8: Tension stiffening diagrams derived from experimental data of reinforced concrete beams (a) ignoring shrinkage (b) after shrinkage elimination

Zanuy, Albajar and de la Fuente (2010) presented the behaviour of a reinforced concrete tension member under repeated loading. The specimen had a dimension of 1.2 m in length and a cross section of 0.26 m x 0.2 m with a foundation of 0.8 m x 0.5 m x 0.2 m dimensions. Authors monitored throughout the test that repeated reversal stresses damaged the concrete around the reinforcement. Zanuy et al. (2011) presented an experimental study on half-scale lightly reinforced concrete bridge deck subjected to fatigue loading. The main parameter was the frequency (2.0 Hz and 1.0 Hz), the dimensions of which are shown in Figure 2-9. Authors found there is a progressive loss of tension stiffening when the number of load cycles is increased.
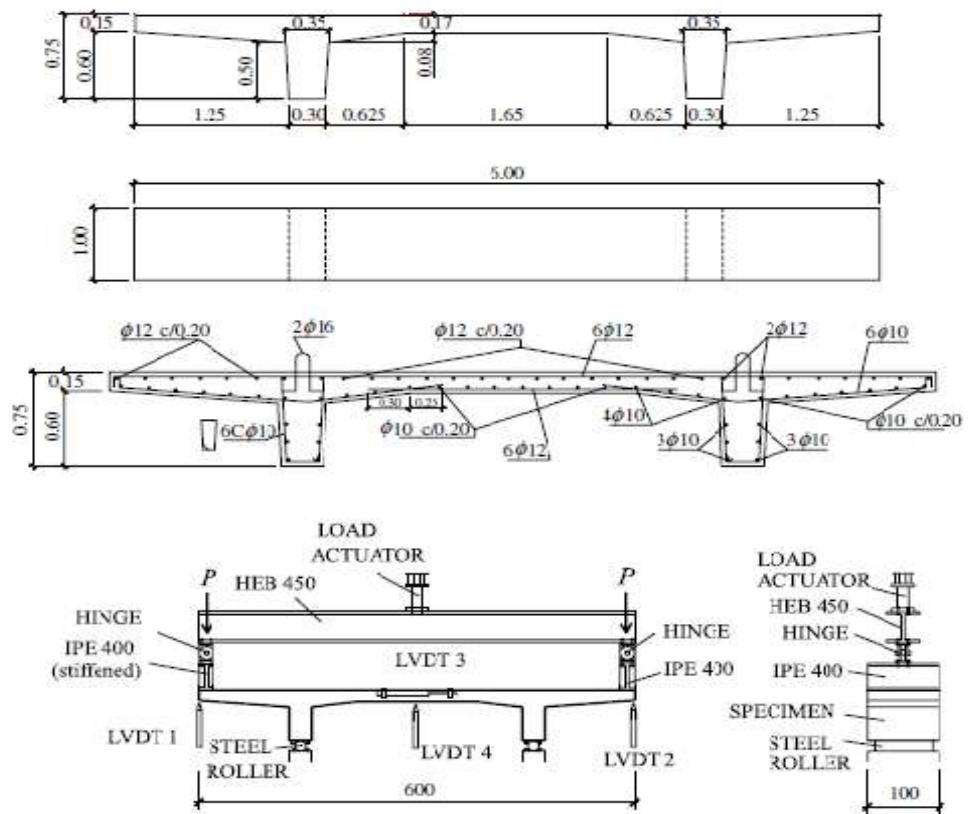
Figure 2-9: (a) Dimensions and reinforcement layout of the specimens; (b) test set-up and instrumentation; (c) view of specimen FT1 during the test. (Zanuy et al., 2011)

2.4 Long-Term Deflection of Reinforced Concrete Beams

When a reinforced concrete beam is subjected to a load, instantaneous deflection (i.e. elastic deflection) takes place. This elastic deflection usually depends on the material properties, reinforcement ratio, loading amount and beam geometry. Once the load is sustained on the beam, the deflection of that member increases due to many factors (i.e. creep, shrinkage, loss of tension stiffening and loading history). In reinforced concrete beams, cracks and deflections must be controlled in order to be serviceable (Gilbert, 2008). Eurocode 2 (2004) suggests L/500 to be the maximum deflection limitation after removed from the framework. A simplified empirical technique was proposed in ACI 318 Code to compute the long-term deflection, where the elastic deflection is modified by a deflection multiplier. Other models have been developed in design codes such as Eurocode 2 (2004) and AS 3600. Fundamentally, the long-term deflection is calculated as the summation of shrinkage and creep deflections. However, all these design codes have drawbacks, as they do not account for the loss of tension stiffening with time under repeated loading as in the Eurocode 2 (2004) and loading history. Hence, more research should be carry out in this field to account for these factors. In addition, long-term deflection of reinforced concrete beams has been studied by many researchers over the past several years. Although, no one has used a nonlinear finite element software to predict the long-term deflection of cracked reinforced concrete beams, nor the effect of the number of cracks on the shrinkage deflection.

2.4.1 Design Codes

Civil engineers employ design codes for the analysis of concrete structures (Gribniak et al., 2013). The Eurocode 2 (2004) and ACI 318 are probably the most commonly used codes to predict the long-term deflection of the reinforced concrete structures.

2.4.1.1 Eurocode 2 (2004)

Eurocode 2 (2004) is based on the CEB-FIP Model Code (1990). The long-term curvature predicted by Eurocode 2 (2004) depends on the section behaviour rather than the beam behaviour and is based on a weighting factor, relating two stages during the life of the structural element, i.e. uncracked (elastic section) and fully cracked section, as presented in equation (2-5).

$$ {}^1\!/_r = \xi \left({}^1\!/_r \right)_{cr} + (1 - \xi)\left({}^1\!/_r \right)_{uc} \qquad\qquad (2\text{-}5) $$

Where

$ {}^1\!/_r $ is the average curvature

$ \left. \begin{array}{l} \left({}^1\!/_r \right)_{cr} \\ \left({}^1\!/_r \right)_{uc} \end{array} \right\} $ are values of curvature calculated for the cracked and uncracked section, respectively

$ \xi $ is the distributed coefficient allowing for tension stiffening given by $ \xi = 1 - \beta \left(\frac{M_{cr}}{M_a} \right)^2 $

$ \beta $ is the coefficient taking account the duration of loading (0.5 for sustained or cyclic loading and 1 for single short-term load)

$ M_{cr} $ is the cracking moment

$ M_a $ is the applied moment

Eurocode 2 (2004) suggests that ξ is $1 - \beta \left(\frac{M_{cr}}{M_a} \right)^2$ when $M_a > M_{cr}$ and zero when $M_a \leq M_{cr}$ (under short-term loading). Espion and Halleux (1990) noticed that when the applied moment is slightly less than the cracking moment the predicted deflection is imprecise, as the deflection is assumed to be purely due to the uncracked section. In reality, shrinkage induced tension stresses in concrete will produce cracks with time and the beam will transform from the uncracked into cracked stage. Daud et al. (2016) showed that, when the beam sustained a load less than the cracking load, creep and shrinkage cracks developed and the beam transformed from the uncracked section into the cracked section a single day after the sustained load was applied.
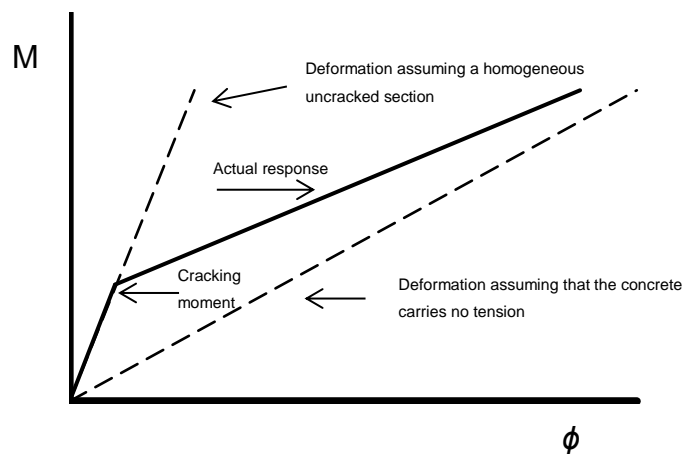
Figure 2-10: Typical behaviour of a reinforced concrete beam under loading

However, Eurocode 2 (2004) is unclear when taking $\beta = 0.5$ for many cycles of repeated loading; does this mean short or long-term repeated loading? Under long-term sustained loading, taking $\beta = 0.5$ is equivalent to reducing the cracking moment by 30%.

This represents the fact that shrinkage induces tension and develops cracks with time (Vollum and Afshar, 2009, Gilbert and Ranzi, 2010). Vollum (2002) suggest equations to calculate β where the duration of peak construction load is known (Equation 2-6). More accurately, β should be taken as 0.7 up to five weeks duration of peak construction loads.

$$\beta(t) = -0.0364\ln(t) + 0.8279 \qquad 0 = t = 12 \text{ days} \tag{2-6a}$$

$$\beta(t) = -0.0008t + 0.7327 \qquad t > 12 \text{ days.} \tag{2-6b}$$

The most appropriate value of β depends on the shrinkage, duration of the load and the time-dependent damage to the bond between the reinforcement and the concrete (Ahmed 2013).

2.4.1.2 ACI 318-14

The ACI 318-14 code suggests that the long-term deflection of a reinforced concrete member due to creep and shrinkage may be obtained by multiplying the elastic deflection by a coefficient. This coefficient depends on the ratio of the time under load to the compression reinforcement as shown in Equation 2-7.

$$\Delta_{long} = \frac{\zeta}{1+50\,\rho'} \tag{2-7}$$

Where

ρ' Compression reinforcement ratio

ζ Coefficient dependent on the time under load

ACI 318-14 suggests the value of ξ between 1 and 2, depending on the duration of the applied load and decreases with the presence of the compression reinforcement in the section (Scanlon and Bischoff, 2008). The variation of ξ with time is shown in Figure 2-8 (Gribniak et al., 2013).
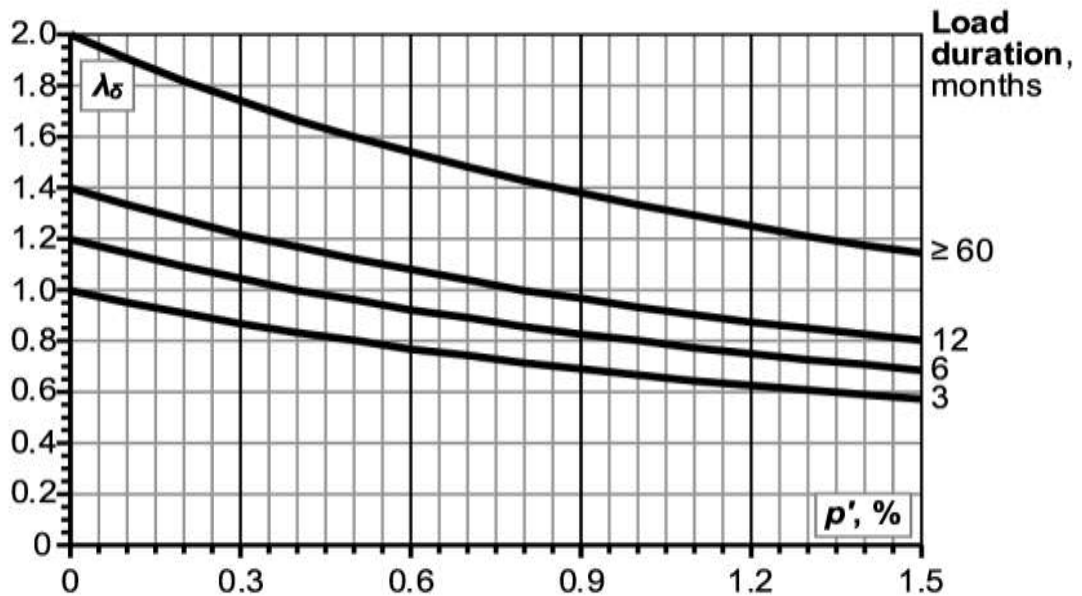
Figure 2-11: Variation of additional long-term deflection factor (Gribniak et al., 2013)

The ACI 318-14 suggested equation to predict the long defection is ignoring many factors which effect the long-term deflection, such as the creep and shrinkage characteristic of the concrete, environmental and age of the section at first loading (Gilbert and Ranzi, 2010).

Moreover, the ACI 318-14 multiplier factor does not consider the loss of tension stiffening with time due to shrinkage and/or crack propagations and other time-dependent parameters which have an effect on deflection. Using a single parameter formula to compute the long-term deflection of reinforced concrete, members cannot give an accurate result for the deflection (Vakhshouri and Nejadi, 2014a).

However, the ACI 318-14 suggested equation and span/depth ratio are widely used by engineers and can be appropriate when there is a lack of information (i.e. age and amount of loading). Nilson (1985) suggests that two factors should be used in the ACI 318-14 μ_m and μ_s, which represent material and a section modifier, respectively. Comparative studies showed that both material and section modifiers can be replaced by one factor μ, which is a function of the compressive strength and the equation of the ACI 318 Code and can be rewritten as follows:

$$\Delta_{long} = \frac{\mu\xi}{1+50\mu\rho'} \qquad\qquad (2\text{-}8)$$

Where $\mu = 1.3 - 0.00005f'_c$ and should be not less than 0.7 nor greater than 1. This equation is suitable for compressive strengths less than 6000 psi (48 MPa). Over the years, for a long span, slender and economy requirement, high and ultra-high strength concrete are developing and Equation 2-8 will not be appropriate to predict the long-term deflection. For that purpose, Paulson et al. (1991) suggested $\mu = 1.4 - f'_c/10000$ for a concrete with a compressive strength ranging from 4000 psi (30 MPa) to 10000 psi (70 MPa).

2.5 Previous Studies of the Long-Term Deflection of Reinforced Concrete Members

Creep, shrinkage and loss of tension stiffening increase the deflection of spanning elements with time. In design it is therefore necessary to consider these factors in order to better estimate the deflection, increase the lifespan of the reinforced concrete elements, and control crack propagation.

Corley and Sozen (1966) studied the long-term deflection of reinforced concrete beams under sustained loading.

They proposed a theoretical model to predict the long-term deflection of reinforced concrete beams based on their experimental work. Their experimental work was carried out on four reinforced concrete beams with different cross sections (i.e. 75 x 150 mm and 75 x 100 mm and with a span length of 1800 mm) subjected to sustained loading for a period of 23 months. Corley and Sozen's (1966) model was verified with other works published by different researchers. The total deflection was suggested to be a superposition of three deflections: instantaneous deflection due to the applied load, deflection induced due to creep and deflection resulting from shrinkage strain.

The elastic curvature was calculated as follows:

$$\kappa_i = \frac{M}{E_{to} I_{cr}}$$

(2-9)

Where

κ_i is the instantaneous curvature,

M is the design moment and

E_{to} & I_{cr} are the modulus of elasticity of the concrete at time t0 and the moment of inertia of the cracked section.

For the creep curvature, authors assumed that the creep strain ε'_{crp} does not change the calculated steel strain and the strain distribution remains linear, as shown in Figure 2-12.
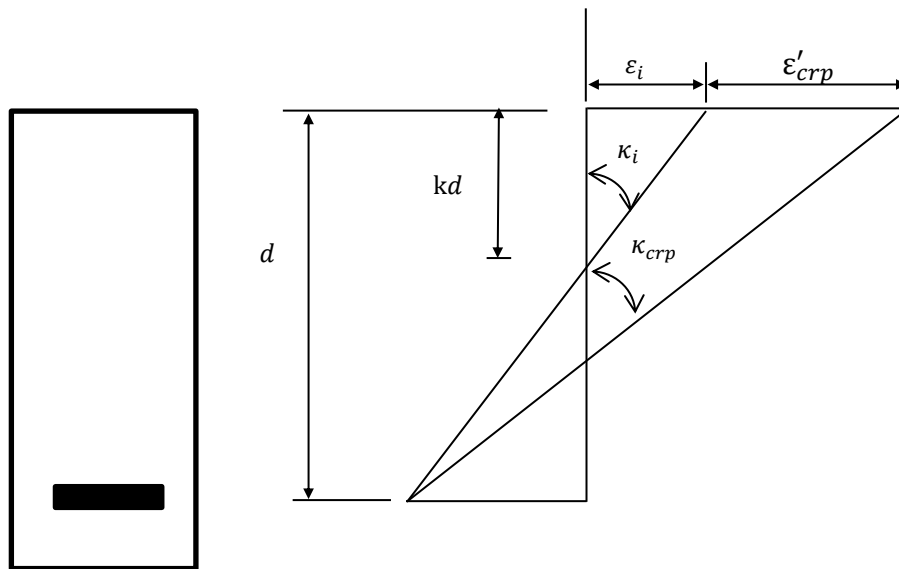
Figure 2-12: Idealized effect of creep strain on curvature at section
(Corley and Sozen, 1966)

The creep strain on the extreme compression fibre was defined by the authors as:

$$\varepsilon'_{crp} = m\varepsilon_i \qquad (2\text{-}10)$$

Corley and Sozen (1966) suggested equation to predict the creep curvature is

$$\kappa_{crp} = km\kappa_i \qquad (2\text{-}11)$$

Where

κ_{crp} is the creep curvature

k   is the ratio of the neutral axis depth to the beam effective depth

m is the he ratio of the creep strain on the extreme compression fibre to instantaneous strain.

Using the proposed method to predict the creep strain on the extreme fibre, the value of *m* can be found at any time t.

A similar approach was used by the authors to develop an approximate expression to predict shrinkage curvature as follows:

$$\kappa_{sh} = \frac{0.035}{d}(\rho - \rho')$$ (2-12)

This equation was developed for concrete that has incurred a shrinkage strain of 500 µε and validated with data from beams where only shrinkage curvature takes place (i.e. no load applied). However, even when there is no load applied on the beam, the beam's own weight still produces a deflection and the long-term deflection will result from the creep and shrinkage defections.

There was a good agreement between the proposed model, their experimental work and the other works (Gilkey and Ernst, 1935, Washa, 1947, Washa and Fluck, 1952, Washa and Fluck, 1956). Moreover, the predicted deflection for a lightly reinforced concrete beam was higher than measured, as the steel reinforcement percentage is an important factor in the deflection. Where tension in the concrete becomes more significant, the percentage of reinforcement decreases.

Though the previous equation could be used only for shrinkages below 500 µε, the following can be used for any value of shrinkage (Wallo and Kesler, 1968):

$$\kappa_{sh} = \frac{0.035}{d} \left(\frac{\varepsilon_{sh}}{500*10^{-6}}\right)(\rho - \rho') \tag{2-13}$$

Bakoss et al. (1982) assessed the instantaneous and long-term deflection predicted by ACI 345 1966 and CP 110 based on the experimental results of two simply supported beams and two continuous beams subjected to long-term sustained loading. The compressive strength of the beams varied from 33 to 55 N/mm^2, and the span length was 1875 mm for the simply supported beam and 3504 mm for continuous beams. The researchers concluded that both the ACI and CP 110 overestimated the short-term deflection, whereas the ACI and CP 110 predicted deflections differed by +16% and -16%, respectively, from the experimental measurements over a period of 500 days.

Clarke et al. (1988) suggested a new method to compute the creep deflection of cracked reinforced concrete beams based on the ratio of the initial neutral depth to the effective depth (x_i), as shown in Figure 2-13.
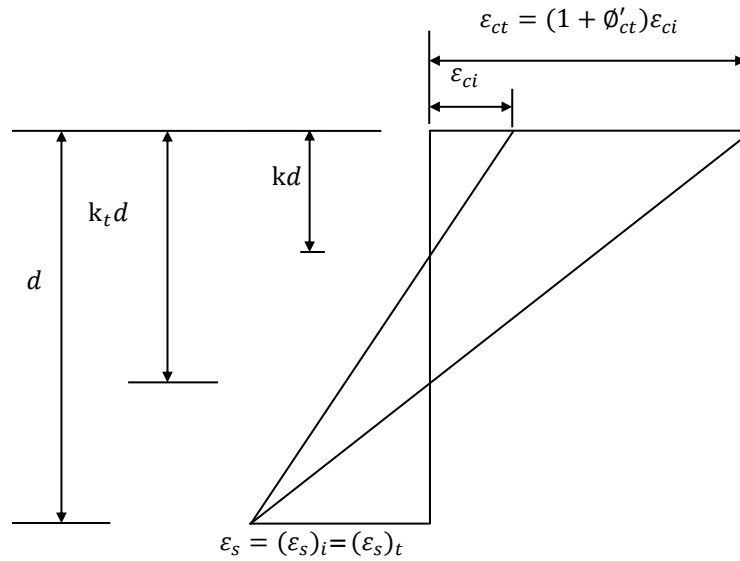
Figure 2-13: Idealized strain distribution through a
fully cracked section (Clarke et al., 1988)

Their method of computing the creep deflection is similar to that of the ACI-318
Code, which modifies the elastic deflection, as shown below:

$$\Delta_c = k\emptyset'_{ct}\Delta_i \qquad (2\text{-}14)$$

Where

Δ_i is the elastic deflection

$\emptyset'_{ct}$ is the creep coefficient prevailing in the compression fibre.

Clarke et al. (1988) had proposed a numerical method to compute $\emptyset'_{ct}$ and then
plot $\emptyset'_{ct}$ versus creep coefficient ($\emptyset_{ct}$) for different values of k as shown in Figure
2-14.

Their approach is based on the assumption that the tensile strain at the level of the tension reinforcement is equal to that of the completely cracked section value and not affected by creep, as shown in Figure 2-13. However, the concrete in tension is still undergoing tensile creep and an inequality should be considered between the tensile and compressive creep in any assessment of neutral axis position (Forth, 2015).
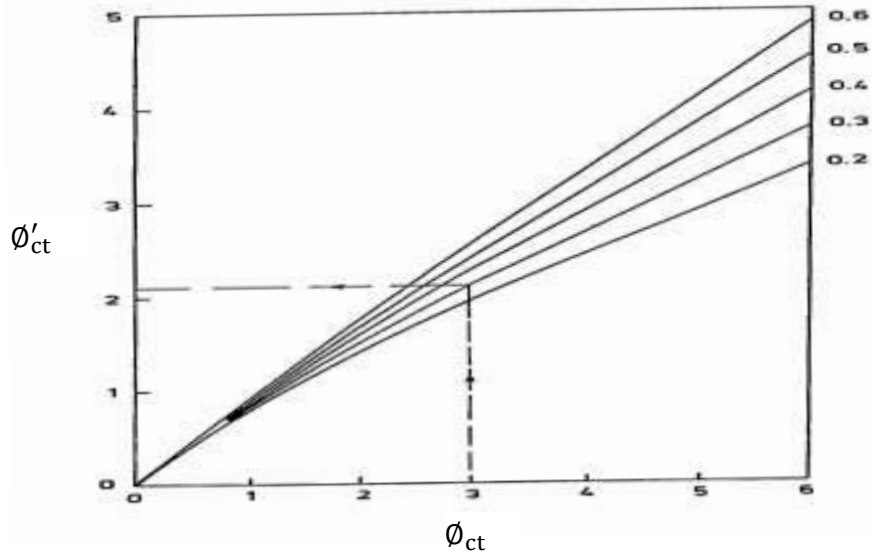
Figure 2-14: $\emptyset'_{ct}$ versus $\emptyset_{ct}$ for different values of k (Clarke et al., 1988)

Ghali (1993) suggested an equation to calculate the mid-span deflection of simple, continuous or cantilever beams with different cross sections from the curvatures at a number of sections, as shown in Figure 2-15.

$$D = \frac{L^2}{96}(\psi_1 + 10\psi_2 + \psi_3)$$

$$D = \frac{L^2}{6}(2\psi_2 + \psi_3)$$

$$D = \frac{L^2}{48}(\psi_1 + 4\psi_2 + \psi_3)$$

$$D = \frac{L}{24}(\psi_2 + 6\psi_2 + 5\psi_3)$$
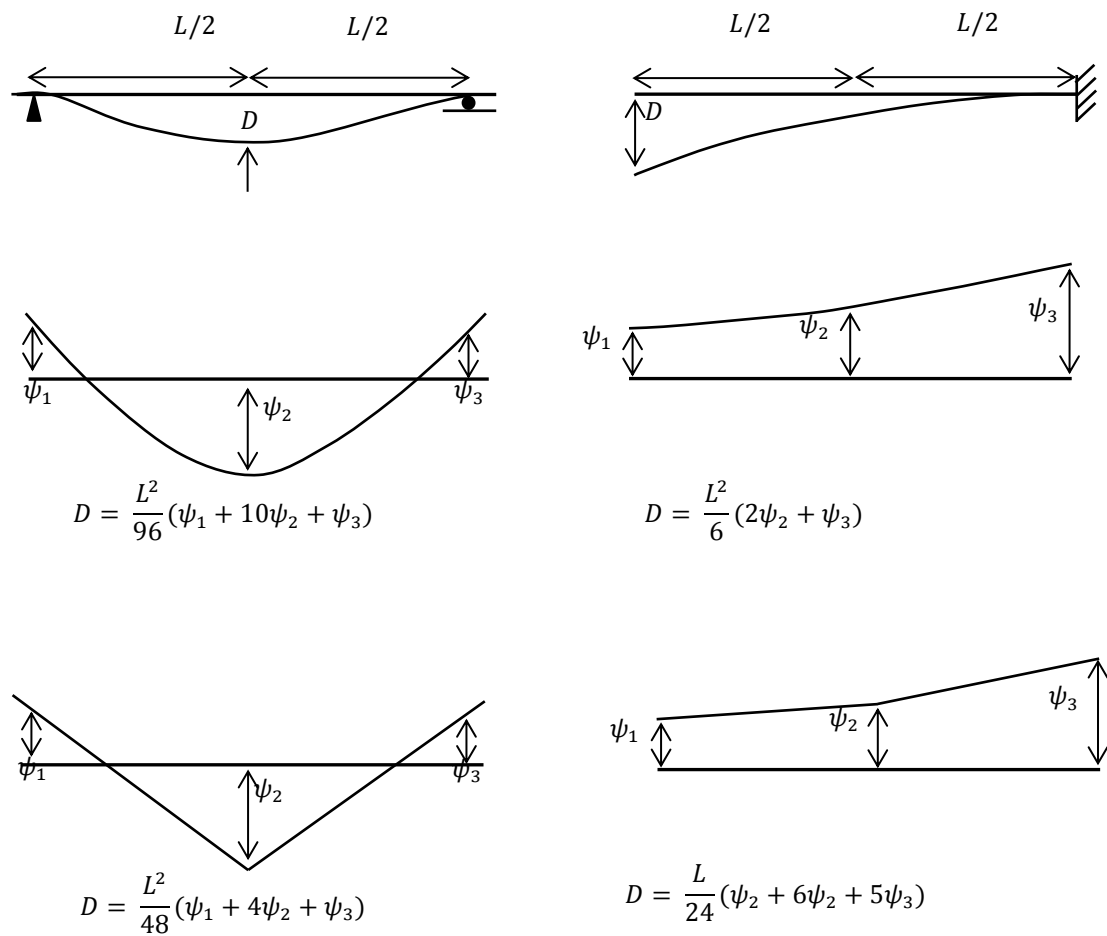
Figure 2-15: Geometric relationships between curvature and deflection
(Ghali, 1993)

For the case of a simply supported beam, the moments at the supports are equal to zero i.e. $\psi_1 = \psi_3 = 0$ and the deflection in the mid-span will be:

$$\mathrm{D} = 0.104 * L^2 * \kappa_{mid} \tag{2-15}$$

Where

L is the span length.

κ_{mid} is the curvature at the middle section.

The curvature ψ can be calculated from the strain variation over the reinforced concrete section as :

$$\kappa = \frac{\varepsilon_c - \varepsilon_s}{d}$$ (2-16)

Where

ε_c is the strain in the concrete compressive fibre

ε_s is the tensile reinforcement strain

d   is the distance of the tensile reinforcement to the top fibre strain as show in Figure 2-16.
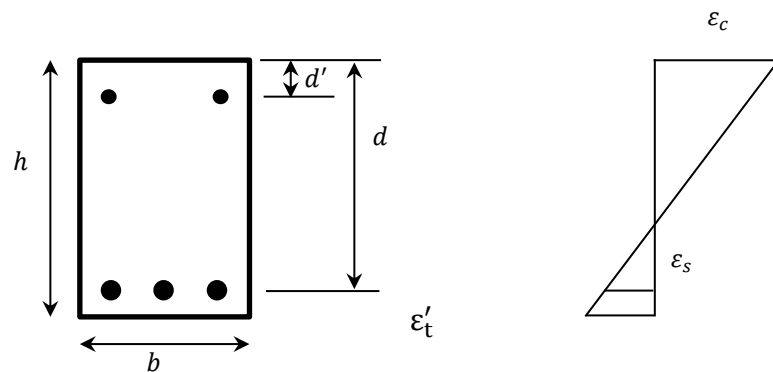
Figure 2-16: Strain caused by bending on a cracked section

Equation 2-15 is suitable for short and long-term deflection, as long as the curvature in the middle of the section is known and the deflection is largely dependent on the curvature at the centre (Hall and Ghali, 2000). This equation will be used in Chapter 5 to predict the long-term deflection of the reinforced concrete beams.

Samra (1997) proposed a method to compute the long-term deflection of cracked reinforced concrete sections based on the ratio of short to long-term flexural rigidity $(E_c I_e)_i$ and $(E_c I_e)_t$. The moment of inertia and concrete modulus of elasticity at time t are given as:

$$(I_c)_t = \frac{\left[\rho(1-k_t)\left(k_t^2 - \frac{1}{3}k_t^3\right) + \rho'\left(\frac{d'}{d} - k_t\right)\left(\frac{d'}{d}k_t^2 - \frac{1}{3}k_t^3\right)\right]bd^3}{2\left[\rho(1-k_t) + \rho'\left(\frac{d'}{d} - k_t\right)\right]}$$

(2-17)

$$(E_c)_t = \frac{E_s}{n_t}$$

Where b, d and d' are the geometry of the section, as shown in Figure 2-17, E_s is the modulus of elasticity of the reinforcement, k_t is the ratio of the neutral axis depth at time t to the beam effective depth and n_t is the modular ratio between the reinforcement and the concrete at time t, and all are given as:

$$k_t = \frac{-\beta_1 + \sqrt[2]{\beta_1^2 + 4\beta_2}}{2}$$

(2-18)

$$n_t = \frac{k_t^2}{2\left[\rho(1 - k_t) - \rho'\left(k_t - \frac{d'}{d}\right)\right]}$$

(2-19)

Where β_1 & β_2 are factors calculated from:

$$\beta_1 = 2E_s \frac{\varepsilon_{ct}}{f_{ct}}(\rho + \rho')$$ (2-20)

$$\beta_2 = 2E_s \frac{\varepsilon_{ct}}{f_{ct}}(\rho + \rho'\frac{d'}{d})$$ (2-21)

The proposed long-term deflection was derived and given as:

$$\Delta_{long} = \frac{\Delta_i(E_cI_e)_i}{(E_cI_e)_t}$$ (2-22)

Where Δ_i is the initial deflection.
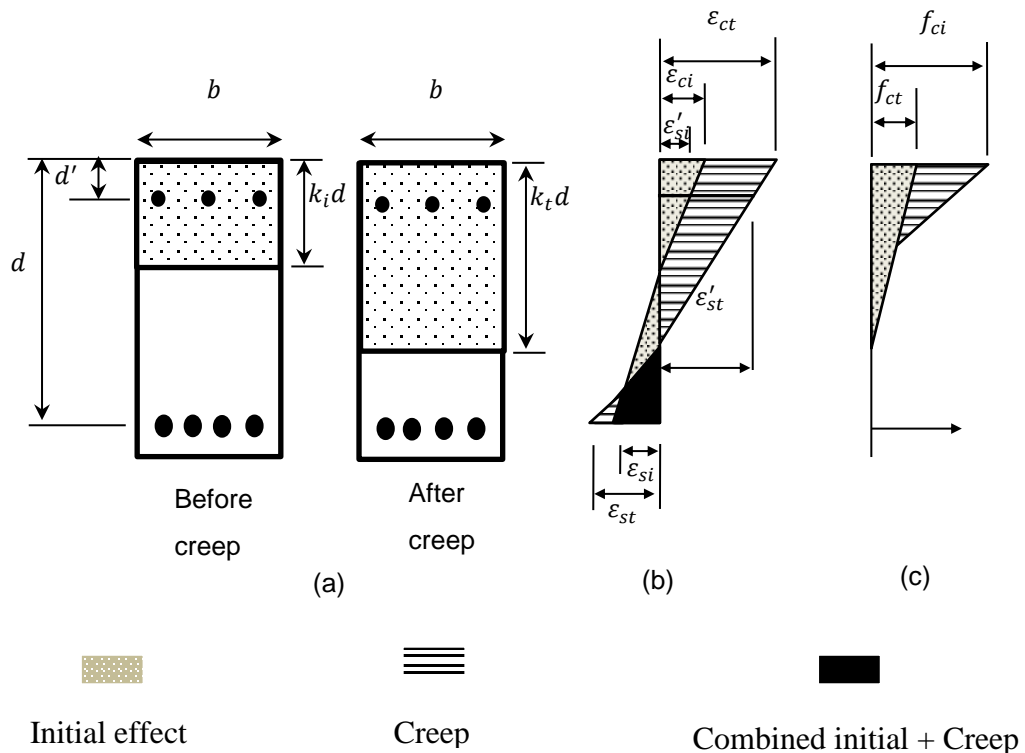
Figure 2-17: Reinforced concrete beam section before and after creep (a) Section; (b) Strain diagram; (c) Stress diagram. (Samra, 1997)

Nie and Cai (2000) experimentally studied the effect of sustained loading on the time-dependent deflection of simply supported beams. They tested twelve beams, eight of which were under sustained loading for a period of 90 days, while the rest were subjected to short-term loading, i.e. up to failure. All beams had the same dimensions (2180 mm clear span with 120 x 400 mm cross section). The main parameters of their work were the compressive strength of the concrete (38 N/mm^2 and 41 N/mm^2), reinforcement ratio (2.3% and 3.5%) and sustained loading amount. The sustained loading amount was a load which produced a crack width of 0.2 mm and 0.3 mm. Test results noted that the developed deflection due to sustained loading ranged from 0.48% to 88% of the elastic deflection in a period of 3 months. In contrast, the work done by Washa and Fluck (1952) indicated that the total deflection after 30 months was nearly two times that of the initial deflection for beams with no compression reinforcement, and was slightly greater than the elastic deflection in the case of double reinforced concrete beams. A recent study shows between 55% to 65% of the total deflection takes place in the first 10 days. Moreover, up to 90 % of the total deflection occurs after 90 days of sustained loading (Mias et al., 2013).

Similar to Washa and Fluck (1952) and Nie and Cai (2000), Pillai and Menon (2003) showed that the long-term deflection of the reinforced concrete members due to shrinkage, creep and temperature could be two to three times the instantaneous deflection.

Nurnbergerova et al. (2000) studied the long-term deflection of reinforced concrete I beams under sustained loading. A total of six beams with varying sustained loads were tested for a period of 200 days. They concluded that the elastic deflection and long-term deflection of reinforced concrete beams can be assumed to be dependent. Moreover, during their test they noticed that the neutral axis position does not change with time. However, recent work carried out by Vakhshouri and Nejadi (2014b) compared the short and long-term deflections of work published by other researchers. They noticed that the parameters that affect the long-term deflection are not the same as for the short-term deflection, thus a linear relationship between them is out of the question. Vakhshouri and

Nejadi (2014b) also stated that there is no distinct expression to show when the short-term deflection ends and the long-term deflection begins. However, the long-term deflection ratio to the initial deflection depends on many factors, such as the type of concrete (i.e. normal, high strength or fibre concrete), environmental conditions (which enhance the creep and shrinkage), concrete age, when first loaded, and the amount of the sustained loading.

Gilbert (1999) suggested empirical equations to predict the long-term curvature in cracked reinforced concrete members. The total curvature will be the summation of the creep and shrinkage curvatures and the instantaneous curvature. The shrinkage curvature of cracked and uncracked reinforced concrete members under sustained loading are shown below:

$$(\kappa_{sh})_{cr} = \left[\frac{0.7\,\varepsilon_{sh}}{D}\right]\left[1 - \frac{A_{SC}}{A_{St}}\right] \tag{2-23}$$

$$(\kappa_{sh})_{uncr} = \left[\frac{1.2\,\varepsilon_{sh}}{D}\right]\left[1 - \frac{A_{SC}}{A_{St}}\right] \tag{2-24}$$

Where

A_{SC}, A_{St}	are the area of tensile and compressive reinforcement respectively, ρ is the reinforcement ratio,
ε_{sh}	is the shrinkage strain
D	is the overall depth of the member.

However, the induced curvature due to the creep was calculated from the equation below:

$$\kappa_{crp} = \kappa_i \left(1 + \frac{\emptyset(t,\tau_0)}{\alpha}\right) \tag{2-25}$$

Where

κ_i is the instantaneous curvature

$\emptyset(t, \tau_0)$ is the creep coefficient and

α is an empirical factor (called the creep modification factor) which accounts for the cracking and reinforcement effect on creep.

For cracked reinforced concrete section in pure bending (i.e. no axial force):

$$\alpha = [20000 \, \rho^2 - 700 \, \rho + 90] \left[1 + 0.7 \frac{A_{sc}}{A_{St}}\right] \tag{2-26}$$

For uncracked section or restressed concrete section:

$$\alpha = 1 + [45\rho - 900\rho^2] \left[1 + \frac{A_{sc}}{A_{St}}\right] \tag{2-27}$$

The typical values for α range from 1 to 1.6 for uncracked sections and from 4 to 10 for cracked sections.

Marí et al. (2010) studied the long-term deflection of cracked reinforced concrete members under sustained loading. They proposed formulae to predict the long-term deflection due to the creep and shrinkage of reinforced concrete members. Their suggested equation was verified by 217 beams tested in flexure under long-term sustained loading, conducted by other researchers. The suggested creep deflection equation was:

$$\Delta_c = \Delta_i k \frac{0.847\emptyset_{(t,t_0)} - 0.20}{1 + 12n\rho'} \tag{2-28}$$

Where

Δ_i	is the instantaneous deflection
kd	is the instantaneous neutral axis depth
$\emptyset_{(t,t_0)}$	creep coefficient
n	modular ratio $(\frac{E_s}{E_c})$

Whereas the shrinkage deflection equation was:

$$\Delta_{sh} = \frac{\varepsilon_{sh}}{d} \frac{1}{1+12n\rho'} k_s \frac{L^2}{8} \qquad (2\text{-}29)$$

Where

ε_{sh}	is the shrinkage strain
L	span length of the beam
k_s	constant which depends on the support conditions.

Approximate values of k_s are: 4.0 for cantilevers, 1.0 for simply supported beams, 0.7 for end spans of continuous beams and 0.5 for intermediate spans of continuous beams and beams fixed at both ends. The total deflection of their model is:

$$y = y_g + \Delta y_{cr} + \Delta y_{sh} \qquad (2\text{-}30)$$

The results of this proposed model gave a better agreement than the ACI method and CEB methods.

Higgins et al. (2013) conducted an experimental study into the effect of two different frequencies and amplitude on the long-term deflection of reinforced concrete beams. They tested 6 beams, two under sustained loading and 4 under repeated loading. All beams had the same dimensions and material properties. The frequencies adopted in their work were 0.2 H_z and 1 H_z, while the amplitudes were ± 2.5 kN and ± 5 kN. Their findings showed that beams which were subjected to repeated loading had more deflection than those subjected to an equivalent sustained loading. Moreover, it was found that beams subjected to larger amplitudes developed more deflection with time. Finally, authors found that the frequency had only a slight effect on the long-term deflection, and that the cyclic action mainly achieved movement in the early stages of loading.

Further studies have been carried out on the behaviour of unbonded reinforcement under short-term loading to study the effects of corrosion of the reinforcement (Raoof and Lin, 1997, Wang et al., 2011, Jnaid and Aboutaha, 2014). Sea structures are more likely exposed to chloride-laden environments which leads corrosion of the reinforcement to occur (Jones et al., 2012) . When the reinforcement is corroded, the bond between the concrete and reinforcement will be deteriorated as the rust breaks the concrete surrounding the reinforcement (Jnaid and Aboutaha, 2015). However, in certain cases a small amount of corrosion (i.e. < 4%) will enhance the bond between the concrete and reinforcement (Almusallam et al., 1996). In reality, the effects of corrosion on the behaviour of the reinforced concrete beams will take time, therefore it is important to study the effect of the long-term behaviour of corroded reinforced concrete beams.

El Maaddawy et al. (2005) studied the long-term performance of reinforced concrete beams with corroded reinforcement. In this study, the authors were interested in the loss of steel mass under long-term loading. More recent studies carried out by Malumbela et al. (2009) reviewed previous work to investigate the loading type and steel corrosion effects on the behaviour of reinforced concrete structures. They concluded that sustained loading had a major influence on the behaviour of the reinforced concrete beams contains corroded reinforcement,

and suggested a further investigation should be carried out to clarify that influence.

2.6 Summary

Creep, shrinkage and loss of tension stiffening are the main factors which affect the long-term behaviour of reinforced concrete structures. Many researchers have proposed empirical equations to predict the long-term deflection of reinforced cracked concrete members, and several design codes suggest equations to calculate the effect of creep and shrinkage on the long-term deflection. The drawbacks and/or the limitations of the suggested equations mean further investigations in this field are required. Table 2-1 summarises the previous work that has been carried out on the long-term behaviour of cracked reinforced concrete beams. This table shows that so far no work has been performed on the effect of the number of cracks on the long-term deflection. Moreover, no research has studied numerically the long-term behaviour of reinforced concrete beams under sustained and repeated load.

Table 2-1: Summary of the literature review

Authors	Journal	Dimension (mm)	Test duration (months)	Conclusion
Corley and Sozen (1966)	*Aci Journal Proceedings*	75 x 150 x 1500 75 x 100 x 1500	23	Authors here proposed a theoretical models to predict the long-term deflection of cracks reinforced concrete beams. They assist there model by an experimental work. However their model to predict the shrinkage curvature does not contain shrinkage strain.
Bakoss et al. (1982)	*Magazine of Concrete Research,*	100 x 150 x 1875 100 x 150 x 3504	16	Both ACI and CP 110 equations to predict the short and long-term deflection were assessed. It was found that both codes were overestimate the elastic deflection whereas the ACI and CP 110 equations predicted deflections + 16 % and -16 % different from

				the experimental measurements respectively in a period of 500 days.
Clarke et al. (1988)	*ACI Materials journal*	100 x 150 x 2100	6	Based on the ratio of the initial neutral depth to the effective depth (x_i), Clarke et al. (1988) proposed a new method to find the creep deflection of cracked reinforced concrete members. They assume the tensile strain at the level of the tension reinforcement is equal to that of the completely cracked section value, and that it is not effected by creep.
Ghali (1993)	*ACI Structural Journal*	-	-	Suggested an equation to calculate the mid-span deflection of simply, continuous or cantilever beams with a different cross sections from the curvatures at a number of sections

Samra (1997)	*Journal of Structural Engineering*	-	-	based on the ratio of short to long-term flexural rigidity $(E_cI_e)_i$ and $(E_cI_e)_t$ respectively. Samra (1997) proposed a new method to compute the long-term deflection of cracked reinforced concrete section
Nie and Cai (2000)	*Journal of Structural Engineering,*	120 x 400 x 2180	3	Authors carried out an experimental test to study the long-term behaviour of reinforced concrete beams under sustained loads. they noticed after three months of sustained loading, the developed deflection is up to 88 % of the elastic deflection
Washa and Fluck (1952)	ACI Journal	200 x 300 x 6000 150 x 200 x 6000 300 x 130 x 6500 300 x 75 x 5500	0	Their experimental outcomes are: the total deflection after 30 months was nearly two times that of the initial deflection for beams with no compression reinforcement,

				The long-term developed deflection is slightly greater than the elastic deflection in the case of the double reinforced concrete beams.
Pillai and Menon (2003)	*Tata McGraw-Hill (Book)*			showed that the long-term deflection of the reinforced concrete members due to shrinkage, creep and temperature could be two to three times the instantaneous deflection.
Nurnbergerova et al. (2000)	*Indian Journal of Engineering and Materials Sciences*	240 x 480 x 4150		Authors concluded that, the elastic deflection and long-term deflection of reinforced concrete beams can be assumed to be dependent. Moreover during their test they noticed that the neutral axis position does not change with time.
Vakhshouri and Nejadi (2014b)	Second International Conference on			They noticed that, parameters effect the long-term deflection are not the same in the short-term deflection, thus a linear relationship

	Vulnerability and Risk Analysis and Management (ICVRAM)			between the long-term and short-term deflections is out of the question. Moreover, Vakhshouri and Nejadi (2014b) stated that, there is no distinct expression to show when the short-term deflection ends and long-term begins.
Gilbert and Ranzi (2010)				Suggest empirical equations to predict the long-term curvature in cracked reinforced concrete members. The total deflection will be the summation of the creep and shrinkage deflections and the instantaneous deflection. The shrinkage curvature of cracked and uncracked reinforced concrete members under sustained loading are given by these equations respectively
Marí et al. (2010)	*Engineering Structures*	-	-	They proposed formulae to predict the long-term deflection due to creep and shrinkage of reinforced concrete members. Their

				suggested equation was verified by 217 beams tested in flexure under long-term sustained loading conducted by other researchers
Higgins et al. (2013)	*Engineering Structures*	300 x 150 x 4200	3	Their findings showed that beams which were subjected to repeated loading had more deflection than those subjected to sustained loading. Moreover, it is expected that repeated load amplitude had an effect on beams deflection, where the developed deflection was higher in beams under larger amplitudes. Whereas the frequency had only a slight effect on the long-term deflection. In addition, the cyclic action was mainly affected in the early stages of loading.

Chapter 3 Experimental Work

3.1 Introduction

The main purpose of this work is to examine the performance of full scale cracked rectangular reinforced concrete beams under sustained and repeated loads. The experimental study involved seven reinforced concrete beams, several samples for creep and shrinkage measurements, and eight pull out specimens, all fabricated in the George Earle Laboratory of The University of Leeds. The main parameters investigated using the reinforced concrete beams were the loading type, reinforcement condition and level of applied load. The load types (i.e. sustained/repeated) and reinforcement condition (i.e. bonded/debonded) were examined experimentally to study the effect of loss of tension stiffening in the early ages, while the level of the applied load was investigated to study the effect of the number of cracks on the long-term shrinkage deflection.

Measurements were taken using the Linear Variable Differential Transformer (LVDT) for deflection, electrical resistance strain (ers) gauges for the strain in the steel reinforcement and DEmountable MEChanical (DEMEC) gauges studs for the concrete surface strains.

In this chapter, beam dimensions, materials used, mix proportion and test procedures are described in detail. All of the mid-span deflections, surface strains, creep and shrinkage were measured for 90 days. Previously, it was shown that up to 80% of the final creep and shrinkage occurs in the first 90 days (Troxell et al., 1958). Also up to 50% of the tension stiffening is lost over the first 30 days; after that the loss in tension stiffening stabilized (Scott and Beeby, 2005). Higgins et al. (2013) showed experimentally that, the extra deflection due to repeated loading occurred in the first 10 days.

Finally, Mias et al. (2013) showed experimentally that, up to 90% of the final long-term deflection in reinforced concrete members occurs by 90 days of loading. Therefore in this study all beams under sustained and repeated loading were tested for a period of 90 days.

3.2 Test Programme

The experimental part of this investigation is primarily based on the four-point flexural test of seven reinforced concrete beams. Type of loading, reinforcement condition and level of applied load are the main parameters investigated.

3.2.1 Beam Description

All beams have a cross-section of 300 x 150 mm with 20 mm cover to the stirrups. The whole length of the beams is considered to be 4200 mm, whilst the beams span was 4000 mm (simply supported). Beam layout and dimensions are shown in Figure 3-1. Beam dimensions and reinforcement amount (i.e. tension reinforcement, compression reinforcement and stirrups) were the same as those used by Ahmed (2013) and Higgins et al. (2013).

The seven beams were divided into two sets.

The first series consisted of two beams under repeated loading. In one of these beams, the reinforcement in the constant moment zone is bonded. However, in the second of these two beams an attempt was made to debond the reinforcement in the constant moment zone (the method of debonding is described in Section 3.3.5).

The second series consists of five beams under sustained loading. The first beam in the second set had debonded reinforcement in the constant moment zone, while the second beam had symmetrically bonded reinforcement, i.e. 3 Ø 16 in the compression and tension zone. The last three beams were normal reinforced concrete beams (see Figure 3-1), while the sustained applied load varied from an amount equivalent to the first cracking load to the amount producing a fully cracked section (i.e. all primary cracks had taken place).

3N B16   2N B10

1250 mm   1500 mm   1250 mm

d=114 mm   Steel Stirrups Ø8@150

b=300 mm
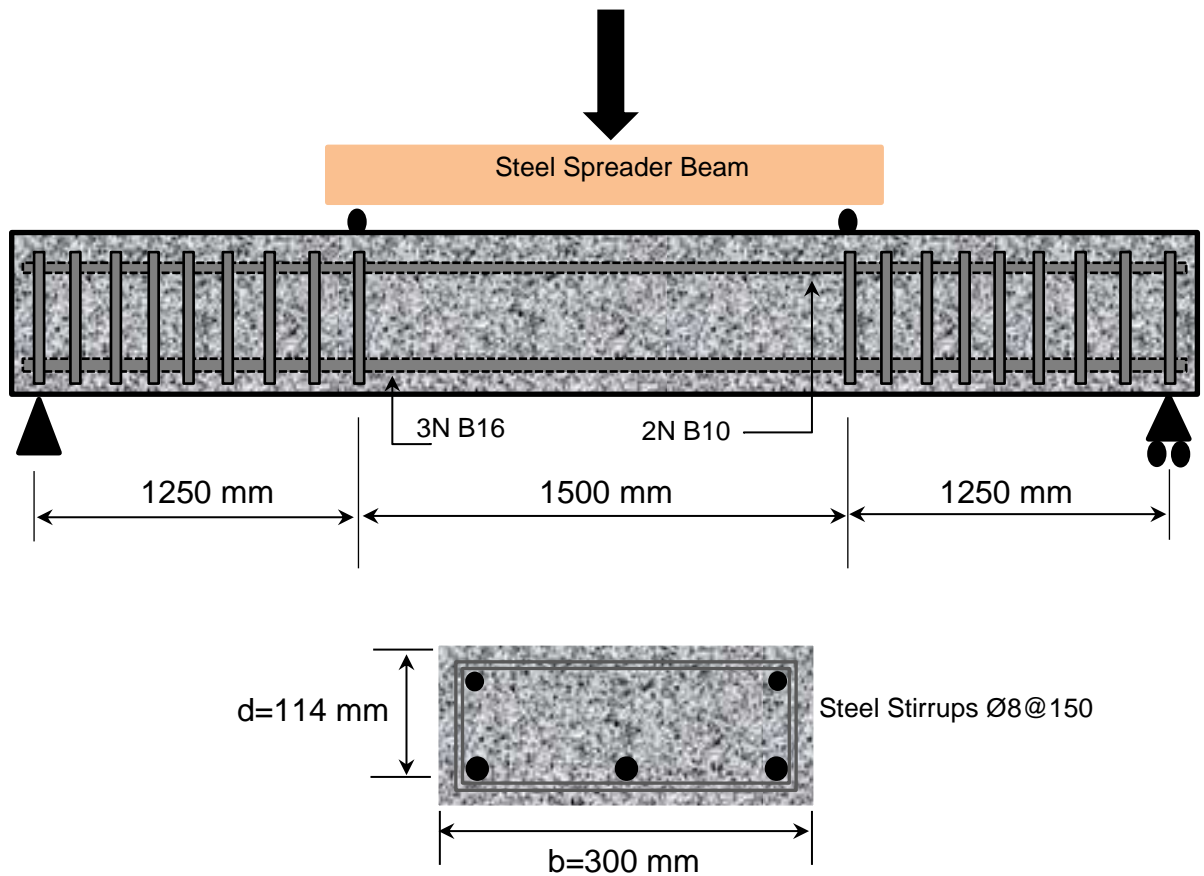
Figure 3-1: Beam Dimensions and Experimental Setup

3.2.2 Beam Identification

Each beam was identified by X#Y#N, where X is a letter indicating the type of loading (static sustained or cyclic repeated), Y is a letter indicating the reinforcement condition (bonded, unbonded or symmetrical reinforcement) and finally, letter N is a number indicating the amount of load. Beams were divided into two series - Series REP and Series SUS - according to types of loading (**REP**eated or **SUS**tained, respectively) and each series was subdivided into three groups (group B, group UB and group SYB) according to the bond and geometry of the reinforcement (**B**onded, **U**n**B**onded and **SY**mmetrical **B**onded reinforcement, respectively).

In summary, the first group consisted of two beams under repeated loading (REP-UB-19 and REP-B-19) and the second group consisted of five beams under sustained loading (SUS-UB-19, SUS-SY-19, SUS-B-19, SUS-B-5 and finally SUS-B-3). The group and beam details are given in Table 3-1.

Table 3-1: Details of the beams

Series designation	Group designation	Beam designation	Loading type	Loading amount (kN)	Type of reinforcement
REP	UB-19	REP-UB-19	Repeated	19	Unbonded
	B-19	REP-B-19	Repeated	19	Bonded
SUS	UB-19	SUS-UB-19	Sustained	19	Unbonded
	SYB-19	SUS-SYB-19	Sustained	19	Symmetrical Bonded
	B-19	SUS-B-19	Sustained	19	Bonded
	B-5	SUS-B-5	Sustained	5	Bonded
	B-3	SUS-B-3	Sustained	3	Bonded

3.3 Materials

Normal concrete is a composite material containing cement, sand, coarse aggregate and water. In this section the basic ingredients will be described.

3.3.1 Cement

The cement used in this work was Portland Cement (CEM 52.5 N) conforming to the requirements of BS EN 197-1: (2011).

The cement was stored in airtight bags to ensure minimum exposure to the environment and therefore to maintain its dryness. The chemical test results are shown in Table 3-2, which was given by the manufacturing company.

Table 3-2: Chemical properties of the cement

Property	Guideline value	Unit	Requirement Standard
Setting time	110	min	≥ 45
Volume consistency	1.1	mm	≤10
Compressive strength 2d	27	MPa	≥20
Compressive strength 28d	58	MPa	≥ 52,5
SO3	2.60	(%)	≤4,0
Cl	0,01	(%)	≤0,10

3.3.2 Fine Aggregate

The fine aggregate was washed natural river sand originating from deposits in North Nottinghamshire (Tarmac Roadstone). The maximum particle size of the fine aggregate that was used in this experimental work was 5 mm. The fine aggregate was oven dried in the University of Leeds laboratory using the drying parker plant with a drying rate of 7 kg/min. Two days after drying, the fine aggregate was cooled in a hopper. At that point, the fine aggregate was ready to be mixed with the other material to produce the concrete matrix. Table 3-3 and Figure 3-2 show the grading of the fine aggregate based on BS EN 12620: (2002 +A1:2008).

Table 3-3: Grading of fine aggregate

Sieve Size	Weight Retained (g)	% Retained	% Passing	BS 882 overall Limits
10 .0 mm	0	0	100	100
5 mm	11.45	2	98	89-100
2.36 mm	57.78	12	86	60-100
1.18 mm	71.91	14	72	30-100
600 µm	108.75	22	50	15-100
300 µm	93.8	19	31	5-70
150 µm	93.7	19	12	0-15
75 µm	54.4	11	1	
Pan	6.21	1	-	
Total	498			
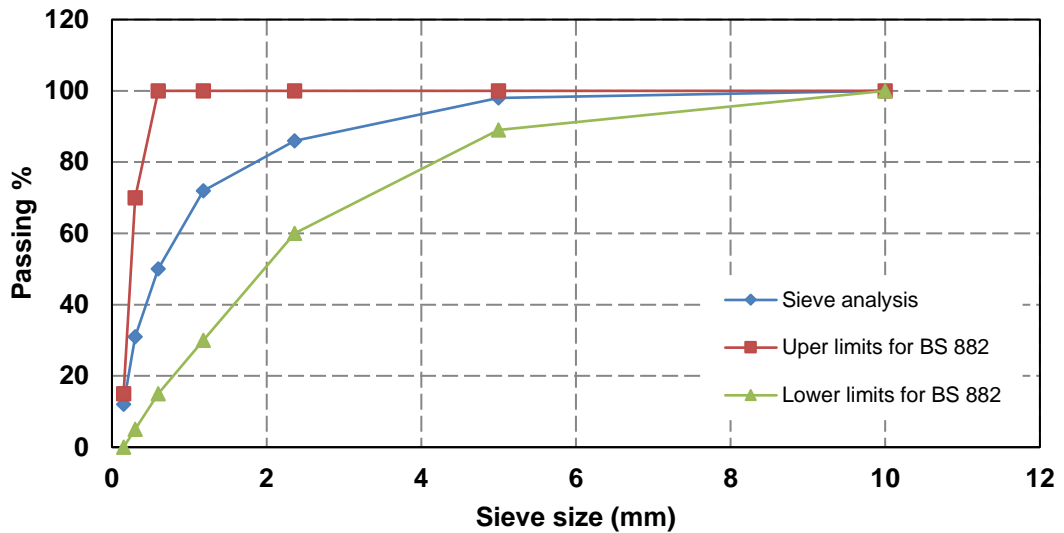
Figure 3-2: Grading of fine aggregate

3.3.3 Coarse Aggregate

A quartzite natural aggregate with a maximum size of 20 mm from North Nottinghamshire (Tarmac Roadstone) was used in this study. Similar to the fine aggregate, the coarse aggregate was oven dried in the University of Leeds laboratory using the same drying parker plant described in Section 3.3.2. After drying, the coarse aggregate was cooled and sorted in preparation for mixing with the other material to produce the concrete matrix. The grading of natural aggregate is shown in

Table 3-4.

Table 3-4: Grading of coarse aggregate

Sieve Size	% Passing	BS 882 Limits
20	100	85 to 100
14	62	0 to 70
10	11	0 to 25

3.3.4 Water

Leeds tap water was used as the mixing water for the concrete (BS EN 1008:, 2002).

3.3.5 Reinforcement

Three bars with a diameter of 16 mm, yield stress of 510 MPa and a modulus of elasticity of 200000 MPa were used as the bottom longitudinal reinforcement. To avoid shear failure, 8 mm diameter shear links were placed outside of the constant moment zone of the beam at 150 mm centre to centre distance. Two 10 mm diameter bars were located in the compression zone to support the links. In order to debond the reinforcement, first the ribs of the tension reinforcement in the constant moment zone (i.e. the central 1500 mm) were ground away. The area was then wrapped with thermal shrinkage wrap (the surface of the shrinkage wrap which would come into contact with the concrete was also treated with degreasing agent) to ensure that the concrete was debonded in the constant moment zone. The degree of debonding was measured and discussed in Section 4.2. The main purpose of debonding the reinforcement in the constant bending moment zone is to study the effect of loss the tension stiffening with due to the cyclic load effect.

3.4 Concrete Mix Design

In this study, concrete was designed with 55 MPa cube compressive strength and 120 mm slump after 28 days, according to the British Standard procedure (BS EN 206:, 2013+A1:2016). The mix proportion of normal concrete is shown in Table 3-5.

Table 3-5: Mix proportions of the normal concrete

Total added water kg/m3	Cement kg/m3	Fine Aggregate kg/m3	Coarse Aggregate kg/m3	Concrete Strength N/mm2
230	485	775	910	55

3.5   Cage and Placement

The longitudinal steel reinforcement and the stirrups were cut and bent to the required shape and dimensions, see Figures 3-3 and 3-4. Appropriate spacers were attached to the bottom and sides of the cage to achieve the required cover (i.e. 20 mm).

Figure 3-3: Steel formwork with reinforcement cage

Figure 3-4: Steel reinforcement beam cage

3.6 Casting and Curing

Two batches of concrete were used to cast each beam (4200 mm in length and 300 mm x 150 mm cross section), 6 cubes (100 x 100 x 100) mm, 8 prisms (200 x 75 x 75) mm and 3 prisms (100 x 100 x 500) mm. A slump test was performed after each mix to ensure the workability of concrete. The maximum workability of 120 ± 10 mm (slump) i.e. S3 class (BS EN 206:, 2013+A1:2016) was achieved in accordance with BS EN 12350-2 (2009)

Each mix was vibrated using a pocket vibrator (see Figure 3-5). The top face of the beams was levelled and finished with a trowel after casting. Beams and all specimens were then covered immediately with a polyethylene sheet to prevent the evaporation of water. After 24 hours, all of the small concrete specimens were de-moulded and placed in the curing room. The beams were de-moulded after four days, before being placed in the curing room (see Figure 3-6). Three days prior to testing a beam at 28 days, beams and all samples were taken out of the curing room to prepare for the test.

Figure 3-5: Using pocket vibrator during casting

Figure 3-6 Beam in the curing room

3.7 Instruments

Three types of data gathering instruments were used to monitor the deformations of each beam.

3.7.1 Electrical Resistance Strain Gauges

Three metallic foil-type electrical resistance strain (ers) gauges were placed at the mid-span of each beam. Each reinforcement was smoothed with sandpaper first then cleaned with acetone before the strain gauge was attached. The strain gauge was first mounted on sticky tape (attached to the back face of the gauge); this was done immediately after the strain gauge was taken from its plastic protection. After a special glue (CN cyanoacrylate adhesive) was put on the front face of the strain gauge, it was positioned on the reinforcement and pressed against the steel using a protective foil. Subsequently, a temperature compensating wire with a resistance of 120 Ohm was soldered to the strain gauge. Finally, a polyurethane coating (M-COAT A) was used as a waterproof liquid. A plastic padding (Chemical Metal+ Hardener) was then used to cover the strain gauges, protecting them against the impact of aggregate during casting, as shown in Figure 3-7.

Figure 3-7: Strain gauges installation

3.7.2 LVDTs

LVDTs (Linear Variable Displacement Transducers) were used to monitor the developed deflection during the 90-day tests of the reinforced concrete beams. Two LVDTs with a resolution of 0.01 mm and displacement capacity of 30-50 mm were placed under each beam in the middle to monitor the mid-span deflection. The results presented in Chapter 4, 5 and 6 are the average reading of the LVDT (no twisting was observed). A dial gauge was placed at the support to ensure there was no differential settlement. It was found that the deflection was minor here (subtracted from the initial readings). Before each test, the LVDTs were recalibrated to ensure accurate readings. The LVDTs were then plugged into the data logger and the readings were recorded every 10 days until the end of the test.

3.7.3 DEMEC Points

A total of 88 DEMEC points were glued to each side of a beam within the constant moment zone. The DEMEC points were fixed using epoxy adhesive at four levels -33, 60, 87 and 114 mm- from the top surface of the beam, as shown in Figure 3-8. The first (33) and the last (114) level were attached at the level of the compression and tension reinforcement, respectively. The DEMEC points were fixed 150 mm apart and allowed the measurement of average surface strain.

Figure 3-8: DEMEC point layout

3.8 Compressive Strength and Tensile Strength Tests.

According to BS EN 12390-3: (2009), the compressive strength of concrete should be carried out using six 100 mm cubes with each beam (i.e. three cubes for each batch). Whereas the indirect tensile strength should be determined from 3 prisms (100 x 100 x 500) mm using BS EN 12390-5: (2009). Both tests were conducted at day 28 and are shown in Figure 3-9.

(a)   (b)
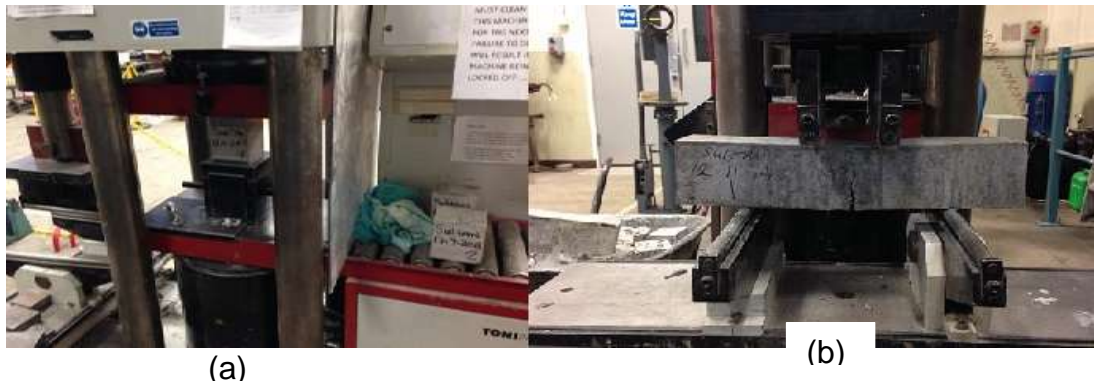
Figure 3-9: Determining the concrete properties a) Compressive strength test b) Tensile strength test

Table 3-6 shows the compressive strength and the indirect tensile strength of each beam.

Table 3-6: Mechanical properties of the concrete mix

Mix	Cube compressive strength (MPa)	STD (MPa)	Flexural tensile strength (MPa)	STD (MPa)	Predicted flexural tensile strength* (MPa)
Mix 1	55	5	4.9	0.81	4.26
Mix 2	55	7	4.73	0.6	4.26
Mix 3	55	4	4.92	0.68	4.26
Mix 4	56	5	4.47	0.55	4.3
Mix 5	56	6	4.9	0.49	4.3
Mix 6	54	5	4.48	0.45	4.22
Mix7	53	2	4.74	0.85	4.18

* ACI 318 suggested equation was used to predict flexural tensile strength ($f_{t,\mathrm{fl}} = 0.623\sqrt{f_c'}$)

Table 3-6 shows a good consistency for both compressive strength and the flexural tensile strength. Moreover the experimental flexural tensile strength was within a good agreement with that calculated using the ACI 318 suggested equation (within 20 %).

Based on the Eurocode 2 (2004), the direct tensile strength could be predicted by multiplying the splitting tensile strength by 0.9. Similarly, 0.744 was suggested by Raphael (1984) to be the reduction factor to predict the direct tensile strength from the modulus of rupture, as both splitting tensile strength and flexural tensile strength are giving values higher than the direct tensile strength. In this study, a reduced modulus of rupture was used as a tensile strength for the calculation of the long-term deflection in Chapter 5.

3.9 Modulus of Elasticity

In this work, the modulus of elasticity of the concrete was obtained from the creep test, where all the samples were applied to 20% of the compressive strength of the concrete. The results of the modulus of elasticity are presented in Table 3-7 with those predicted from the Eurocode 2 (2004), where the Eurocode 2 (2004) suggested equation to predict the modulus of elasticity of the concrete from the compressive strength. It can be seen that the average modulus of elasticity of the concrete matched well with those predicted by the Eurocode 2 (2004).

Table 3-7: Modulus of elasticity of concrete from the creep test

Beam number	Modulus of elasticity (GPa)	
	Test	Eurocode 2*
Beam 1	33.784	34.94
Beam 2	32.154	34.94
Beam 3	34.000	34.94
Beam 4	33.223	35.132
Beam 5	34.000	35.132
Beam 6	35.335	34.7501
Beam 7	36.000	34.556

*Eurocode 2 suggested equation was used to predict modulus of elasticity from the compressive strength ($E_{cm} = 2200(fcm/10)^{0.3}$

3.10 Tensile Strength of the Reinforcement

The tensile mechanical properties of the steel reinforcement used in this work were also determined in the School of Civil Engineering, University of Leeds.

. Figure 3-10 shows the stress-strain relationship of the steel reinforcement.
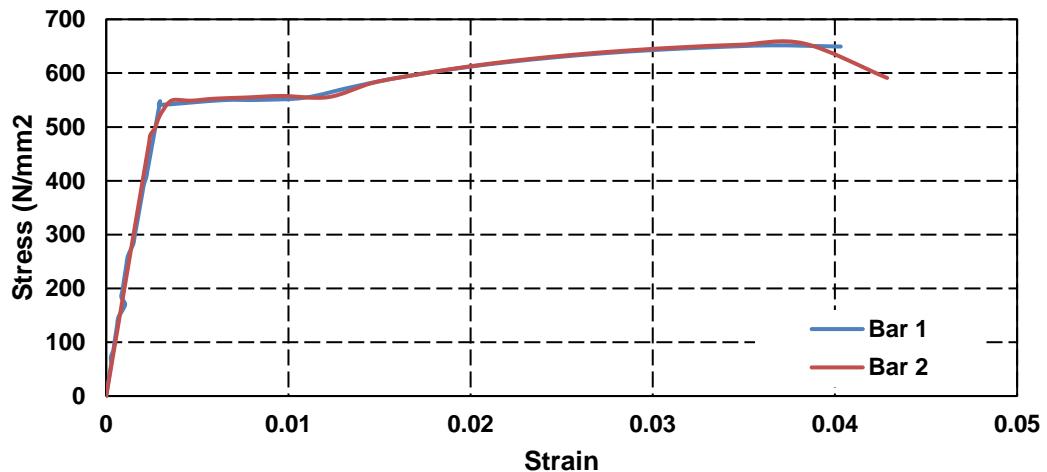
Figure 3-10 Stress-stain of steel

3.11 Long-Term Beam Deflection Tests Procedure.

The beam tests monitored the long-term performance of reinforced concrete beams subjected to repeated and sustained loading. These tests lasted for 90 days. Three days prior to testing a beam at 28 days, the beam was taken out of the curing room, placed in the test rig and prepared for the test. Four sets of DEMECs were placed on both sides of the beams in order to monitor the curvature and average concrete surface strain with time. Two LVDTs were placed under the middle of each beam to monitor the mid-span deflection along the beam. A four point bending test was adopted for the beams. The constant moment zone was 1500 mm and the span of the beams was 4000 mm. Both sides of the beams were painted with white paint to help monitor crack development during the test.

Loading for the first beam set (REP Group) was applied using the hydraulic system, while the system for the second group (SUS Group) was manually applied using a jack and load cell located at the top in the middle of the beam. Beams SUS-B-19, REP-B-19, SUS-SYM-19, SUS-UB-19 and REP-UB-19 were initially preloaded to 19 kN (the magnitude of the sustained load) so that a stabilised crack pattern was produced. It is assumed that the average crack spacing of a fully cracked reinforced concrete beam is 2/3 of the theoretical crack spacing, $2 S_0$ (Beeby and Scott, 2004b). Where $S_0 = 3C$, the cover depth of the tested beams was 28 mm (or 36 mm from the centroid of the section of reinforcement to the concrete surface), hence the average crack spacing should be 112 mm or 144 mm. So, the typical crack numbers in the constant moment zone should range from 11-14.

The tensile steel stresses were checked at this load and were found to be 198 MPa (it is estimated that a steel stress of 200 MPa would produce stabilised cracking for this type of beam). For the beams subjected to a repeating load, the load was then cycled between an upper and lower limit of the constant sustained load of 19 kN. This cyclic amplitude was selected to be 2.5 kN, which is 13% of the sustained load (Vollum, 2009, Higgins et al., 2013) . A cyclic frequency of 0.2 Hz was chosen; this is considerably lower than the beam natural frequency, which is about 4 Hz and close to the rotor frequency of offshore wind turbines i.e. 0.15-0.2 Hz (Bhattacharya, 2014). For the cyclic/repeating tests, when a reading was recorded, the frequency was gradually reduced to zero, so readings were always taken at 19 kN when the load cycling was stopped. The deflection on application of the sustained load (19kN) was recorded and represented the elastic deflection at time t_0. The other beam (i.e. SUS-B-5) was subjected to sustained load of 5 kN, which produced 5 cracks. The last beam (i.e. SUS-B-3) was subjected to a load less than the load required to produce the first crack (i.e. 3.5 kN).

3.12 Concrete Prism Shrinkage and Creep Tests

3.12.1   Concrete Prism Shrinkage Test.

The test specimens had dimensions of 200 x 75 x 75 mm. Two DEMEC points were attached at 150 mm on two opposite sides of the prism, as shown in Figure 3-10.

The shrinkage readings taken from the prism are used directly in the theoretical model and also in the numerical model as a shrinkage and creep coefficient input; see Section 5.5.

Figure 3-11: Shrinkage test

Between 28 to 30 days after casting, all specimens were stored in a controlled room at 21 ± 1C° with a relative humidity of 60 ± 5%. Immediately after being placed in the curing room, the initial readings were taken and the DEMEC was attached on the specimen in the same day, as specimens were sorted in the control room. The shrinkage was taken as an average of the four prisms reading. Figure 3-11 shows the 150 mm strain gauge that was used to measure the creep and shrinkage.

Figure 3-12: 150 mm of DEMECs gauge, calibrated bar and fitting bar

3.12.2   Concrete Prism Creep Test

Four prisms of 200 x 75 x 75 mm were used to calculate the creep strain of the concrete used in this work. An applied stress of 20% of the compressive strength of the concrete at 28 days was used. Each rig was laid horizontally, as shown in Figure 3-13, and the stress was applied manually. As can be seen, each rig can hold two prisms in addition to a steel cylinder. Before applying the stress, initial readings were taken. The second reading was taken after the stress was applied, therefore, providing the elastic strain. As with the beams, the test was carried out for 90 days. The creep strain was calculated by subtracting the elastic strain of the prism and the shrinkage strain of unloaded samples from the total strain of loaded samples.

Figure 3-13: Creep rig test

The purpose of these test was to calculate the creep coefficient and the modulus of elasticity of the concrete; these will be used in Chapter 5 and Chapter 6 to predict the long-term behaviour of the reinforced concrete beams. Tables 3-9 to 3-17 give the measured long-term properties of the mixes (i.e. elastic strain, creep, shrinkage and creep coefficient). In this study the average of the shrinkage and creep coefficient were used in the Chapter 5 and Chapter 6.

Table 3-8: Long-term properities of beam 1

Load Level	Strain (με)	Age testing (days)		
		30	60	90
20 %	Elastic	-296		
	Total	610	625	-786
	Shrinkage	-285	-354	-385
	Creep	-325	-371	-401
	Creep Coefficient	1.1	1.25	1.35

Table 3-9: Long-term properties of beam 2

Load Level	Strain (με)	Age testing (days)		
		30	60	90
20 %	Elastic	-311		
	Total	-620	-735	-797
	Shrinkage	-275	-328	-374
	Creep	-345	-405	-423
	Creep Coefficient	1.11	1.3	1.36

Table 3-10: Long-term properties of beam 3

Load Level	Strain (με)	Age testing (days)		
		30	60	90
20 %	Elastic	-295		
	Total	-600	-750	-877
	Shrinkage	-276	-360	-412
	Creep	-324	-390	-465
	Creep Coefficient	1.1	1.32	1.57

Table 3-11: Long-term properties of beam 4

Load Level	Strain (με)	Age testing (days)		
		30	60	90
20 %	Elastic	-301		
	Total	-603	-77	-907
	Shrinkage	-281	-377	-427
	Creep	-322	-400	-480
	Creep Coefficient	1.07	1.33	1.59

Table 3-12: Long-term properties of beam 5

Load Level	Strain (με)	Age testing (days)		
		30	60	90
20 %	Elastic	-295		
	Total	-530	-740	-781
	Shrinkage	-250	-371	-392
	Creep	-280	-370	-389
	Creep Coefficient	0.95	1.25	1.32

Table 3-13: Long-term properties of beam 6

Load Level	Strain (με)	Age testing (days)		
		30	60	90
20 %	Elastic	-283		
	Total	-553	-758	-806
	Shrinkage	-248	-385	-448
	Creep	-305	-373	-358
	Creep Coefficient	1.08	1.32	1.55

Table 3-14: Long-term properties of beam 7

Load Level	Strain (με)	Age testing (days)		
		30	60	90
20 %	Elastic	-278		
	Total	-561	-724	-811
	Shrinkage	-281	-371	-416
	Creep	-280	-353	-395
	Creep Coefficient	1.01	1.27	1.42

From Tables 3-9 to 3-15 it can be seen that both the shrinkage and the creep coefficient were reasonably consistent. The average shrinkage of the concrete used in this study after 90 days was 408 με with a standard deviation of 26 με. However, the difference between the maximum and minimum shrinkage was 74 με. This 74 με difference results from the ambience of the control room where the relative humidity and the temperature was not constant over the whole test duration.

The average creep coefficient of the prisms subjected to a stress equal to 20% of the compressive strength of the concrete was 1.46 with a standard deviation of 0.11. (8% difference). The difference between the maximum and minimum creep coefficient was 0.27. In addition to the control room conditions, the stress was applied manually and from experimental practices, only a 10% accuracy can be achieved with this method.

3.13 Pull-Out Test

In order to assess the efficiency of the artificial debonding method adopted in the investigation, a series of pull-out tests were performed. A total of 8 concrete cubes of (200 x 200 x 200) mm were cast, each with a single protruding rebar. The concrete cubes had the same material properties as that of the beams. The variable in these pull-out tests was the bonding of the reinforcement; for four of the samples the steel was composite and bonded with the steel; the other 4 samples contained bars which were artificially debonded. The embedment length-to-bar diameter (*L/d*) ratio was 5. All the specimens were demoulded after 1 day and cured in the fog room until testing (Figure 3-14). The cube dimensions and the embedded length were similar to that adopted by (Garcia-Taengua et al., 2016, El-Zaroug, 2008)
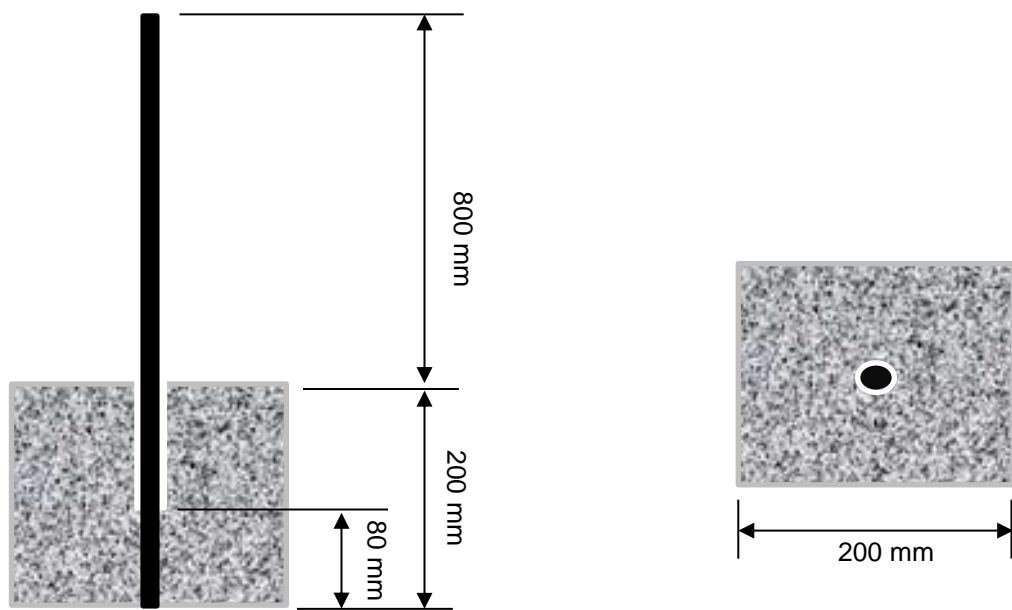
Figure 3-14: Test specimen details

Figure 3-15: Preparation of pull-out specimen

Figure 3-15 illustrates the preparation of the specimen. A loading rate of 2 kN/min was utilised. Three LVDTs were attached to the specimen (as shown in Figure 3-16). The first two samples were tested at an age of 14 days to study the compressive strength development with time effects for the bond strength loss for both bonded and debonded samples.

The rest of the samples were tested at 28 days. None of the reinforcement bars reached their yield stress during the tests.
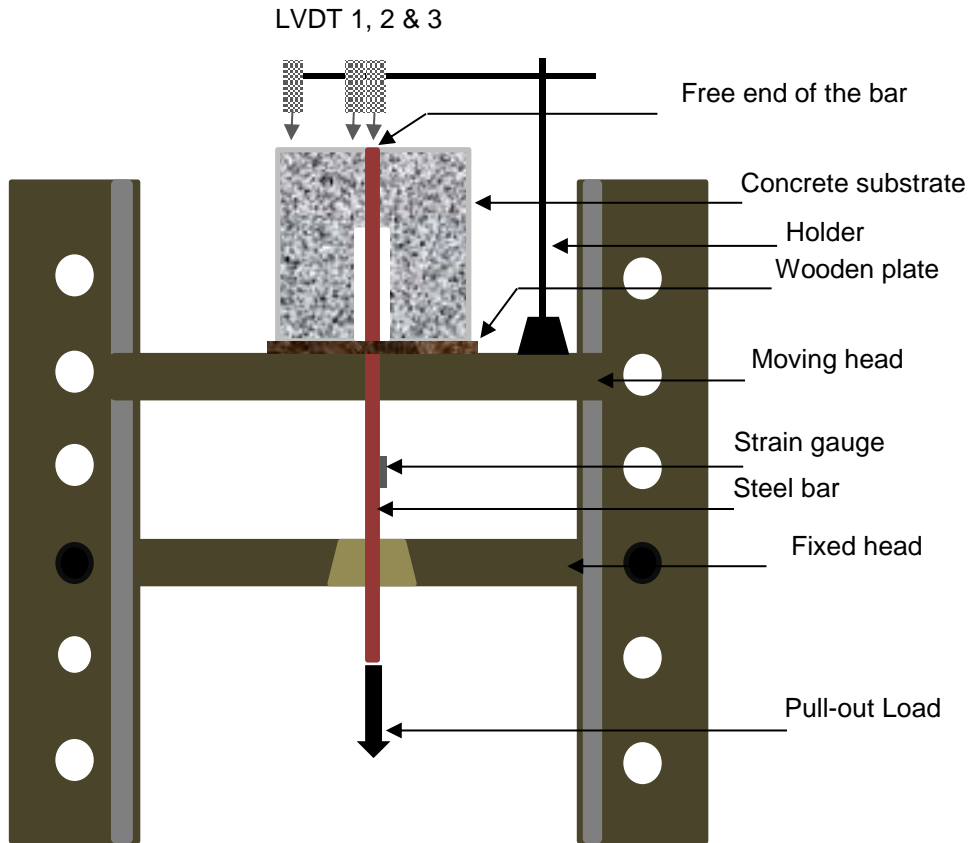
Figure 3-16: Test setup for pull-out test

The results of the pull-out tests will be presented in Chapter 4, where they will be discussed and used to explain the adequacy of the artificial debonding method and its effect on the long-term beam result

Chapter 4 Experimental Results and Discussions

4.1 Introduction

This chapter comprises the results of the flexural behaviour of reinforced concrete beams under long-term loading. The main parameters considered in this study were loading type (i.e. static sustained and cyclic/repeating load), reinforcement conditions (i.e. bonded, unbonded and symmetrical reinforcement) and the magnitude of the sustained loading (i.e. 19 kN, 5 kN and 3 kN). Both mid-span developed deflection and concrete surface strain in the constant moment zone were recorded for a maximum period of 3 months. The load-slip results for the bonded and unbonded samples, results related to the long-term developed deflection and the surface stain are also presented in this chapter.

4.2 Bond Strength, Load-Slip Behaviour and Slip at Maximum Load.

In order to gain a better understanding of the behaviour of cracked reinforced concrete beams and to assess the method of debonding the reinforcement in the constant moment zone, pull-out tests for bonded and unbonded samples were conducted at the University of Leeds.

The average bond strength τ over the embedded length was calculated using the maximum load sustained during the test, assuming a uniform stress distribution along the embedded length of the reinforcement (CEB-FIP, 1990):

$$\tau = \frac{P}{\pi d_b l_b} \hspace{5cm} \text{(4-1)}$$

Where:

P   is the ultimate load (kN)

l_b is the embedded length (mm)

d_b is the diameter of the reinforcement (mm)

This equation has been widely used to determine the bond strength, although it is based on the uniform stress distribution along the embedded length of the reinforcement, which is not true. Whereas, stress distribution varies greatly as the slip develops (Abrishami and Mitchell, 1996, Hamad, 1979).

However, the experimentally obtained bond strength values are presented in Table 4-1 and

Table 4-2 where it can be seen that the artificial method of debonding did not display 100 % loss of bond as expected since there is still adhesive bond between reinforcement and the surrounding concrete. At 14 days, the loss of bond was approximately 94%. At 28 days, it was approximately 93% which agreed with Weathersby (2003) outcome, i.e bond-slip of smooth reinforcement is not significantly affected by the compressive strength of the concrete.

Previous study showed that, up to 50 % of the bond is lost in the case of plain reinforcement (Edwards and Yannopoulos, 1979). Obviously, in this study (i.e. unbonded specimens) the bond lost is higher than that in plain reinforcement as the reinforcement ribs were artificially ground and then treated with thermal shrinkage wrap (the surface of the shrinkage wrap was also treated with a degreasing agent). In addition, the concrete cover adopted in this research was nearly three times that of Edwards and Yannopoulos (1979) specimens.

Unsurprisingly, the unbonded reinforcement was pulled continuously out of the concrete and the slip was very high when compared to that of the bonded specimens (nearly 10 times) which is similar to the findings of Mo and Chan (1996). This is because the ribs of the reinforcement were artificially ground

and once the bond (adhesion) was lost, the reinforcement quickly pulled out of the concrete.

Table 4-1: Bond strength and slip at 14 days

Sample No.	Reinforcement condition	Ultimate load (kN)	Bond strength (N/mm^2)	Slip at ultimate load (mm)	Bond strength loss (%)
1	Bonded	96	22.5	7.3	-
2	Unbonded	6	1.4	14.9	94

Table 4-2: Bond strength and slip at 28 days

Sample No.	Reinforcement condition	Ultimate load (kN)	Average Bond strength (N/mm^2)	Slip at ultimate load (mm)	Bond strength loss (%)
1	Bonded	-		-	
2	Bonded	117	25.8	1.3	
3	Bonded	104		1.2	
4	Unbonded	9.8		13.2	
5	Unbonded	7	1.9	10.5	93
6	Unbonded	7.5		12	

The load-slip behaviour of the bonded and unbonded specimens are shown in Figure 4-1. It can be seen that the ultimate load in the case of bonded

reinforcement was higher than that of the unbonded reinforcement. The average ultimate load was 110.5 kN for the bonded specimens whereas it was only 8.1 kN for the unbonded specimens. The slip at ultimate load in the case of unbonded samples was about ten times more than that of the bonded specimens. Therefore, it can be assumed that debonding the reinforcement increases the failure slip and decreases the ductility (as the unbonded samples has less ultimate load than the bonded samples).

Figure 4-2 indicates that although the same technique was used for the artificial debonding of the reinforcement, the degree of debonding was not quite the same in all samples. This agreed with a previous work carried out by (Feldman and Bartlett, 2007), where they found bond stress magnitude is not uniform along the embedded length of the plain reinforcement.

However, the artificial method of debonding does appear to have worked reasonably well where the unbonded beams subjected to both loading cases are compared (Sections 4.3.2.1 and 4.4.2).
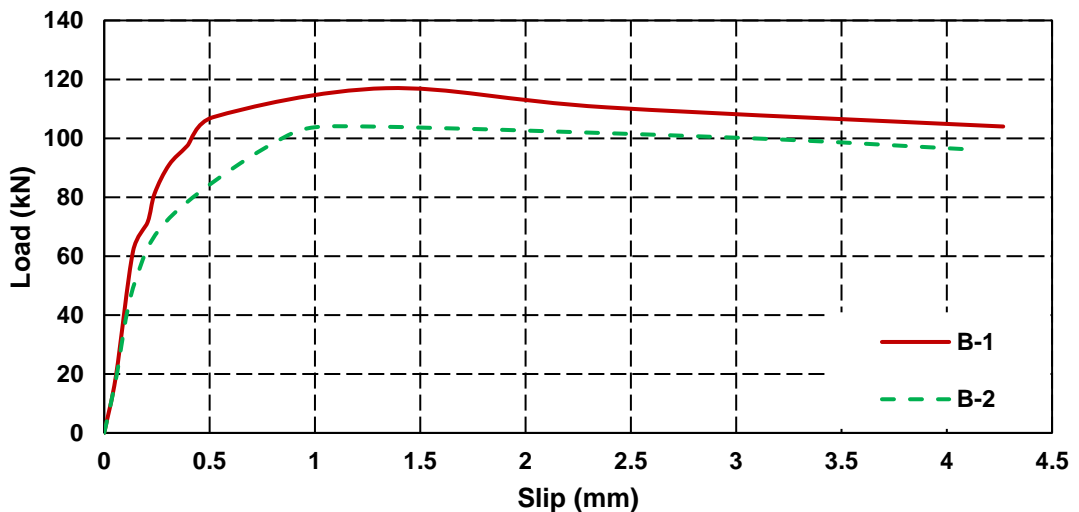
Figure 4-1: Load-slip behaviour of reinforced concrete bonded samples
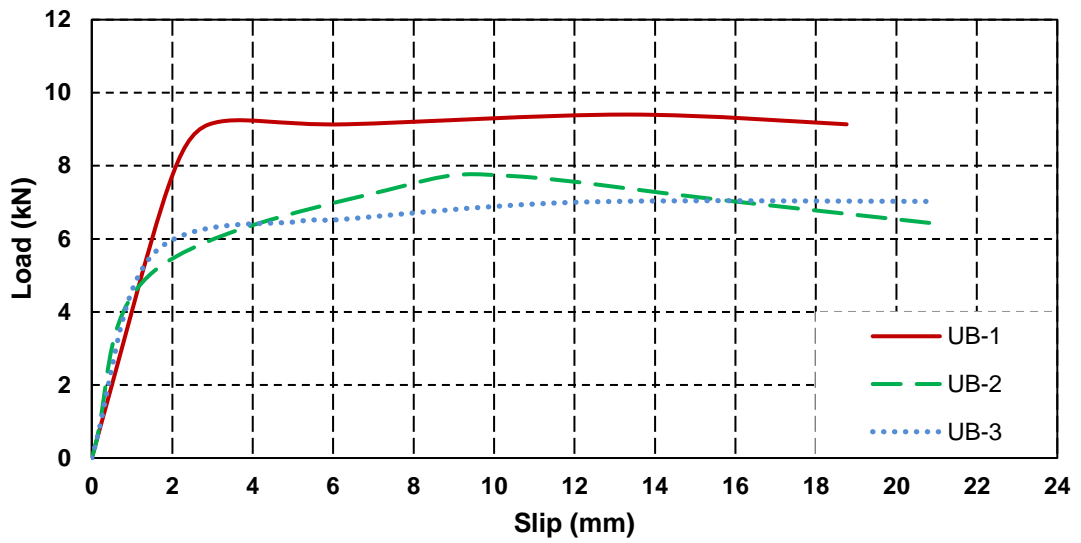
Figure 4-2: Load-slip behaviour of reinforced concrete unbonded samples

Two types of failure modes were recognised during the test for the bonded samples; the first one was a pull out failure i.e shear failure between the reinforcement and the concrete interface. While the second one was by crushing of the concrete i.e. the concrete around the reinforcement was subjected to radial stresses which lead to splitting failure (Garcia-Taengua et al., 2016). Whereas in unbonded samples, only bond failure was recognised and that because there is 8 % bond left, and the bond transfer by adhesion between the reinforcement and the surrounding concrete (Feldman and Bartlett, 2007) (see Figure 4-3).

(a)   (b)

Figure 4-3: Failure mode through pull-out test a) Bonded samples, b) Unbonded samples

4.3 Mid-Span Deflection

4.3.1 Effect of Load Type

The Eurocode 2 (2004) suggests using a single factor for loss of tension stiffening to represent both a sustained and repeating long-term load (i.e. $\beta=0.5$). In order to assess Eurocode 2 (2004) suggested equation and to gain knowledge of the reinforced concrete beams subjected to relatively low frequency (i.e. 0.2 H_z). Two reinforced concrete beams subjected to static sustained and cyclic/repeating loads were tested to achieve these objectives. The reinforcement in the tension zone was fully bonded. The first beam was subjected to a 19 kN sustained load whereas the second beam was subjected to a 19 kN cyclic/repeating load. For the beam subjected to the repeating load, the load was cycled between an upper and lower limit about the constant sustained load of 19 kN. This cyclic amplitude was selected to be 2.5 kN which is between 10% to 15% of the sustained load (Vollum, 2009, Higgins et al., 2013). The elastic deflection for SUS-B-19 and REP-B-19 was 27 mm and 26 mm, respectively. The developed deflection with time will be presented in the results.

Figure 4-4 compares the developed mid-span deflection of the two beams. In this figure it is clear that the beam under repeated loading developed more deflection than the beam under sustained loading, which agreed with Higgins et al. (2013) i.e. beams under repeated loading held more deflection than beams under sustained loads. Where the bond between the concrete and the reinforcement is damaged due to the effect of repeated loading. It can also be seen that, the increased deflection in beam REP-B-19 occurs during the first 20 days while the increase in the deflection of Higgins et al. (2013) beams occurs in the first 10 days. The reason of the extra deflection stabilised after 20 days in this study is due to the shrinkage strain where the shrinkage here is higher than in Higgins et al. (2013) work (1.5 higher). Both Vollum (2002) and Gilbert (1999) believed that shrinkage induced tension between cracks, which leads further cracking and consequent loss of tension stiffening. However, as both beams were cast with the same concrete and the elastic deflection was similar and deflection was recorded at same load level (19 kN). This extra deflection after 90 days shown in Figure 4-4 should be due to the previous loading history (i.e. repeated loading) not the current loading condition. Hence the extra deflection after 90 days in the case of repeated loading (i.e 5.6 mm) is due to the loss of tension stiffening after the case of stabilized crack pattern when the bond between the reinforcement damaged due to cyclic effect (Zanuy et al., 2010). Which indicates that there is still some amount of tension stiffening presents even after stabilized crack pattern has been achieved.
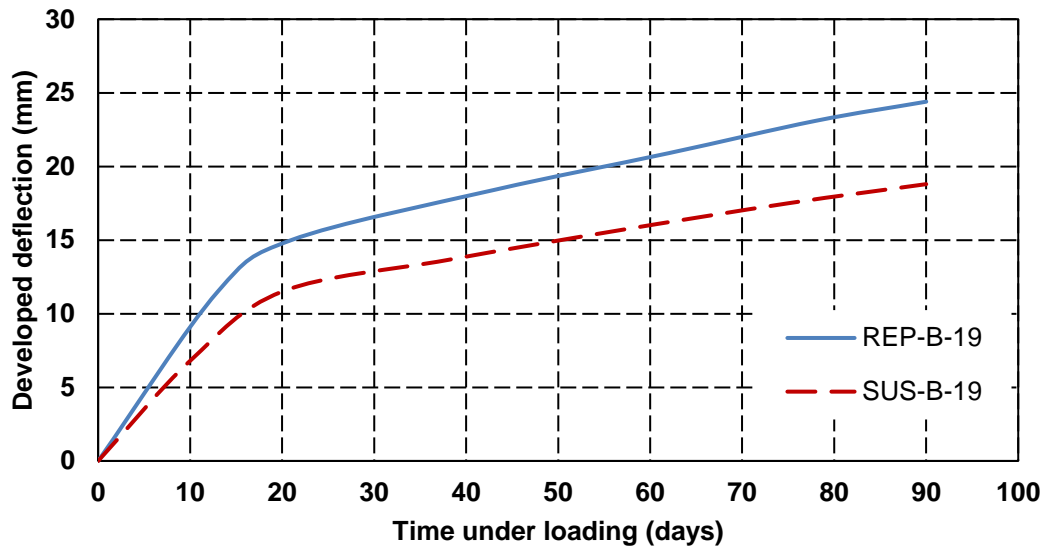
Figure 4-4: Developed mid-span deflection with time (REP-B-19 and SUS-B-19)

4.3.2 Effects of Reinforcement Bond and Compression Reinforcement

In this section, the effect of reinforcement condition (bonded, unbonded and symmetrical) on the tension stiffening and shrinkage deflection of reinforced concrete beams was investigated experimentally. Three beams were tested. The first two beams were unbonded beams; one was subjected to static sustained loading while the second beam was subjected to repeated loading. The third beam had symmetrical reinforcement and was subjected to a sustained load. The mean load for all three beams was 19 kN. The results are compared to that of the fully bonded beams.

4.3.2.1 Unbonded Reinforcement.

Section 4.3.1 showed that, under long-term loading, beam under repeated loading developed more deflection than beams under sustained loading. The extra deflection in the case of repeated loading resulted from the damage of the concrete surrounding the reinforcement due to the effect of repeated loading as was also witnessed by Higgins et al. (2013). In order to investigate

the influence of low frequency (0.2Hz) on debonding the reinforcement from the concrete, this section compares the results of the fully bonded beams with the artificially debonded beams. Figure 4-5 compares the long-term mid-span developed deflection of the unbonded and bonded reinforced beams under sustained loading. From Figure 4-5 it can be seen that during the early ages of sustained loading, the debonded beams developed more deflection than the bonded beam. After 90 days, the debonded beam had approximately 36 % extra deflection than the bonded beam. This extra deflection here is due to the effect of debonding the reinforcement.
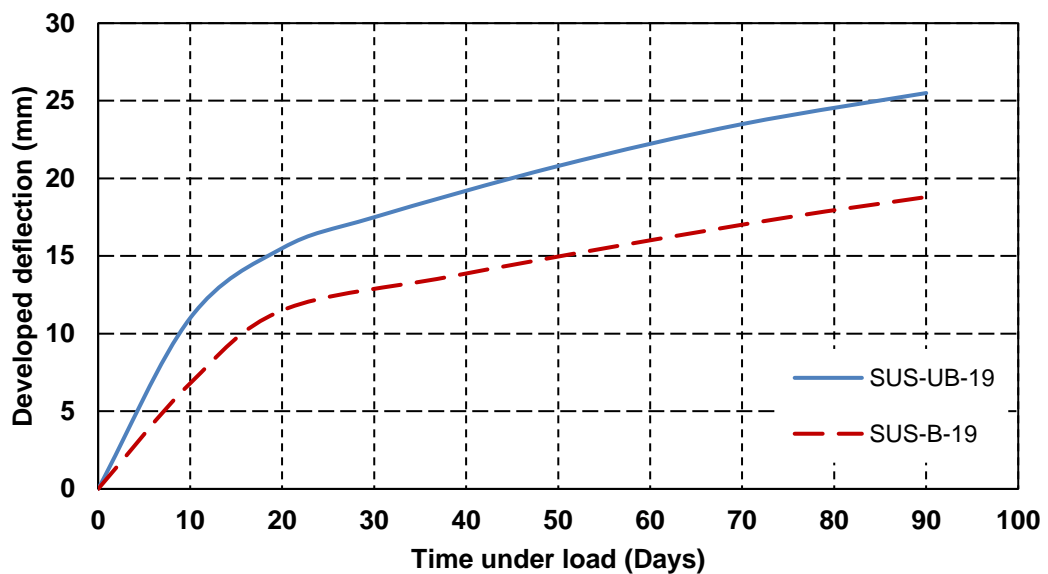
Figure 4-5: Developed mid-span deflection with time (SUS-UB-19 and SUS-B-19)

Figure 4-6 compares the development in the mid-span deflection of the debonded beams under two different load types (i.e. sustained and repeated loads). It can be seen that the deflection of both beams was similar during the first 20 days, however, at the end of the test, the beam subjected to the repeating load exhibited more deflection (+7%) than the beam subjected to the sustained load. The comparison also further illustrates the success of the artificial debonding method as previously Higgins et al. (2013) showed that the difference in deflection between the bonded beams subjected to the two

loading cases mainly occurred in the first 10 days (as the repeating load enhanced internal cracking, destroyed tension stiffening and hence increased the deflection). Thus the extra deflection after 90 days due to repeated loading is thought to be due to the effect of cyclic creep, since the cyclic creep increases static creep (Neville and Hirst, 1978).

In Figure 4-7 the behaviour of the debonded beam under sustained loading was compared with the fully bonded beam under a repeating load. After 20 days, there was only a minimal difference in the deflection (debonded beam has slightly greater deflection than bonded beam) which again shows the success of the artificial debonding method. After 20 days of loading, the deflection rate in both beams was almost identical, suggesting that the bond between concrete and reinforcement in both beams had been removed.

This implication is important as it indicates that the bond between concrete and steel in reinforced concrete beams subjected to a repeating load can be significantly damaged (see Figure 4-7) due to the loading even though the frequency is relatively low (i.e. 0.2 H_z).
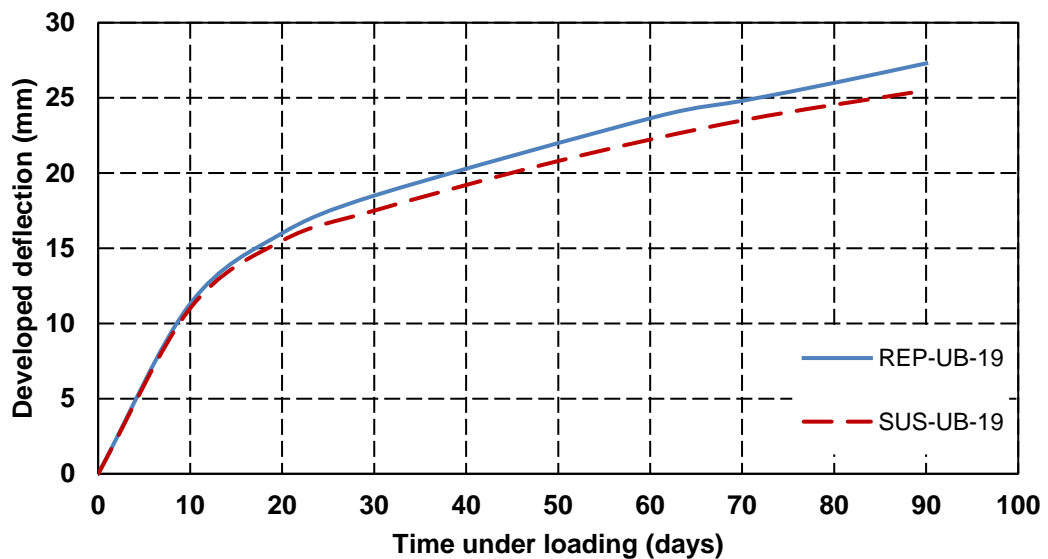

Figure 4-6 Developed mid-span deflection with time (REP-UB-19 and SUS-UB-19
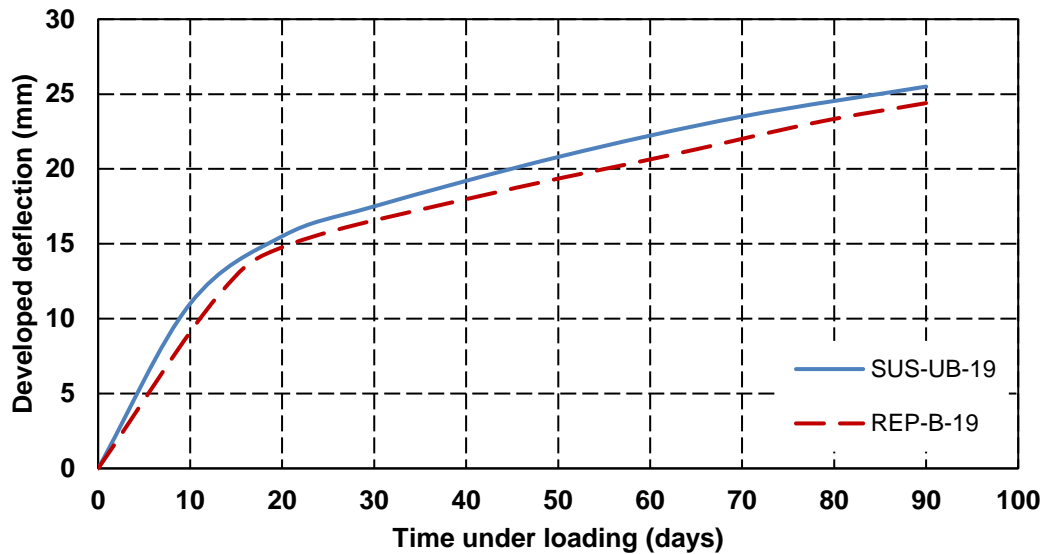
Figure 4-7: Developed mid-span deflection with time (SUS-UB-19 and REP B-19)

4.3.2.2 Symmetrical Reinforcement

For the symmetrically reinforced concrete beam, the long-term developed deflection was compared with that of the normally reinforced concrete beam (see Figure 4.8). Both beams were subjected to the same amount of sustained load (i.e. 19 kN) to study the effect of additional reinforcement in the compression zone on the long-term deflection. Clearly, it can be seen that the beam with symmetrical reinforcement has less long term deflection than the first beam (i.e. SUS-B-19); this agrees with Paulson et al. (1991).

Both beams had the same number of cracks (15) in the constant moment zone. This suggests that, adding reinforcement in the compression zone has slightly affected the tension zone (Washa and Fluck, 1952) by increasing the stiffness and reducing the creep and shrinkage deflections.

In Figure 4-8 it can be seen that, 10 days after loading both beams had the same amount of developed deflection which indicates both beams lost the same amount of tension stiffening. After that, the developed deflection in the symmetrical reinforced beam is less than that in the normally reinforced concrete beam by 30 %. The 30 % lower deflection can be explained by the

additional reinforcement in the compression zone producing extra restraint to the shrinkage and creep of concrete.

Mu et al. (2008) showed numerically that 50 % of the total long-term curvature is likely to be due to creep while the other 50 % is due to shrinkage – this is however dependent on this section geometry and ratio of steel reinforcement. Based on this ratio, the shrinkage deflection for the symmetrically reinforced concrete beam is 7.6 mm whereas it is 9.4 mm for the normal beam (i.e. SUS-B-19).
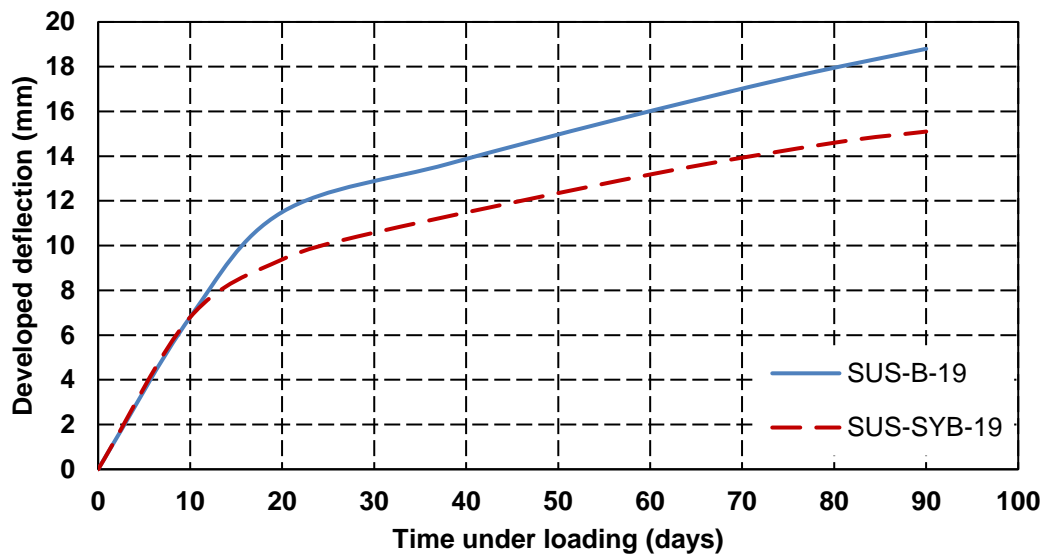
Figure 4-8: Developed mid-span deflection with time (SUS-B-19 and SUS-SYB-19)

4.3.3 Effect of Loading Level

Further tests were performed in order to understand the effect of the amount of applied load in relation to the load required to produce the cracking moment and stabilized crack pattern. Figure 4-9 illustrates the developed long-term deflection of three reinforced concrete beams tested under different levels of sustained loading (i.e 19 kN, 5 kN and 3 kN). As expected, it can be seen that the beam sustained under a higher amount of load has more developed

deflection. According to Mu et al. (2008), for the first beam considered here (i.e. SUS-B-19), the shrinkage curvature should be 9.4 mm and it would be 5.5 mm and 5 mm for SUS-B-5 and SUS-B-3, respectively. From these tests, it can be seen that identical beams having a higher number of cracks develop a greater deflection due to shrinkage; this will be further discussed in Chapter 5.

For the beam with a stabilized crack pattern (i.e. SUS-B-19), no more cracks were developed after loading. Whereas in the SUS-B-5 and SUS-B-3 cases more cracks developed during the 90 days of testing. This suggested that:

1. In the case of stabilized crack pattern, the concrete between cracks acts elastically.

2. As beam SUS-B-3 was subjected to a load which was actually less than that required to cause cracking (3.5 kN) and yet cracks were observed the day after loading, it appears that, the tensile strength of the concrete was exceeded due to creep and shrinkage curvature. As such, these long-term effects (i.e. creep and shrinkage) appear to be influential only one day after loading: this contradicts the guidance in Eurocode 2 (2004) which suggest long-term means 28 days.
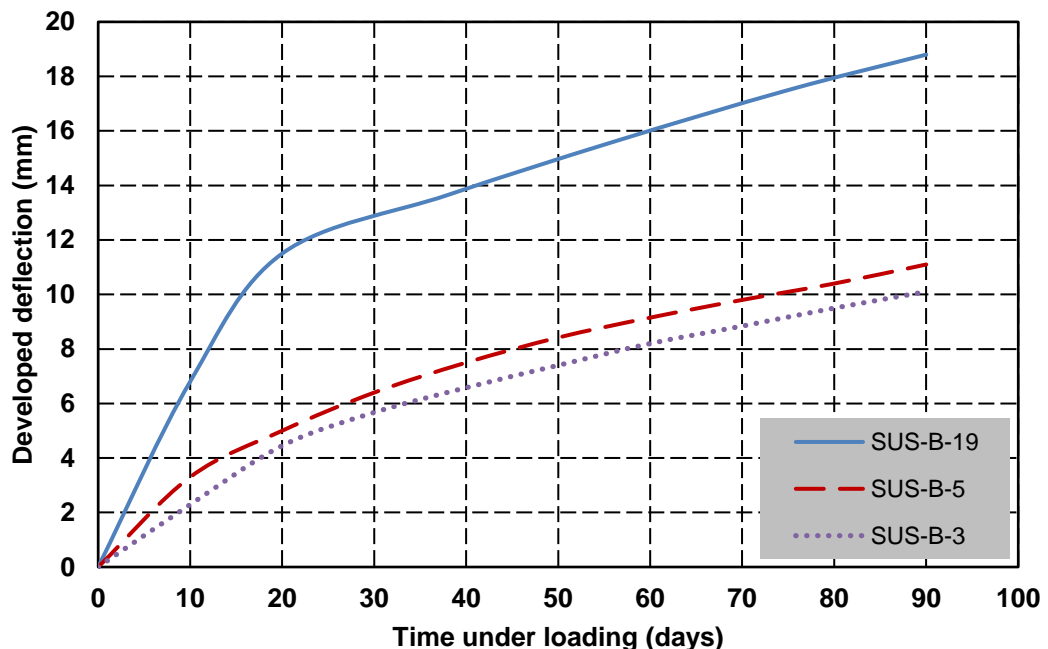

Figure 4-9: Developed mid-span deflection with time (SUS-B-19, SUS-B-5 and SUS-B-3)

4.4 Surface Strain Development

The surface strain development with respect to time in the compression and tension zone was monitored for a period of 90 days. In all cases, it can be seen that, the surface strain development is higher in the compression zone than in the tension zone. This is attributed to the effects of creep and shrinkage and how they act on the two stress zones, i.e. creep and shrinkage are in the same direction in the compression zone – they are effectively a contraction; whilst shrinkage (a contraction) is in the opposite direction to creep (an extension) in the tension zone. In addition, there is more reinforcement in the tension zone than in compression zone and so more restraint to movement. Finally the concrete stress in the compression zone is higher than that in the tension zone.

4.4.1 Effect of Load Types.

Figure 4-10 compares the surface strain development for the fully bonded beams, under repeated and sustained loading. It can be seen that in the compression zone there is an additional deformation developed with time in the repeated load case to that seen in the sustained loading case whereas in the tension zone the more difference occurs in the first 25 days.

The fact that this has happened further confirms the effect of cyclic creep (Neville and Hirst, 1978). Where cyclic creep is present in the compression zone and in the tension zone. However cyclic creep is more dominant in the compression zone than the tension zone (Forth, 2015). Where cyclic creep depends on the applied stresses and the concrete in the compression zone holds more stress than that in tension zone (the extra strain development between the repeated and sustained beam in the compression zone and tension zone after 25 days was 28 $\mu\varepsilon$ and 19 $\mu\varepsilon$, respectively)

Both beams had the same number of cracks after loading (15 cracks). After 90 days no more cracks were developed in the beam subjected to sustained loading and three additional cracks (internal cracks developed into surface) in the beam subjected to repeated loading (all developed in the first 15 days).

These extra cracks occurred because of the effect of repeated loading as the repeated loading damaged the concrete around the reinforcement which is similar to the work carried out by Zanuy, Albajar and de la Fuente (2010).
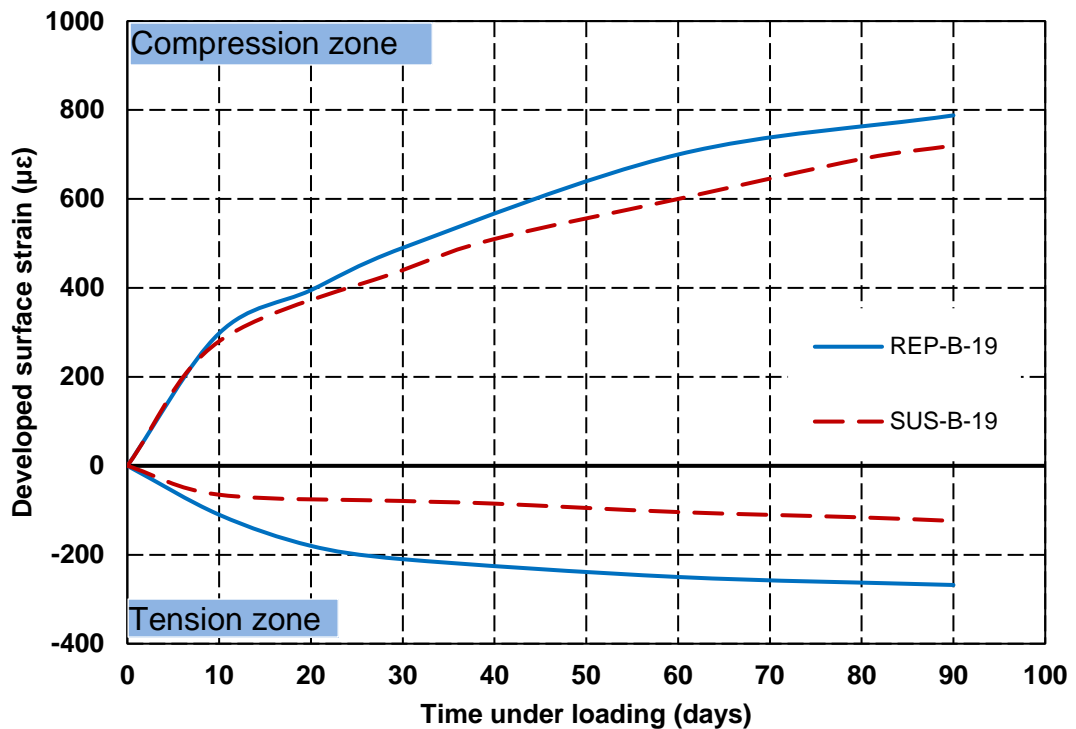
Figure 4-10: Surface strain development in the compression and tension zone with time (REP-B-19 and SUS-B-19)

4.4.2 Effects of Reinforcement Bond

Figure 4-11 illustrates the surface strain development with time for beams where the reinforcement has been artificially debonded. From the Figure it can be seen that, both beams had almost the same development of strain in the compression zone, although there is still more strain in the beam subjected to the repeating load. In the tension zone, the surface strain in beam subjected to repeated loading is more than that in the beam subjected to the sustained load. No more cracks were produced in either beam after loading (eight cracks were observed); this additional deformation of the repeated load beam is due

to the increasing crack width. Unsurprisingly, beams with debonded reinforcement had less number of cracks in the constant moment zone than the beams with deformed reinforcement. Previous research had also shown that beams with smooth reinforcement have less surface cracks than beams with deformed reinforcement (Mohammed et al., 2001).

Although, the pull out tests and the long-term developed deflection of unbonded samples show the success of debonding process. Eight cracks in the debonded beams could be relatively high. This could be explained by two main reasons:

1. The tension reinforcement was unbonded only in the constant moment zone and both beams have anchorage length.
2. The unbonded beams were tested under flexural loading i.e. concrete around the reinforcement in the tension zone under tension whereas in pull out samples, concrete surrounding reinforcement was under compression (Feldman and Bartlett, 2008)
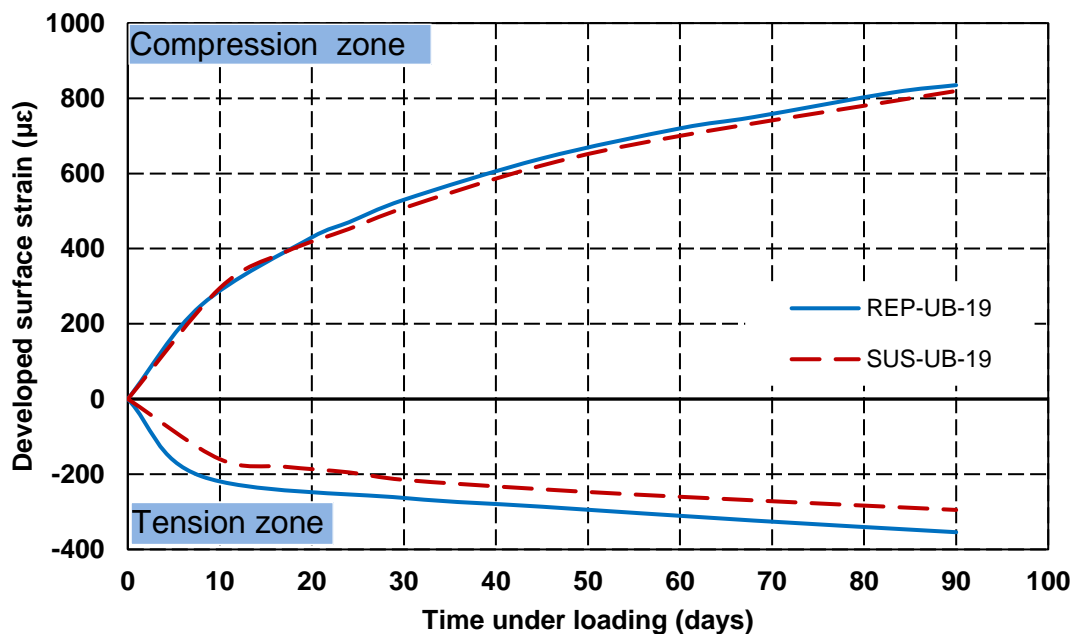

Figure 4-11: Surface strain development in the compression and tension zone with time (REP-UB-19 and SUS-UB-19)

Figure 4-12 shows the effect of debonding the reinforcement on the development of surface strain for the beams under sustained loading only. Clearly the debonded beam had more strain development in both the compression and tension zones. In the compression zone, the higher surface strain development is because the debonded beams had higher developed deflection due to the artificial loss of the tension stiffening. Whereas the higher surface strain development in the tension zone indicates that the crack width is higher in the debonded beams that that of the bonded beam although the debonded beam had a lower number of cracks (average crack width after 90 days was 0.35 mm and 0.12 mm for unbonded and bonded beams, respectively.

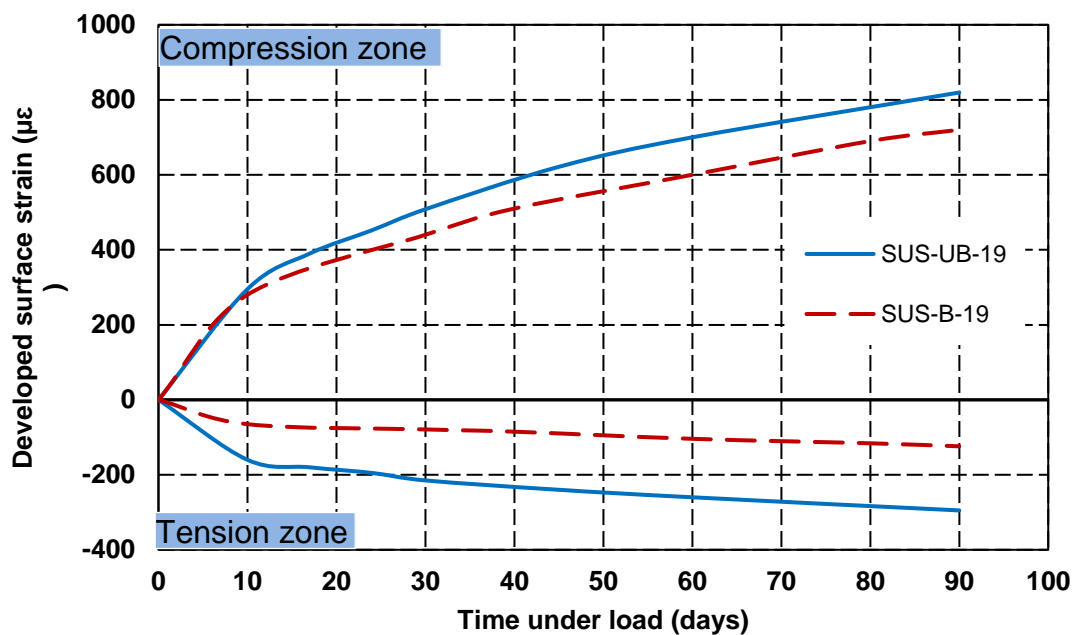Figure 4-12: Surface strain development in the compression and tension zone with time (SUS-UB-19 and SUS-B-19)

For the fully bonded beam subjected to repeated loading, the surface strain development in the compression and tension zones was compared with the debonded beam subjected to sustained loading as shown in Figure 4-13. It can be seen that both beams behaved almost identically; this is again confirming

that, all the bond between the concrete and reinforcement was eliminated in repeating load case.

Figure 4-13: Surface strain development in the compression and tension zone with time (REP-B-19 and SUS-UB-19)

4.4.3 Effects of Compression Reinforcement

Figure 4-14 compares the surface strain development in the compression and tension zone of two beams with different compression reinforcement. The reinforcement is bonded in both beams. One beam is unsymmetrically reinforced while the other is symmetrically reinforced (i.e. 3Ø16 in the compression and tension zone).

It can be seen that the developed surface strain in the tension zone for the symmetrical reinforced concrete beam is less than that of the other beam (i.e. SUS-B-19) by 13 %. The 13 % less strain in the tension zone is because of the less developed deflection due to creep and shrinkage in the symmetrical reinforcement beam and less crack width in the tension zone as both beams

95

had same number of cracks. Whereas beam with symmetrical reinforcement i.e. SUS-SYB-19 has 20 % less surface strain than that in SUS-B-19 in the compression zone.

It can be seen also that the effect of compression reinforcement are more influential in the compression zone than the tension zones which agreed with Washa and Fluck (1952). Washa and Fluck (1952) noticed about 60 % less surface strain by adding compression reinforcement equal in the amount in the tension reinforcement. The surface strain is 60 % less once the authors compare the results of double reinforcement beams with beams without compression reinforcement. While in this study SUS-B-19 still has compression reinforcement but less amount than that in the tension reinforcement.
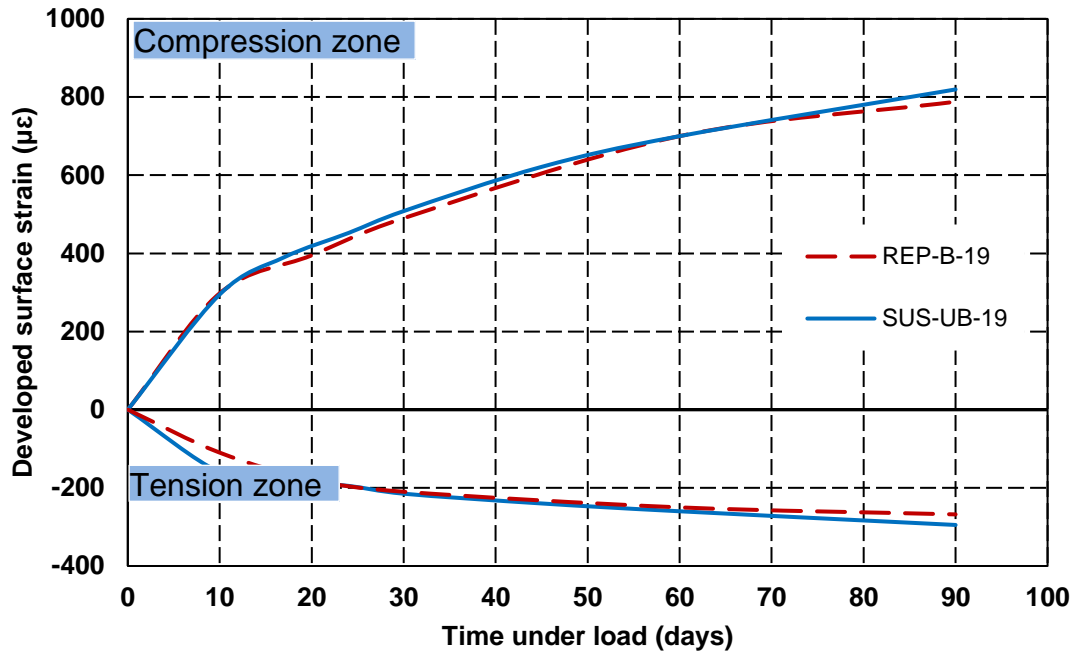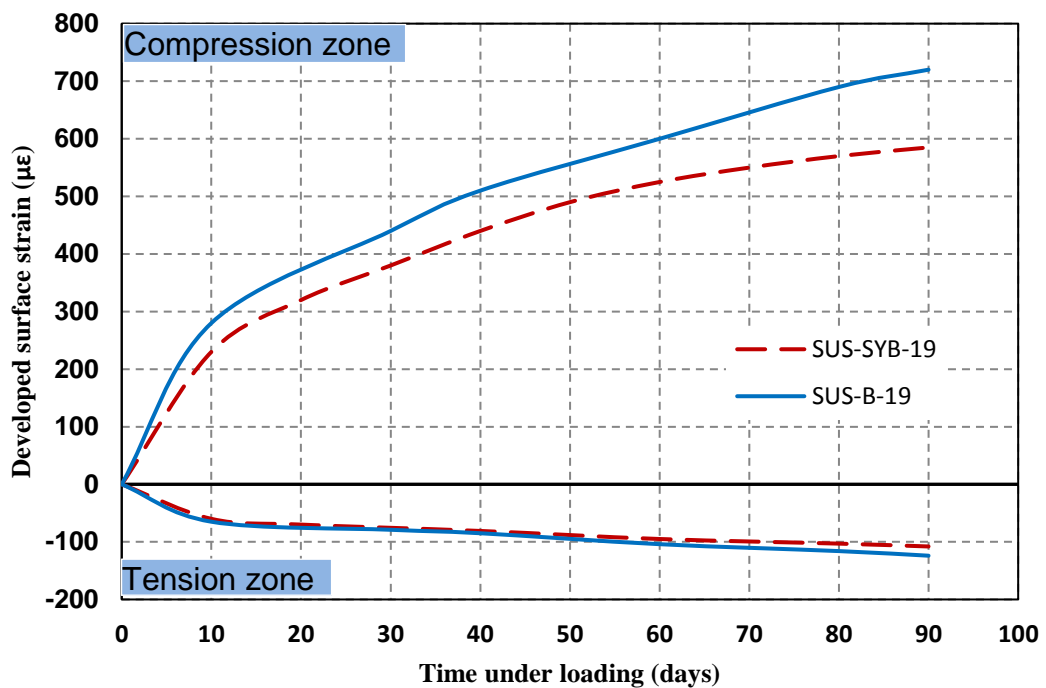

Figure 4-14: Surface strain development in the compression and tension zone with time (SUS-SYB-19 and SUS-B-19)

4.4.4 Effect of Loading Level

Figure 4-15 compares surface strain development of the three fully bonded beams under different loading level. It can be seen that, in both compression and tension zone the surface strain was increased with time in all beams regardless of loading level. However compared with beam tested by Ahmed (2013), the surface strain in the tension zone increased in the first 40 days then started to decreased after that during the 90 days. This is because the shrinkage strain in Ahmed (2013) beams was higher (545 µε), moreover Ahmed (2013) did not mention any cracks developed during the 90 days. In this study both beams SUS-B-5 and SUS-B-3 developed cracks during the 90 days.
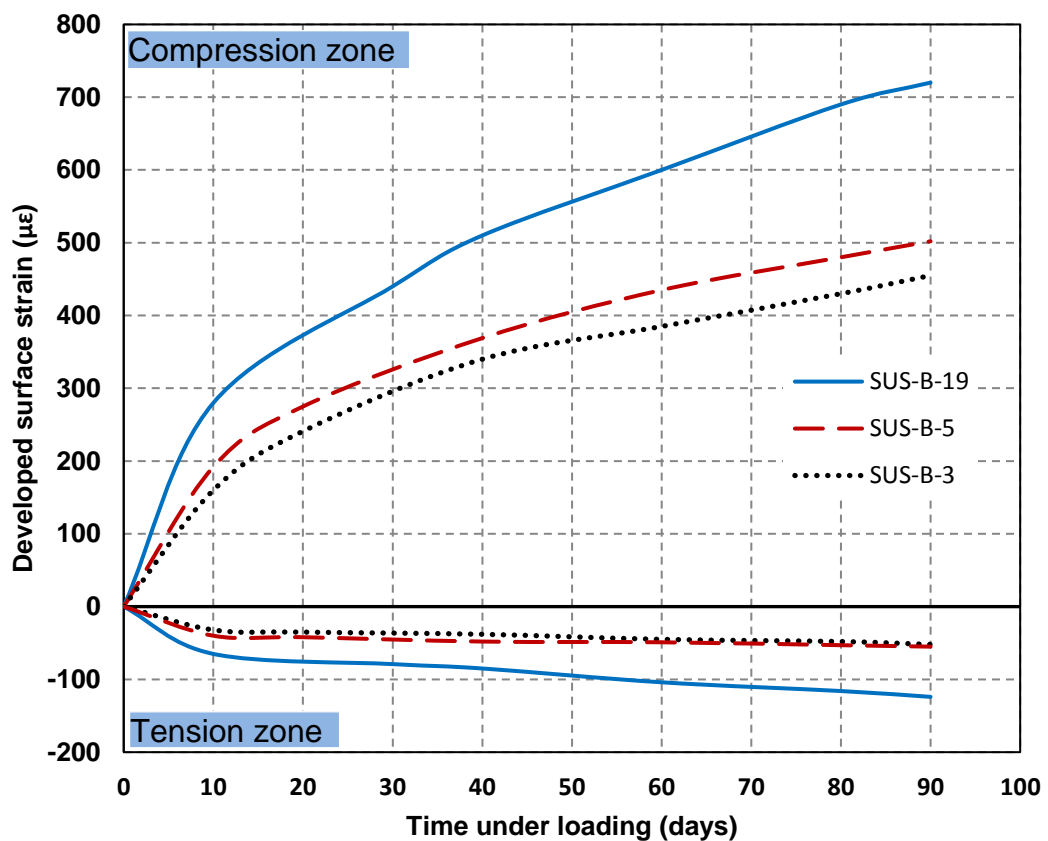

Figure 4-15: Surface strain development in the compression and tension zone with time (SUS-B-19, SUS-B-5 and SUS-B-3)

4.5 Summary

The first part of this Chapter has attempted to present the knowledge of artificial debonding of the reinforcement. It should be realised that the artificial method of debonding the reinforcement in the constant moment zone has been achieved successfully where the bond strength lost was about 93%. The effect of loading level, reinforcement type and adding compression reinforcement were examined experimentally. Based on the data gathered in the University of Leeds for a duration of 90 days, the following conclusions can be drawn:

1. The bond between concrete and steel in reinforced concrete beams subjected to a repeating load can be significantly damaged due to the loading, even though the frequency is relatively low (i.e. 0.2 H_z).

2. The additional deformation caused by repeated load is shown to occur within 10 to 20 days, depending on the material properties of the concrete.

3. For the case of cyclic repeated loading, further coefficients should be added to the Eurocode 2 (2004) equation to reflect the effect of repeated loading on long-term deflection.

4. The behaviour of a fully bonded reinforced concrete beam under repeated loading with small amounts of amplitude and frequency was almost equal to the behaviour of reinforced concrete beams with debonded reinforcement.

5. Beams having a high amount of compression reinforcement have less developed deflection with time.

6. Compression reinforcement does not have significant effect on the number of cracks nor the surface strain development in the tension zone.

7. The long-term mid-span developed deflection of the artificially debonded beam, subjected to sustained loading, is 36% higher than that of fully bonded beams.

8. The long-term deflection starts potentially only a single day after the sustained loading has been applied.

9. In the case of stabilized crack patterns, the concrete between the cracks acts elastically.

10. As expected, creep and shrinkage-induced cracks are a function of the sustained applied moment. The higher this sustained moment (i.e. closer to the stabilized crack pattern) the fewer number of cracks that develop after initial loading.

Chapter 5 Theoretical Analysis of Reinforced Concrete Beams under Long-Term Loading

5.1 Introduction

In this chapter, the mid-span developed deflections of the bonded beams (i.e SUS-B-19, REP-B-19, SUS-SYM-19, SUS-B-5 and SUS-B-3) are compared with the values predicted by Eurocode 2 (2004). The 90 day data is also extrapolated using Ross Hyperbolic function to determine the ultimate deflection; these are also compared with those predicted by Eurocode 2 (2004). The compressions show that Eurocode 2 (2004) tends to overestimate the deflection at early stages but underestimate the long-term values; Eurocode 2 (2004) is particularly inaccurate when it comes to estimating the movement of elements subjected to repeated loading.

5.2 Calculation of Curvature Based on Eurocode 2 (2004).

Eurocode 2 (2004) predicts the long-term deflection by superposition of creep and shrinkage curvatures. It proposes that the long-term curvature induced by the effect of creep can be calculated by using an effective modulus of elasticity according to the following equation:

$$E_{c\,eff} = \frac{E_{co}}{1+\emptyset_{(t)}}$$ (5-1)

Where:

E_{co} is the elastic modulus of concrete at time t_0

$\emptyset_{(t)}$ is the creep coefficient that depends on time and duration of loading.

Eurocode 2 (2004) suggests Equation 5-2 to calculate the shrinkage curvature:

$$\frac{1}{r_{cs}} = \varepsilon_{cs}\alpha_e \frac{S}{I}$$
(5-2)

Where:

$1/r_{cs}$ is the shrinkage curvature.

ε_{cs} is the free shrinkage strain at time t.

α_e is the effective modular ratio $\left(\frac{E_s}{E_{c\,eff}}\right)$.

S is the first moment of area of the reinforcement about the centroid of the section.

I is the second moment of area of section (cracked or uncracked as appropriate).

E_s is the elastic modulus of the steel reinforcement.

However, the curvature $1/r$ is calculated as:

$$1/r = \xi\left(1/r\right)_{cr} + (1 - \xi)\left(1/r\right)_{uc}$$
(5-3)

Where

$1/r$ is the average curvature.

$\left.\begin{array}{l}\left(1/r\right)_{cr} \\ \left(1/r\right)_{uc}\end{array}\right\}$	are the values of curvatures calculated for the cracked and uncracked section, respectively.
ξ	is the coefficient allowing for tension stiffening given by $\xi = 1 - \beta\left(\dfrac{M_{cr}}{M_a}\right)^2$.
β	is the coefficient taking account of the duration of loading (0.5 for sustained or cyclic loading and 1 for a single short-term load).
M_{cr}, M_a	are the cracking moment and the applied moment, respectively.

5.3 Models to Predict Creep Coefficient and Shrinkage Strain

5.3.1 Eurocode 2 (2004)

5.3.1.1 Creep Coefficient

Eurocode 2 (2004) provides an equation to predict the creep coefficient based on compressive strength of the concrete, relative humidity and type of cement used. This equation is:

$$\varphi(t, t_0) = \varphi_0 * \beta_c(t, t_0) \tag{5-4}$$

Where

φ_0	Is the notional creep coefficient which can be calculated from this equation $\varphi_0 = \varphi RH * \beta(f_{cm}) * \beta(t_0)$
$\qquad\varphi RH$	is a factor to allow for the effect of relative humidity on the notional creep coefficient

$$\varphi RH = \left[1 + \frac{1 - RH/100}{0.1 * \sqrt[3]{h_s}} * \alpha_1\right] \alpha_2$$

RH   is the relative humidity %

h_s is the notational size of member in mm ($h_s = \frac{2A_c}{u}$)

A_c section area.

u   perimeter in contact with atmosphere.

$$\beta(fcm) = \frac{16.8}{\sqrt{f_{cm}}}$$

f_{cm} mean compressive strength of concrete

$\beta(t_0)$ is a factor to allow for the effect of concrete age at
loading on the notional creep coefficient $\beta(t_0) = \frac{1}{(0.1 + t_0^{0.2})}$

$$\beta_c(t, t_0) = \left[\frac{(t - t_0)}{(\beta_H + t - t_0)}\right]^{0.3} \tag{5-5}$$

β_H a coefficient depending on the relative humidity (*RH* in %) and
the notional member size. It may be estimated from

$$\beta_H = 1.5[1 + (0.012RH)^{18}]h_s + 250\alpha_3 \tag{5-6}$$

$$\alpha_1 = [\frac{35}{f_{cm}}]^{0.7}$$

$$\alpha_2 = [\frac{35}{f_{cm}}]^{0.2}$$

$$\alpha_3 = [\frac{35}{f_{cm}}]^{0.5}$$

5.3.1.2 Shrinkage

The drying shrinkage strain suggested by Eurocode 2 (2004) can be calculated from:

$$\varepsilon_{sh} = \varepsilon_{cd0} * \beta_{ds}(t, t_s) * k_h \tag{5-7}$$

Where

k_h is a constant depending on the notational size h_s accoring to the Table 5-1

Table 5-1: Values of k_h (Eurocode 2, 2004)

h_s	k_h
100	1
200	0.85
300	0.75
≥500	0.7

$$\varepsilon_{cd,0} = 0.85 \left[(220 + 110 * \alpha_{ds1}) * \exp\left(-\alpha_{ds2} * \frac{f_{cm}}{f_{cm0}}\right)\right] 10^{-6} * \beta_{RH} \tag{5-8}$$

$\alpha_{ds1}, \alpha_{ds2}$ are factors depend on type of cement (4 and 0.12 respectively)

f_{cm0} =10 Mpa

$$\beta_{RH} = 1.55 \left[1 - \left(\frac{RH}{RH_0} \right)^3 \right]$$

RH_0 =100

$$\beta_{ds}(t, t_s) = \frac{t - t_s}{(t - t_s) + 0.04 \sqrt{h_s{}^3}} \tag{5-9}$$

5.3.2 Model code (2010)

The Mode Code (2010) available to predict the creep and shrinkage of the concrete is valid for a concrete with a compressive strength ranging from 12 MPa to 80 MPa.

5.3.2.1 Creep Coefficient

The Mode Code 2010 predicts creep is a similar to Eurocode 2 (2004); both depend on the relative humidity, temperature, and the compressive strength of the concrete. However, the factors in the Model Code (2010) are less than that of the Eurocode 2 (2004) such as factors depend on the cement type (α_{ds1}, α_{ds2}) and the coefficients to consider the influence of the concrete strength ($\alpha_{1,2,3}$). The equations for creep coefficient calculation are:

$$\varphi(t, t_0) = \varphi_0 * \beta_c(t, t_0) \tag{5-10}$$

$$\varphi_0 = \varphi RH * \beta(f_{cm}) * \beta(t_0) \tag{5-11}$$

$$\varphi RH = \left[1 + \frac{1 - RH/100}{0.1 * \sqrt[3]{h}} \alpha_1 \right] \alpha_2 \qquad (5\text{-}12)$$

$$\beta(f_{cm}) = \frac{16.8}{\sqrt{f_{cm}}} \qquad (5\text{-}13)$$

$$\beta(t_0) = \frac{1}{0.1 + (t_0)^{0.2}} \qquad (5\text{-}14)$$

$$\beta_c(t - t_0) = \left[\frac{(t - t_0)}{\beta_H + (t - t_0)}\right]^{0.3} \qquad (5\text{-}15)$$

$$\beta_H = 1.5 * h * \left[1 + \left(1.2 \frac{RH}{100}\right)^{18}\right] + 250 * \alpha_3 \leq 1500 * \alpha_3 \qquad (5\text{-}16)$$

Where

$$\alpha_1 = \left(\frac{35}{fcm}\right)^{0.7}, \ \alpha_2 = \left(\frac{35}{fcm}\right)^{0.2} \text{ and } \alpha_1 = \left(\frac{35}{fcm}\right)^{0.5}$$

Also, the Model Code (2010) proposed equations which are only suitable when the sample is subjected to a compressive stress of less than 40 % of the compressive strength of the concrete, a relative humidity between 40-100 % and a mean temperature between 5⁰C and 30⁰C.

5.3.2.2 Shrinkage

The drying shrinkage of the concrete can be calculated using the following Model Code (2010) equations:

$$\varepsilon_{sh} = \varepsilon_{cds0}(fcm) * \beta_{RH}(RH) * \beta_{ds}(t - t_s) \qquad (5\text{-}17)$$

$$\varepsilon_{cds0} = [(220 + 110\alpha_{ds1}) * \exp(-\alpha_{ds2} * fcm)]10^{-6} \tag{5-18}$$

$$\beta_{RH} = -1.55 * \left[1 - \left(\frac{RH}{100}\right)^3\right] \tag{5-19}$$

$$\beta_{ds}(t - t_s) = \left(\frac{(t - t_0)}{0.035 * h^2 + (t - t_0)}\right)^{0.5} \tag{5-20}$$

Where

$\alpha_{ds1} = 6$ and $\alpha_{ds2} = 0.012$

5.4 Shrinkage Strain and Creep Coefficient Results

Figure 5-1 and Figure 5-2 show the shrinkage strain and creep coefficient development with time, respectively, for a period of 90 days. Both creep and shrinkage test data were obtained from the concrete once it reached an age of 28 days.
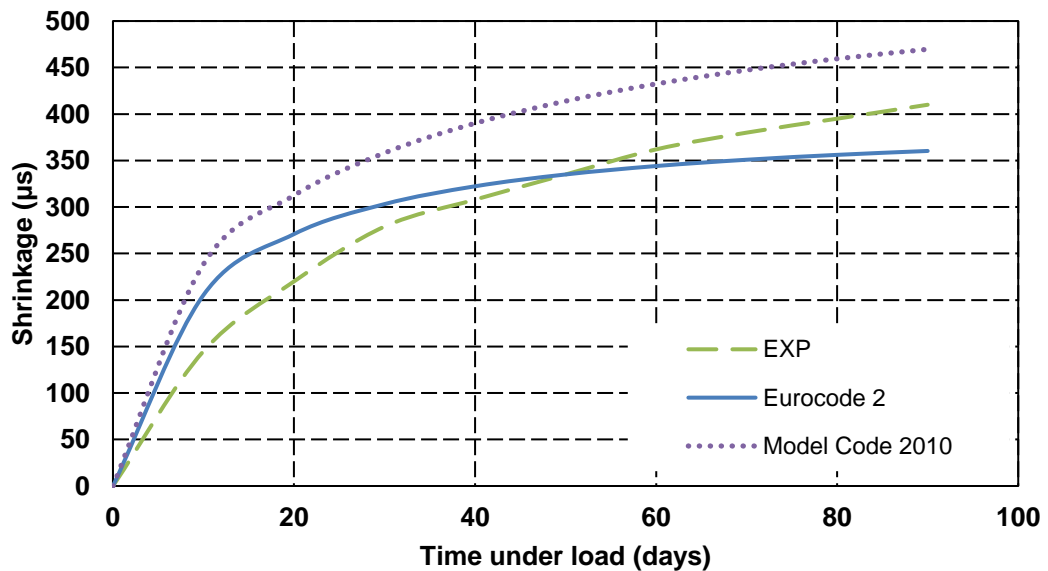

Figure 5-1: Shrinkage development with time

In Figure 5-1, it can be seen that the Model Code (2010) overestimates the shrinkage during the 90 days. The Model Code (2010) does not consider the time when the concrete starts undergoing drying shrinkage. Whereas the Eurocode 2 (2004) overestimates the shrinkage at early ages (25 days). The overestimation in the code results from the missing reading in the experiment, where the samples were taken out from the curing room at 25 days and the reading started at 28 days. However, the Eurocode 2 (2004) seriously underestimates the long-term shrinkage (Vandewalle, 2000, Gribniak et al., 2008). From this figure, it can be noticed that both Model Code (2010) and Eurocode 2 (2004) predict the shrinkage within a reasonable agreement after 90 days (+15 and -13% difference, respectively). However, the rate of shrinkage of the measured specimen is greater than that predicted by the codes. This difference will further amplify the error in the code prediction in the ultimate result.

The creep coefficient development with time for the experimental samples was also compared with that predicted from the Model (Code 2010) and Eurocode 2 (2004) (see Figure 5-2).
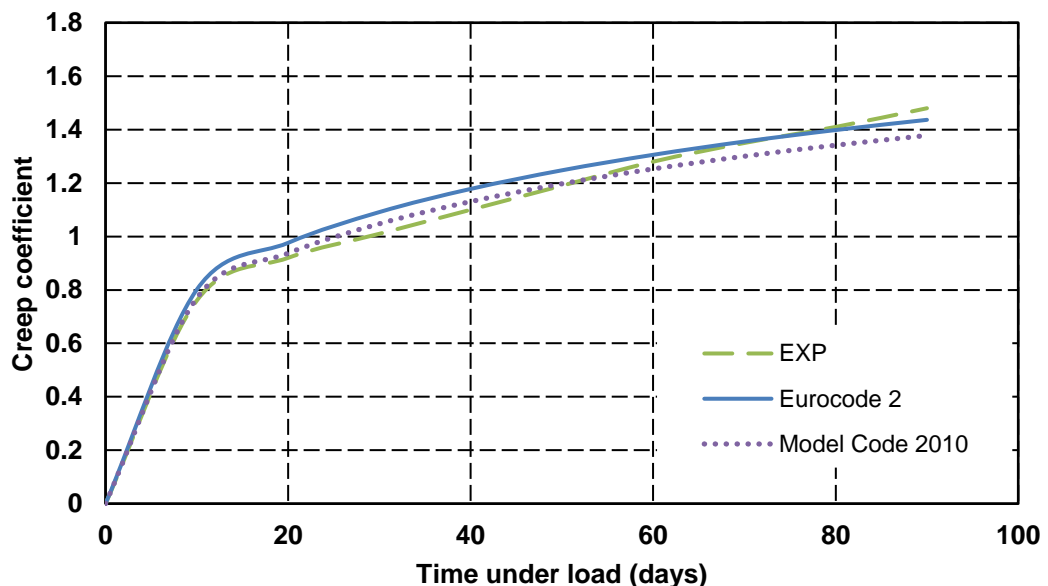

Figure 5-2: Creep coefficient with time

From Figure 5-2, it can be seen that both Model Code (2010) and Eurocode 2 (2004) predict the creep coefficient accurately during the 90 days.

5.5 Mid-Span Deflection

5.5.1 Single Reinforcement

Figure 5-3 compares the developed mid-span deflection of two reinforced concrete beams (i.e. REP-B-19 and SUS-B-19) with that predicted by Eurocode 2 (2004) for a period of 90 days. The 90 days was chosen based on previous studies, where studies showed about 50% of the tension stiffening lost over the first 20 to 30 days, at which point the loss stabilised (Scott and Beeby, 2005). Moreover Higgins et al. (2013) showed that the extra deformations due to repeated load take place significantly within the first 10 days.

For the beam under sustained loading (i.e. SUS-B-19), it is clear that Eurocode 2 (2004) overestimates the developed deflection in the first 22 days. After 22 days, Eurocode 2 (2004) underestimates the developed deflection. However, by 90 days, the error is only 8%, which is still acceptable.

The overestimation of deflection at early ages possibly results from an error in the amount of tension stiffening. Eurocode 2 (2004) suggests a constant factor β (β is the coefficient taking account of the duration of loading, and is 0.5 for sustained or cyclic loading and 1 for a single short-term load). However, Forth et al. (2014) observed that keeping the factor β constant helps to overestimate the predicted curvature in the case of sustained loading (particularly at early ages).

Any difference between measured and predicted values at 90 days may be due to the variation in the storage environment used to obtain beam curvature and concrete shrinkage. Experimentally, the ambient environment will never match exactly and that disparity could lead to this error.

For the case of a cyclic/repeating load beam, Eurocode 2 (2004) suggests the use of the same equations to predict the long-term deflection of those used for the sustained load beam (assume β=0.5). Now, Eurocode 2 (2004) overestimates the deflection by 30% after 90 days, emphasising even more how critical it is to use a varying value of β.
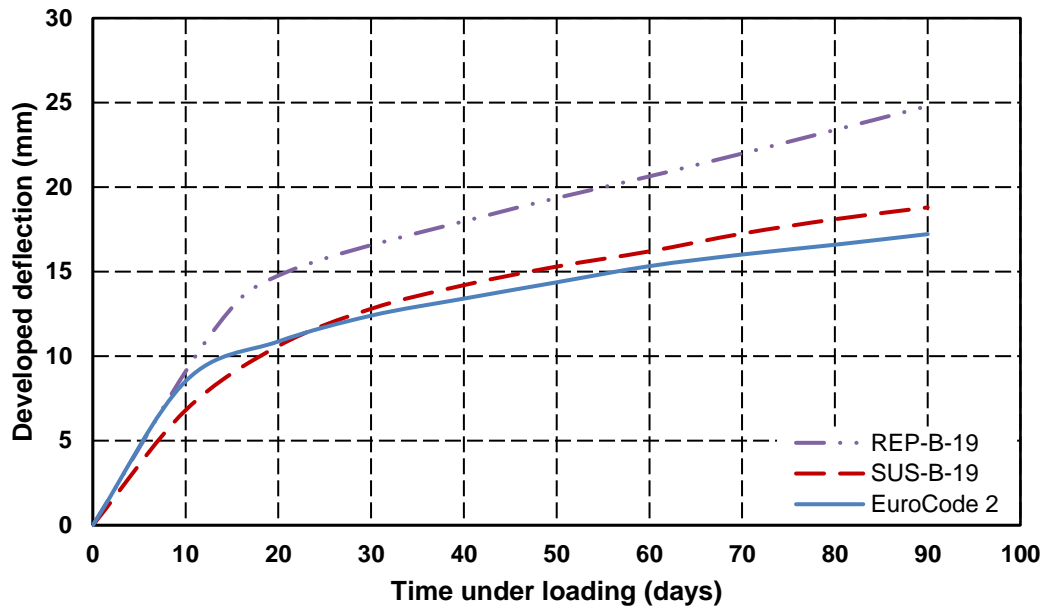

Figure 5-3: Mid-span developed deflection with time (REP-B-19, SUS-B-19 and Eurocode 2)

Figure 5-4 and Figure 5-5 compare the developed long-term deflection predicted by Eurocode 2 (2004) with beams SUS-B-5 and SUS-B-3 for a period of 90 days. Although at 90 days Eurocode 2 (2004) appears to predict the long-term deflection of the both beams reasonably well -16% and 11% for SUS-B5 and SUS-B-3, respectively - it can also be seen that the code overestimates the deflection for the first 50 days and 62 days, respectively, and that the rate of deflection is underestimated at 90 days. By comparing the measured and predicted curves for the three levels of applied load (19 kN, 5 kN and 3 kN), it can be seen that the code tends to overpredict the most when the applied load is the least. In other words, the code is more accurate when the applied load is close to the load which produces a stabilised crack pattern.

This affects the fact that the code theory has been developed around cases where a stabilised crack pattern exists. In reality, this is inappropriate, as this is frequently not the case.

The inaccuracy is thought to be related to the degree of the tension stiffening. Clearly, a beam loaded to 3 kN just below the cracking moment will possess more tension than one loaded to 19 kN, which produces a stabilised crack pattern. In the first case, no cracks were produced and all the concrete acts elastically. While in the second case (beam under 19 kN load), a stabilised crack pattern is produced and only the concrete between cracks acts elastically.
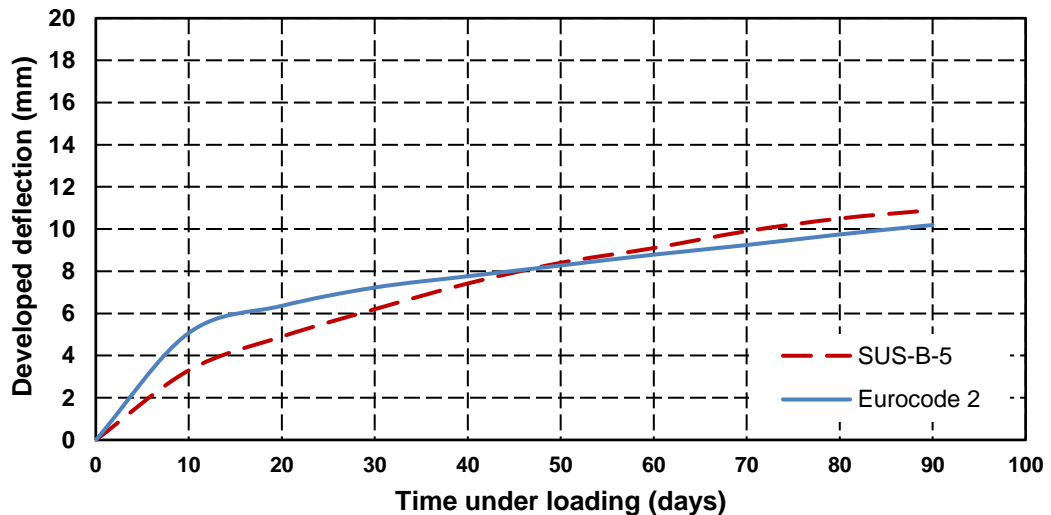

Figure 5-4: Mid-span developed deflection with time (SUS-B-5 and Eurocode 2)
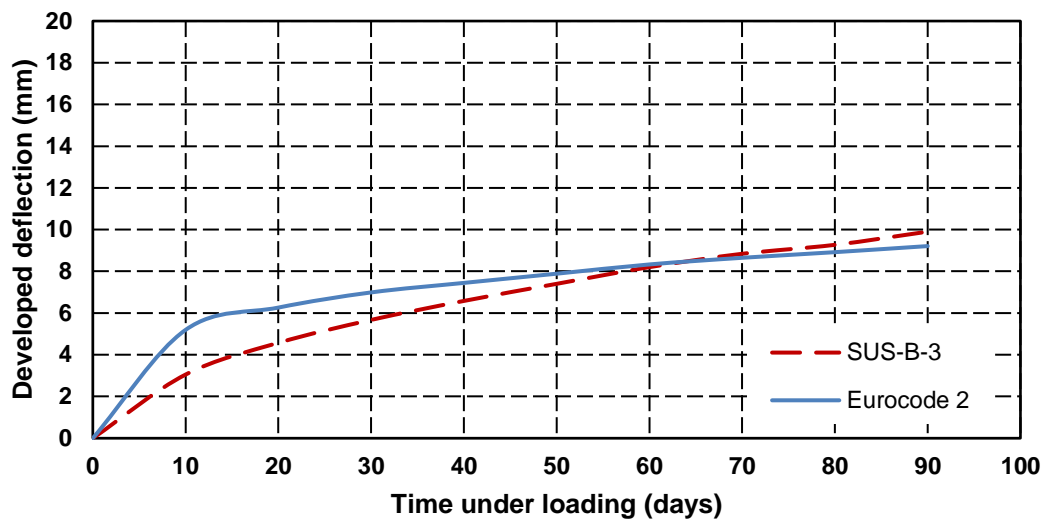
Figure 5-5: Mid-span developed deflection with time (SUS-B-3 and Eurocode 2)

Once the creep and shrinkage strains were adjusted to the environment of the lab where the beams were tested, using the Eurocode 2 (2004) suggested equations, Figure 5-6, Figure 5-7 and Figure 5-8 show good agreement between the Eurocode 2 (2004) and the experimental deflections after 90 days. However, there is still overestimation in the Eurocode 2 (2004) predicted deflection at early ages. This overestimation results is due to tension stiffening.
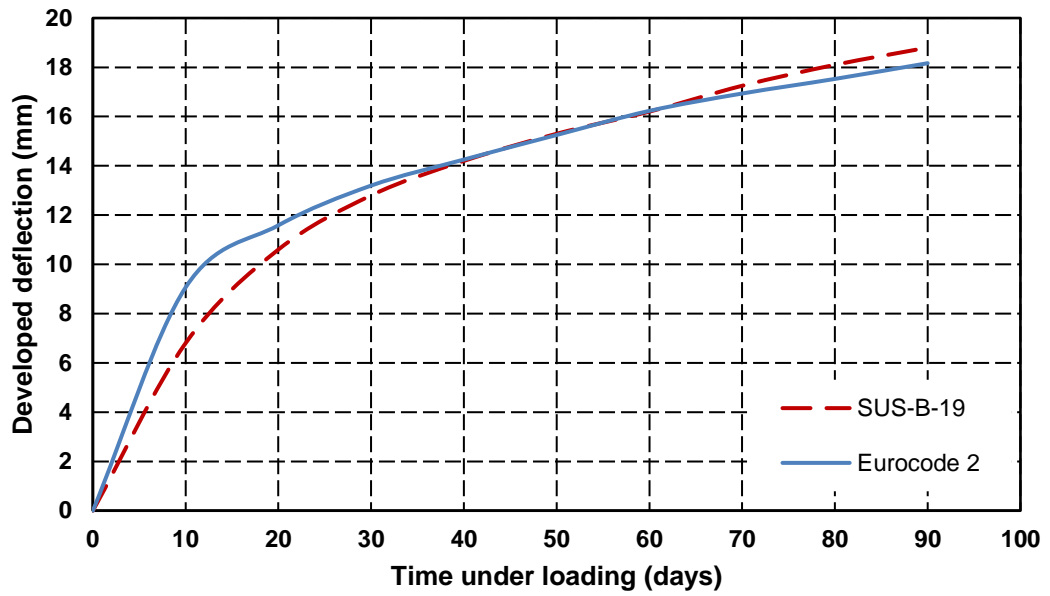
Figure 5-6: Mid-span developed deflection with time (SUS-B-19 and Eurocode 2)

Figure 5-7: Mid-span developed deflection with time (SUS-B-5 and Eurocode 2)

Figure 5-8: Mid-span developed deflection with time (SUS-B-3 and Eurocode 2)

An attempt was made to optimise the value of β during the 90 day period. Initially, β was suggested to start from 0.75 and then reduce gradually to the day of intersection between predicted and measured deflection. After the intersection β was kept at 0.5, as suggested by Eurocode 2 (2004). The suggested values of β showed a great match between the experimental deflection and that suggested by the Eurocode 2 (2004), as shown in Figure
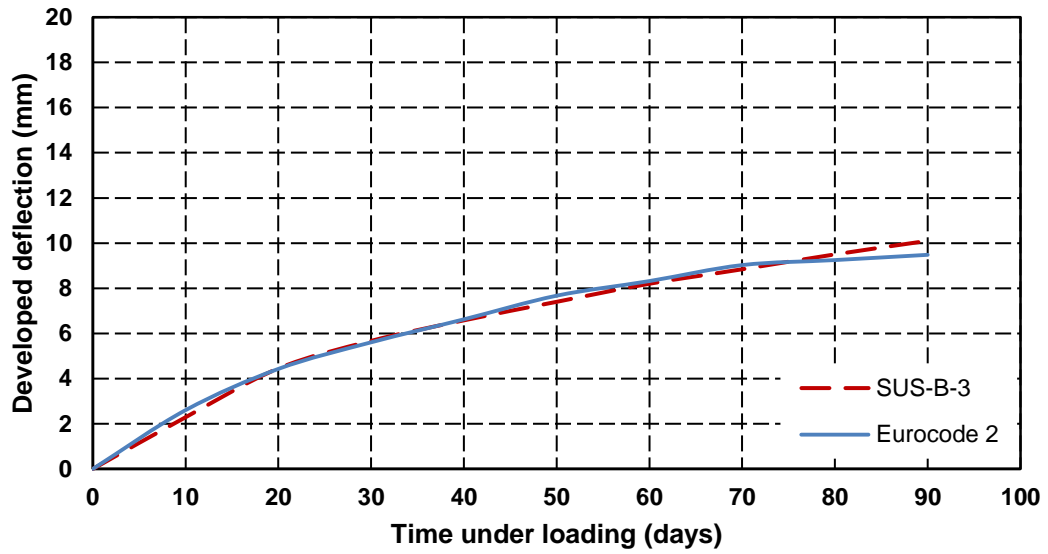
Figure 5-10. The suggested 0.75 value for β will be verified in the next section using beams with a different geometry. The 0.75 value for β was chosen based on a previous work done by Vollum (2002) (i.e. it should be taken as 0.7 up to a five week duration of peak construction loads).
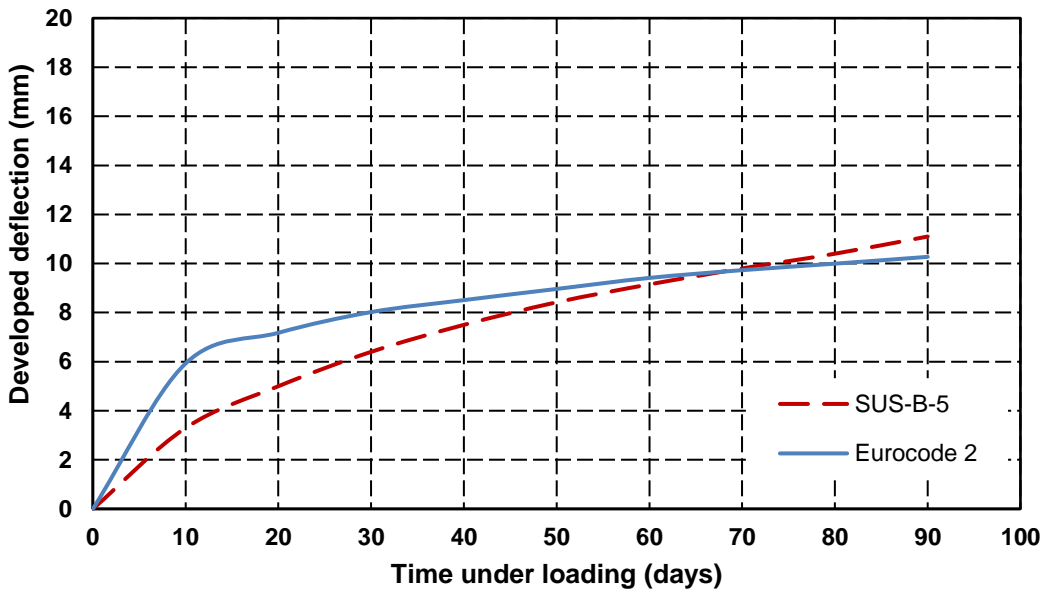
Figure 5-9: Mid-span developed deflection with time (SUS-B-5 and Eurocode 2)

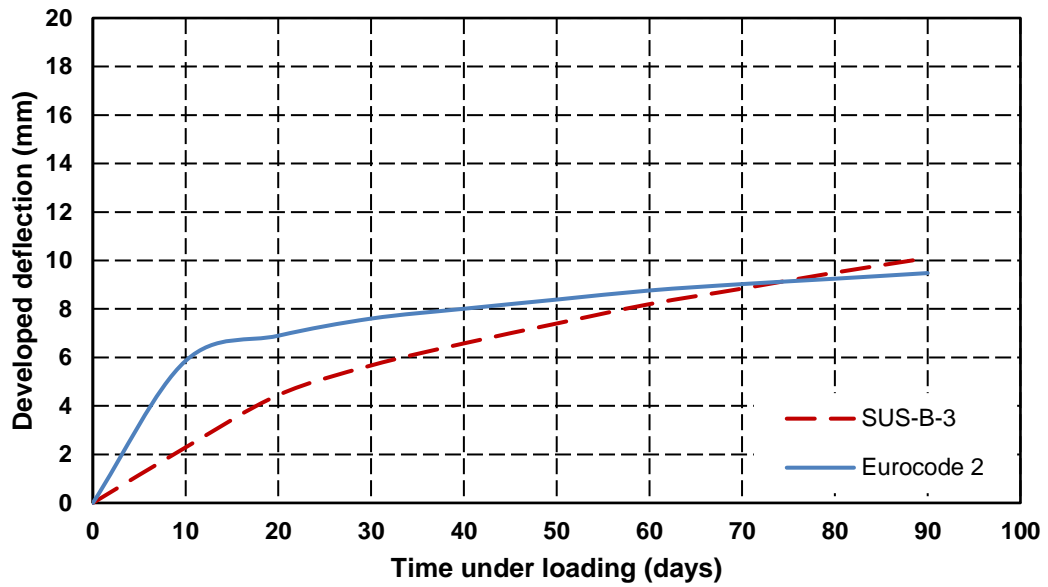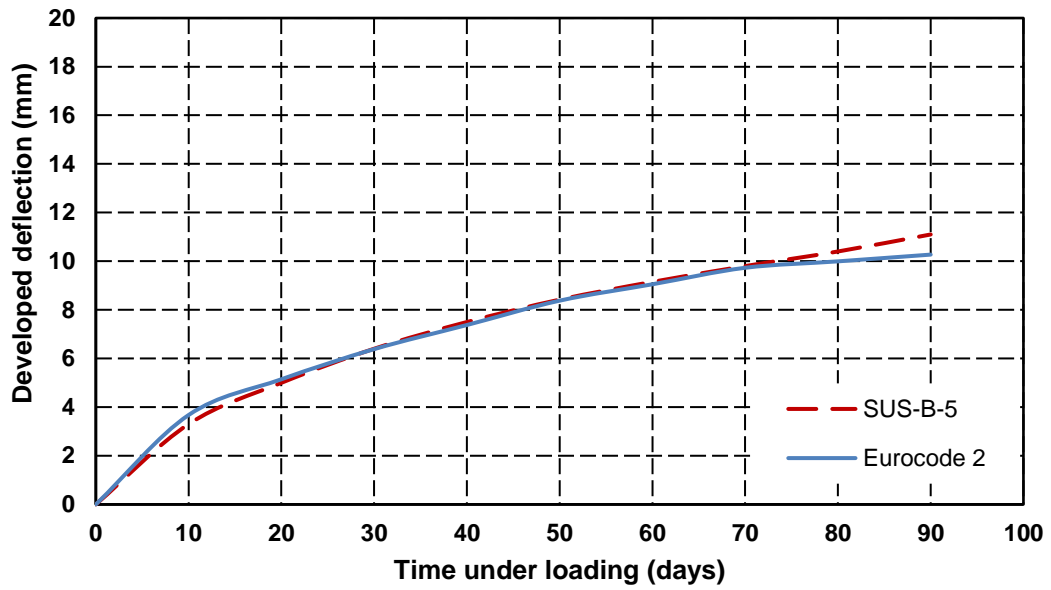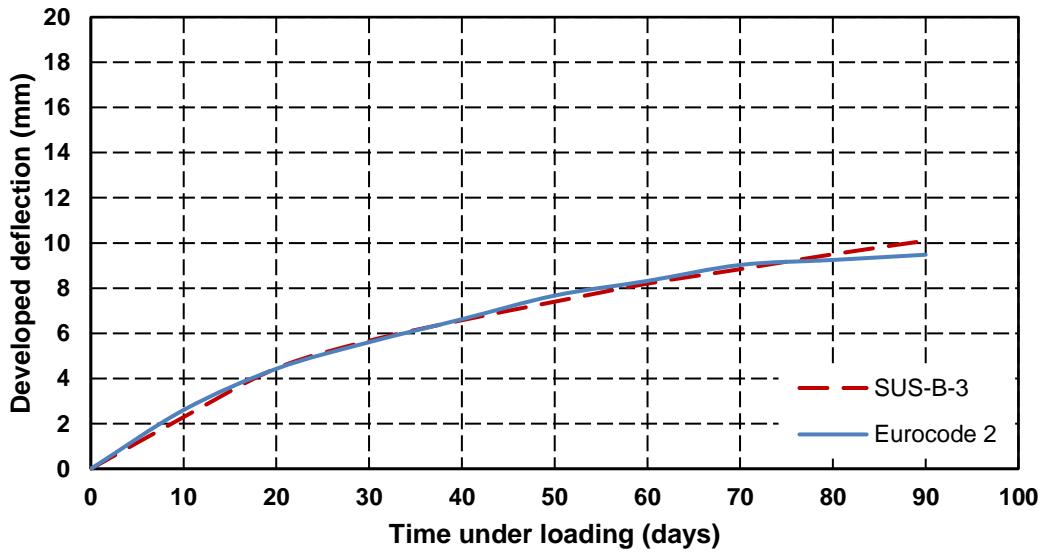Figure 5-10: Mid-span developed deflection with time (SUS-B-3 and Eurocode 2)

Again, the underestimated deflection in 90 days may be due to the variation in storage environment used to obtain beam curvature and concrete shrinkage.

5.5.1.1 Using Eurocode 2 (2004) to Predict Long-Term Deflection of Previous Work.

A comparison between Eurocode 2 (2004) and other experimental works carried out by a different researcher was conducted in this section to support the idea that β is not constant and to verify the suggested values of β.

Mias et al. (2013) study experimentally the long-term deflection of reinforced concrete beams. The main parameters of their work were the reinforcement type (i.e. steel and GRFP rebars), sustained loading amount, and the material compressive strength. All beams had the same dimensions, 140 x 190 x 2450 mm with a clear span of 2200mm. Table 5-2 provides the experimental details utilized by Mias et al. (2013), i.e. material properties and loading amount. The sustained load was chosen to obtain concrete compressive stress on the top fibre of the mid-span section of 0.3 f_c and 0.45 f_c. All beams with steel reinforcement had Ø 10 mm tension reinforcement only.

Table 5-2: Beam designation, material properties and loading amount (Mias et al., 2013)

Beam reference	Concrete compressive strength on the top fibre	Sustained load amount (kN)	Modulus of elasticity at 28 days (GPa)	Compressive strength at 28 days (MPa)
N_L1_S10	0.3 f_c	10	25.7	27.7
N_L2_S10	0.45 f_c	14		
H_L1_S10	0.3 f_c	17	29	56
H_L2_S10	0.45 f_c	22		

Mias et al. (2013) loaded their beams for 250 days (N_L1_S10, N_L2_S10) and 700 days (H_L1_S10, H_L2_S10). The developed mid-span deflection predicted by Eurocode 2 (2004), was compared with their deflection for a 90-day period. Figure 5-11 and Figure 5-12 compare the developed mid-span deflection of the normal concrete beams under two different loading amounts. It can be seen that the Eurocode 2 (2004) overestimates the deflection in the first 35 days, when the beam is sustained at 10 kN load, and underestimates the deflection by 6% after 90 days, while the code overestimates the deflection in the first 20 days when the beam is sustained into a higher load (i.e. 14 kN) and thus underestimates the deflection by 13%.

Figure 5-11: Mid-span developed deflection with time (N_L1_S10 and Eurocode 2)
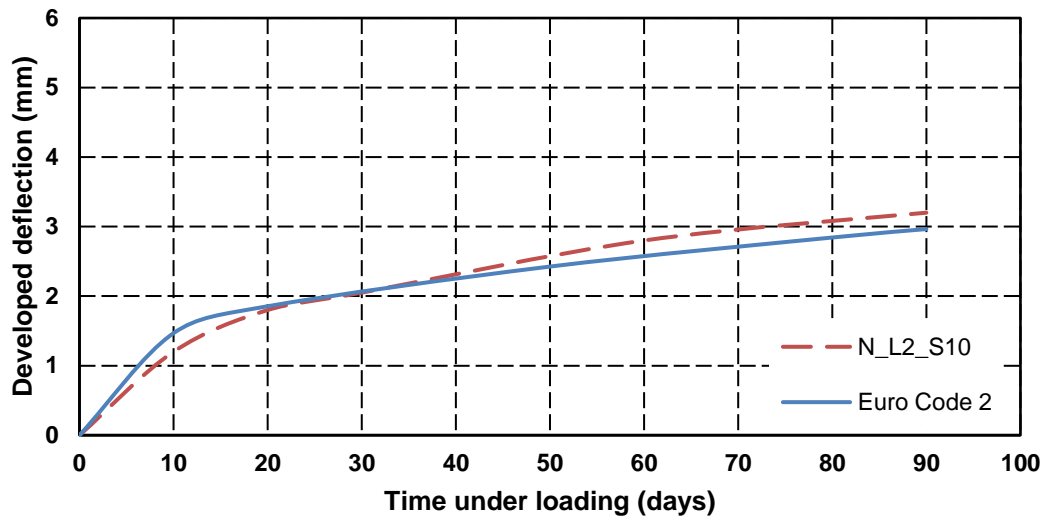
Figure 5-12: Mid-span developed deflection with time (N-L2_S10 and Eurocode 2)

Similarly in the other two beams (i.e. H_L1_S10 and H_L2_S10), the Eurocode 2 (2004) overestimates the deflection in the first 60 days and 40 days when the beams sustained into 17 kN and 22 kN, respectively, as shown in Figure 5-13 and Figure 5-14, whereas the deflection predicted by the Eurocode 2 (2004) agreed with the experimental deflection after 90 days.
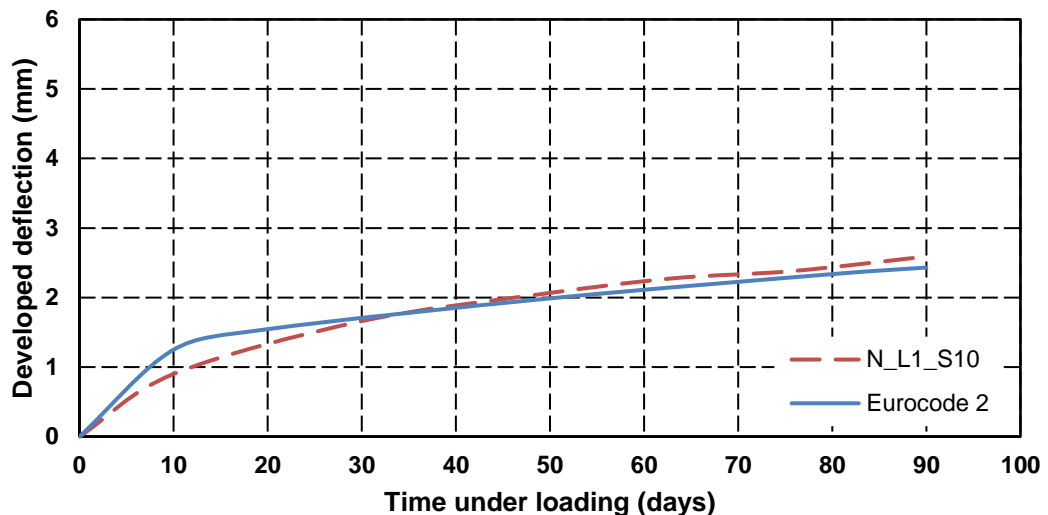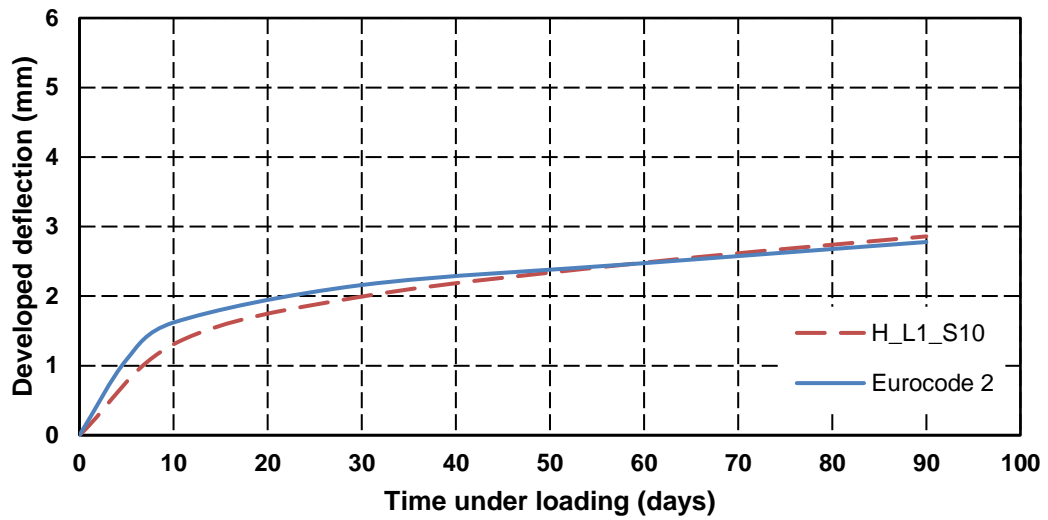
Figure 5-13: Mid-span developed deflection with time (H-L1_S10 and Eurocode 2)
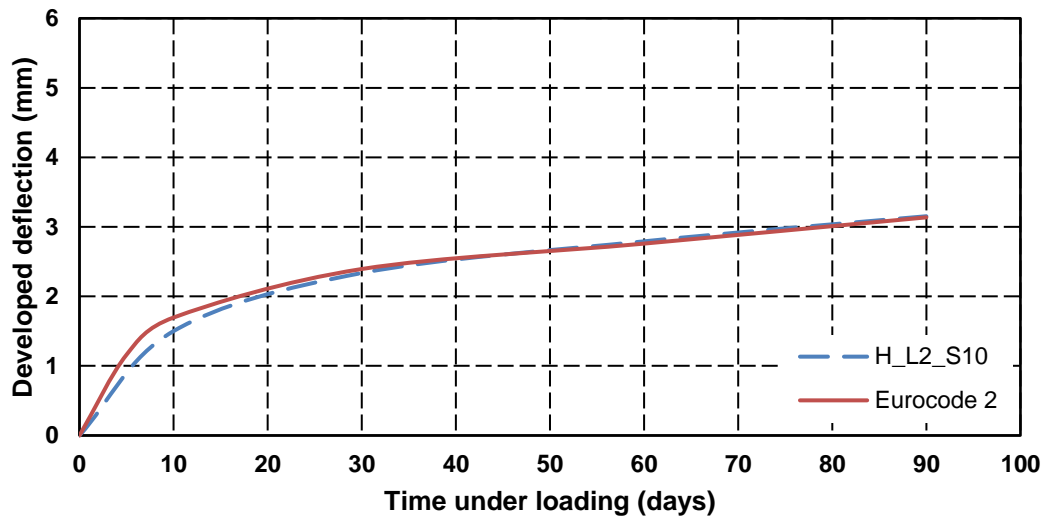
Figure 5-14: Mid-span developed deflection with time (H-L2_S10 and Eurocode 2)

After using the suggested values of β (i.e. β start from 0.75 and reduced gradually to the day of intersection between predicted and measured deflection when β=0.5), Figures 5-15 to Figure 5-18 show better matching at the early

ages. Still, after 90 days the deflection predicted by Eurocode 2 (2004) almost equalled the experimental result of Mias et al. (2013). This matching result could be explained by the beams' geometry and the clear span length, where the clear span was almost half the span of that used in the experiment.
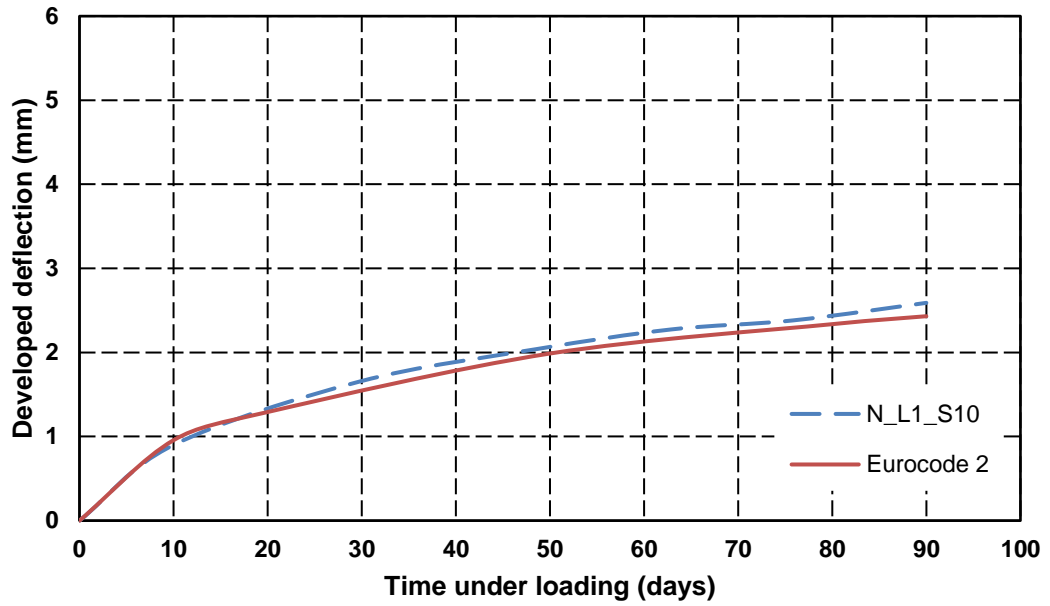
Figure 5-15: Mid-span developed deflection with time (N-L1_S10 and Eurocode 2) with new values of β
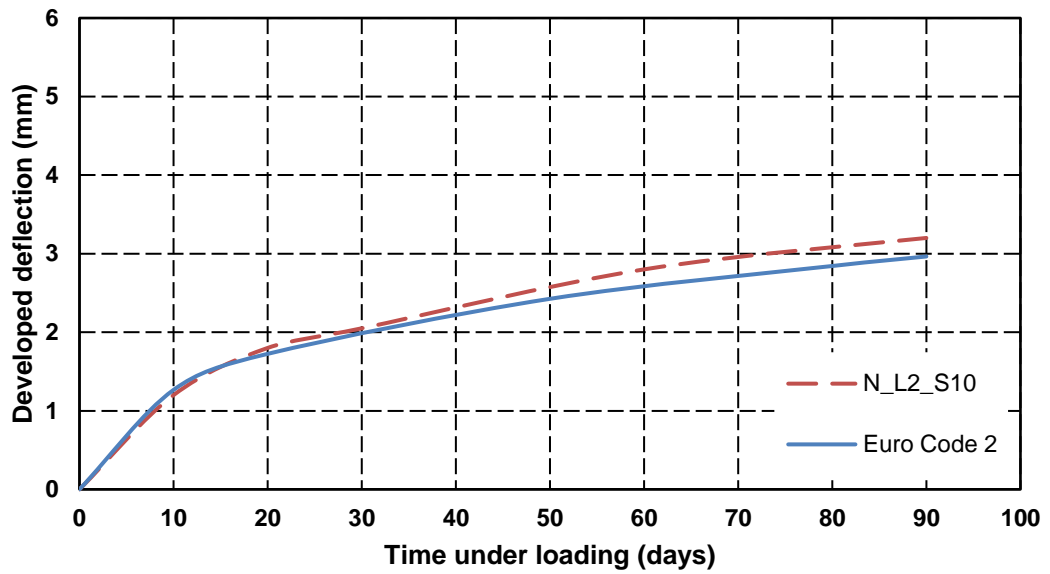
Figure 5-16: Mid-span developed deflection with time (N-L2_S10 and Eurocode 2) with new values of β
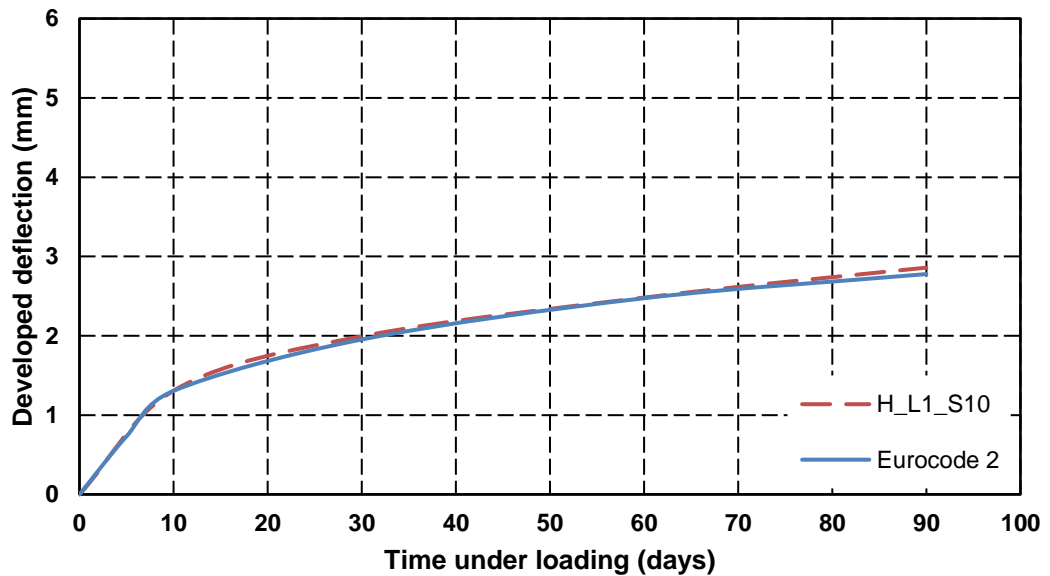
Figure 5-17: Mid-span developed deflection with time (H-L2_S10 and Eurocode 2) with new values of β
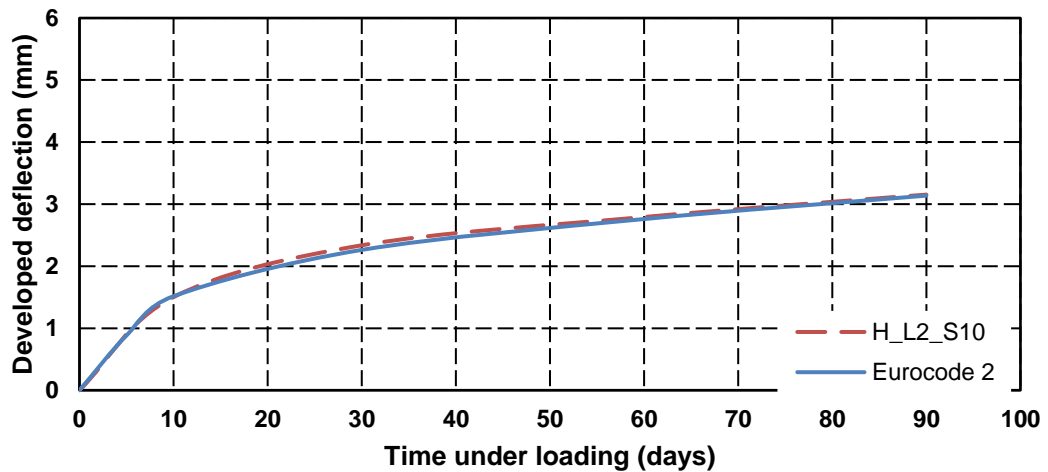
Figure 5-18: Mid-span developed deflection with time (H-L2_S10 and Eurocode 2) with new values of β

5.5.2 Symmetrically Reinforced Concrete Beam.

In this section the mid-span long-term developed deflection of the symmetrically reinforced concrete beam subjected to a 19 kN sustained load was compared with that predicted by Eurocode 2 (2004). It can be seen in Figure 5-19 that the Eurocode 2 (2004) suggested equation predicts the deflection very well.
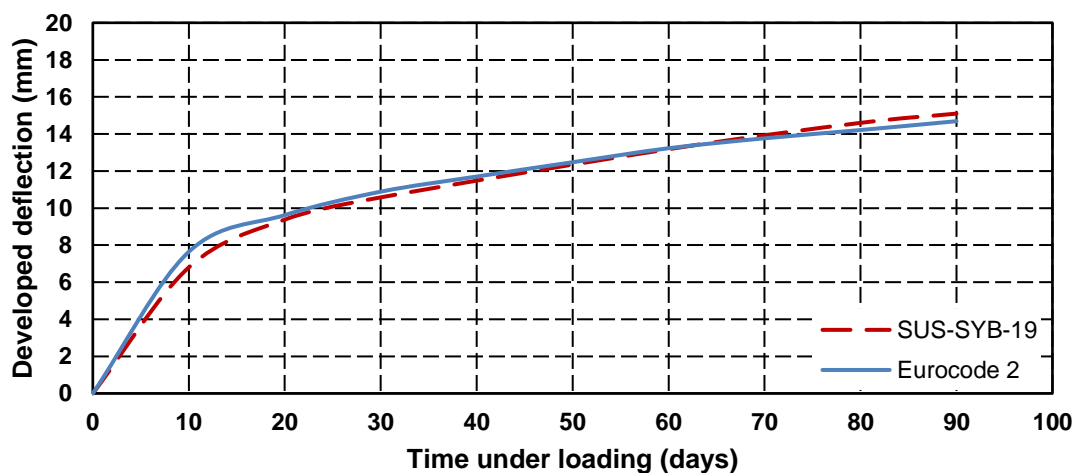
Figure 5-19: Mid-span developed deflection with time (SUS-SYB-19 and Eurocode 2)

Eurocode 2 (2004) predicts the deflection of a symmetrically reinforced beam better than the normally reinforced beam. It believes that in an uncracked section, shrinkage induces curvature when the reinforcement is placed asymmetrically; however, there is no shrinkage curvature when the section is reinforced symmetrically (Hobbs, 1982, Gilbert, 2001). Moreover, although Eurocode 2 (2004) suggests an equation to predict the shrinkage curvature (Equation 5-3) allowed to use cracked section properties, it derived this based on an uncracked section (Mu et al., 2008).

This better prediction for the deflection in cases of symmetrical reinforcement might result from the shrinkage curvature. Where in the case of uncracked sections, there is no shrinkage curvature in symmetrical reinforcement.

5.6 Shrinkage Induced Deflection Predicted by the Eurocode 2 (2004)

Concrete creep and shrinkage are the major parameters which influence the long-term deflection of reinforced concrete members. Figure 5-20 illustrates the long-term developed deflection of the three reinforced concrete beams tested under different levels of loading. Mu et al. (2008) showed numerically that 50% of the total long-term curvature is likely due to creep while the other 50% is due to shrinkage – this is, however, dependent on geometry and percentage steel reinforcement. According to this rationale, for the first beam considered here (i.e. SUS-B-19), the shrinkage curvature should be 9.4 mm (see Figure 5-20). Similarly, it should be 5.5 mm and 5 mm for SUS-B-5 and SUS-B-3, respectively.
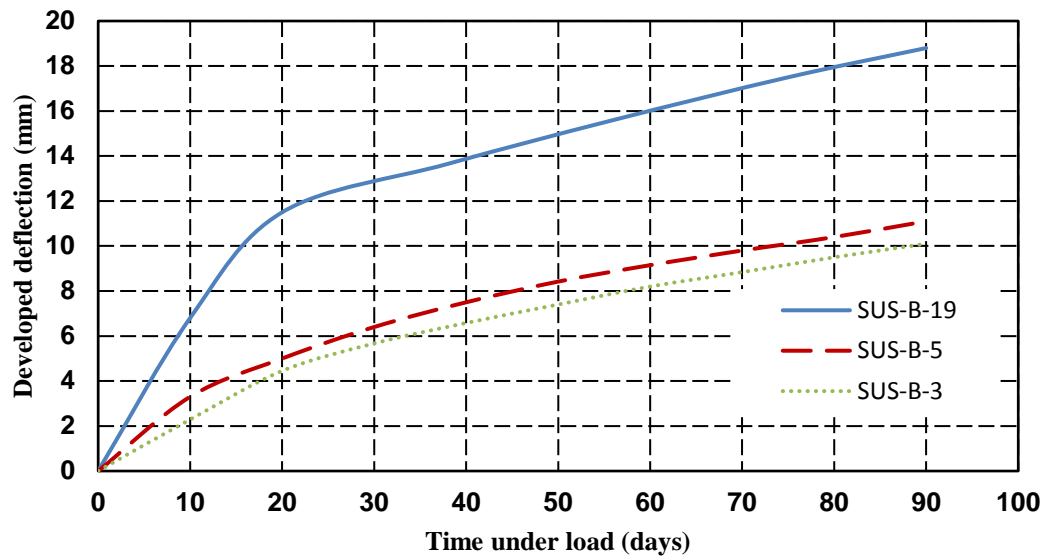
Figure 5-20: Mid-span developed deflection with time (SUS-B-19, SUS-B-5
and SUS-B-3)

Based on Mu et al. (2008) findings, the shrinkage curvature of the three beams
(i.e SUS-B-19, SUS-B-5 and SUS-B-3) can be shown in Figure 5-21. It can be
noted that identical beams having a higher number of cracks develop a greater
deflection due to shrinkage. This is because of the stiffness of the sections.
As the shrinkage curvature results from the cracked and uncracked sections,
in an uncracked section, all beams have the same shrinkage curvature (due to
the non-symmetrical reinforcement). While in a cracked section, beam SUS-
B-3 is stiffer than SUS-B-5 and SUS-B-19 (due to the moment of inertia and
the neutral axis position). Thus the shrinkage curvature in SUS-B-3 is less than
that in the other two beams. Similarly, SUS-B-5 has less shrinkage curvature
than SUS-B-19. However, based on the Eurocode 2 (2004), all beams have
the same moment of inertia (I_{cr} and I_{uc} are same in all beams) and the stiffness
results from ξ (the distributed coefficient allowing for tension stiffening).
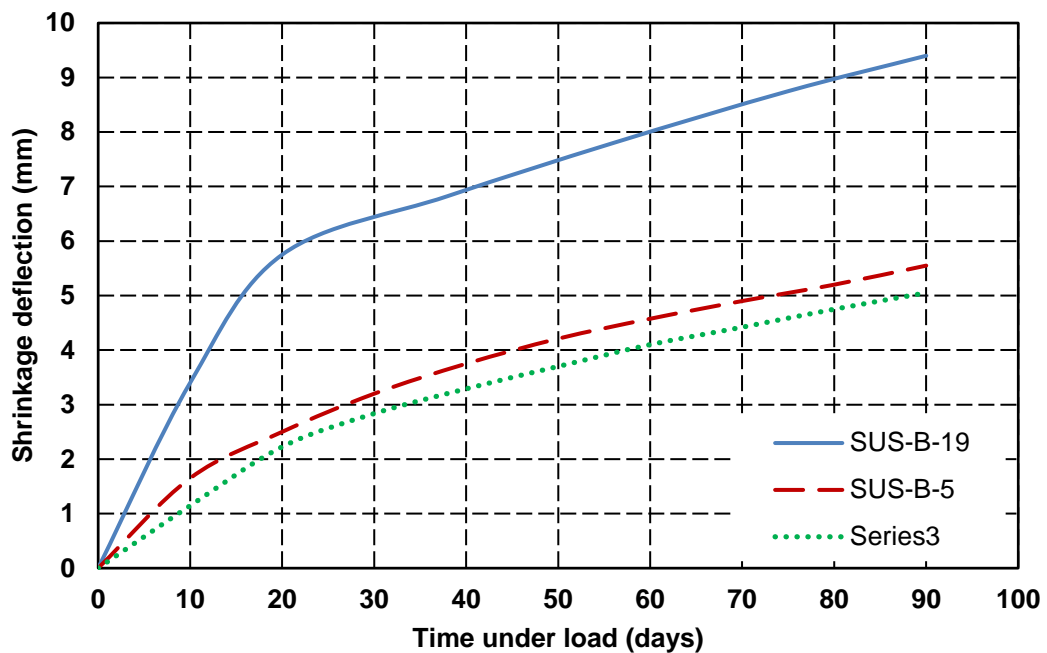
Figure 5-21: Mid-span shrinkage developed deflection with time based on Mu et al (2008)

For the beam with a stabilized crack pattern (i.e. SUS-B-19), no more cracks were produced after loading, whereas both SUS-B-5 and SUS-B-3 developed more cracks during the 90 days testing period. (Note that beam SUS-B-3 was subjected to a sustained load, which produced an applied movement just below the nominal cracking moment.)

Figure 5-22 compares the shrinkage deflections predicted by Eurocode 2 (2004) of the three beams. For the third beam (i.e SUS-B-3), as the sustained moment was less than the cracking moment, the shrinkage deflection predicted by the Eurocode 2 (2004) was calculated twice. The first one from the elastic section and the second using both cracked and uncracked section properties. It can be seen that Eurocode 2 (2004) predicts the shrinkage deflection by considering the degree of cracking, i.e. the shrinkage deflection for SUS-B-19 is higher than that in SUS-B-5 and SUS-B-3 and the shrinkage deflection of SUS-B-5 is higher than that in SUS-B-3.
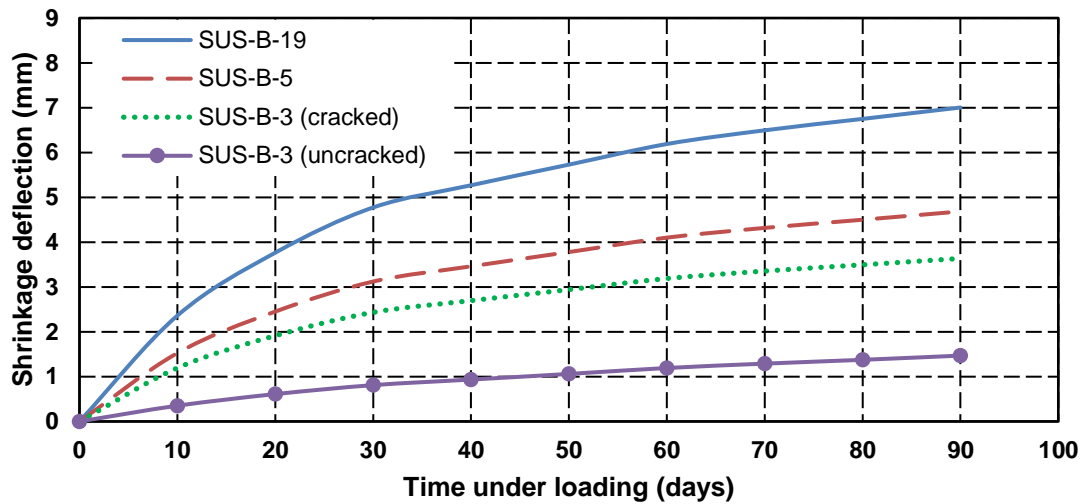
Figure 5-22: Mid-span shrinkage deflection with time based on Eurocode 2

The above figure shows the shrinkage deflection depends on the number of cracks developed in the section. Figure 5-23 shows the calculated shrinkage deflection as a function of the number of cracks. The increase in the shrinkage deflection is linear with the number of cracks.
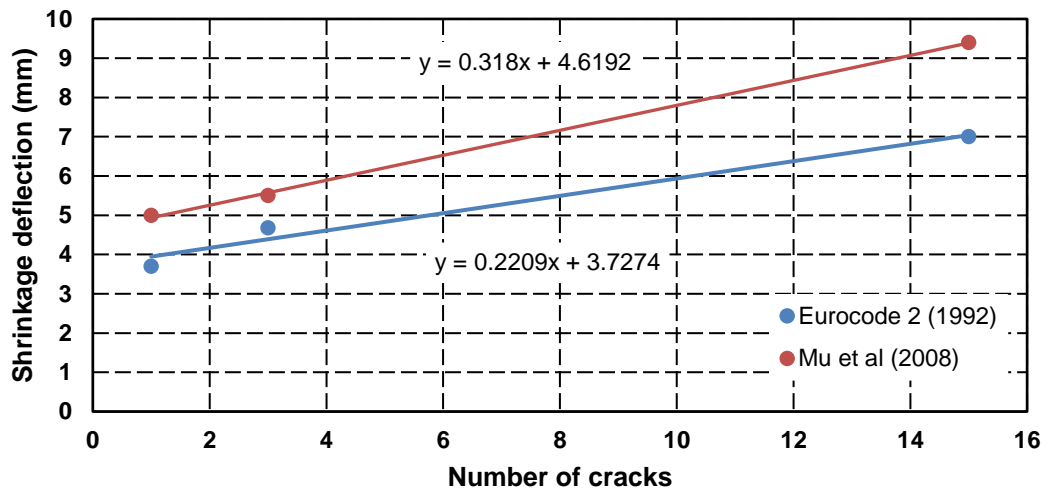
Figure 5-23: Variation of shrinkage deflection with number of cracks

5.7 Extrapolated Deflection From 90 days

As mentioned in section 5.5.1, the mid-span long-term deflection is greater in the repeating load case than in the sustained load case at 90 days, in both the unbonded and fully bonded beams. During the 90 days, the deflection was developed, then stabilized in a hyperbolic shape (the rate of developed deflection in the first 20 days was nearly 5 times than that after 20 days). In this section, the experimentally developed mid-span deflection for the beams under sustained and repeating load will be extrapolated to estimate the ultimate deflection. The aim here is, again, to investigate the use in Eurocode 2 (2004) of a single identical parameter to represent both sustained and repeating long-term loading (i.e. β=0.5). Adopting the theory of the Eurocode 2 (2004) suggests that the ultimate deflection, regardless of load case, will be the same. Although the 90 day data gained during this investigation suggests that this will not be the case, the extrapolation below will allow this to be investigated. The average deflection curve was extrapolated using the Ross (1937) and Lorman (1940) hyperbolic creep model, as show below (Neville et al., 1983):

$$d(t, t_0) = \frac{(t - t_0)}{A + B * (t - t_0)} \qquad (5\text{-}26)$$

Where,

$d(t, t_0)$ is the deflection at anytime

A and *B*   are constants

$t - t_0$ is time under loading (days)

When $(t - t_0)$ reaches infinity, the limiting (ultimate) deflection will be $1/B$. Hence, the limiting deflection can be found from the experimental results by plotting $[(t - t_0)/d(t, t_0)]$ against $(t - t_0)$. The slope of the straight line will be B and the intercept of the ordinate will be A. Figure 5-24 shows the extrapolated developed deflection for the fully bonded beams under sustained and repeating load. The constants A and B for the beams under sustained loading are 1.0966 and 0.042, respectively, and are 0.7901 and 0.0336, respectively, for the beam under repeating load. Thus, the limiting developed deflection for the beam under sustained loading will be 23.8 mm and for the beam under repeated loading, it will be 29.7 mm. This finding disagrees with the Eurocode 2 (2004) and suggests that the beam under sustained loading is unlikely to have the same deflection as the beam under a repeating load.
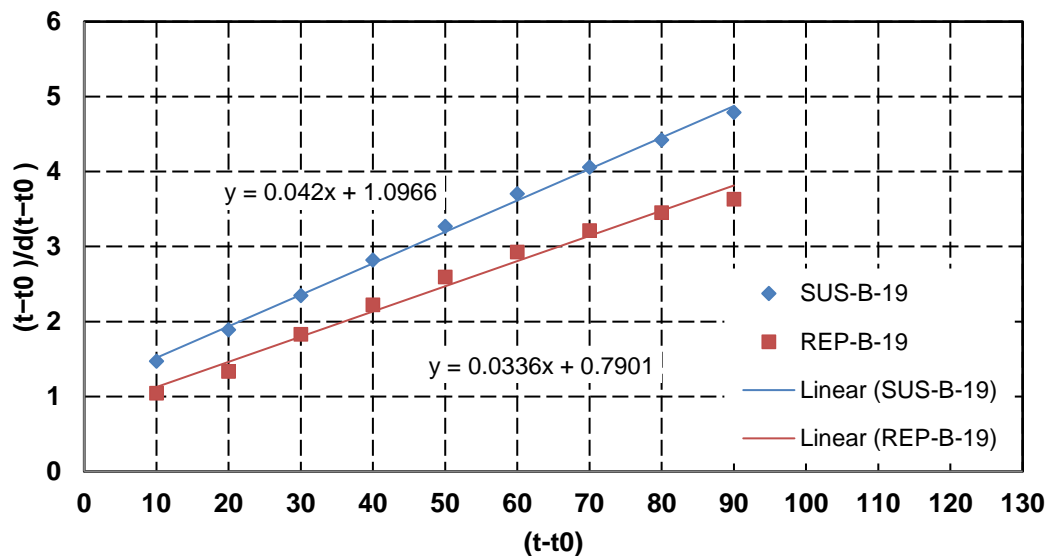
Figure 5-24: Hyperbolic relations proposed by Ross (SUS-B-19 and REP-B-19)

For the case of the unbonded beams of this investigation (Figure 5-25), the ultimate deflection will be 29.7 mm and 31.8 mm for the beam under sustained and repeating loads, respectively. As both beams were effectively debonded (section 4-2 shows the success of artificial deboning), this additional deflection is thought to be due to cyclic creep. It can be noted that the ultimate deflections

are the same for REP-B-19 and SUS-UB-19 (i.e. 29.7 mm), which further illustrates that a small amount of frequency could destroy the bond between the reinforcement and the surrounding concrete.
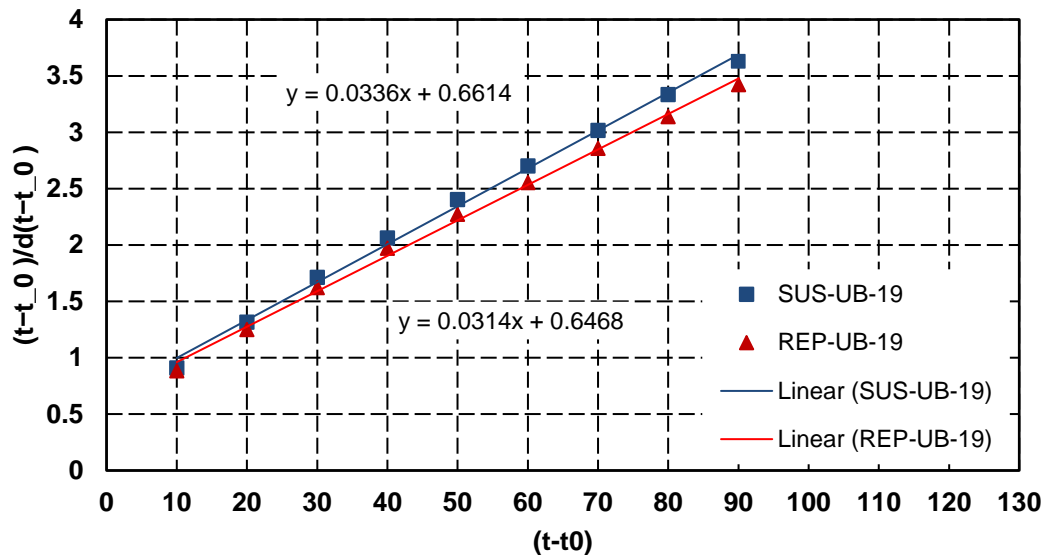
Figure 5-25: Hyperbolic relations proposed by Ross (SUS-UB-19 and REP-UB-19)

A similar procedure was performed by (Higgins et al., 2013). The extracted details of their work are shown in Table 5-3.

Table 5-3: Beam designation and applied load details Higgins et al. (2013)

Beam Reference	Applied Load Type	Mean Applied Load (kN)	Beam Dimensions	Amplitude (kN)	Frequency (Hz)
S	Static Sustained	21	300X150X4200	-	-
C-0.2-5	Cyclic Repeated	21	300X150X4200	5	0.2
C-1-10	Cyclic Repeated	21	300X150X4200	10	1

Figure 5-26 compares the extrapolated developed deflection of the three beams. From Figure 5-26 figure, it can be concluded that the ultimate developed deflection for the beam under sustained loading will be 24.6 mm, while it is 26.4 and 27.4 mm for C-0.2-5 and C-1-10, respectively.
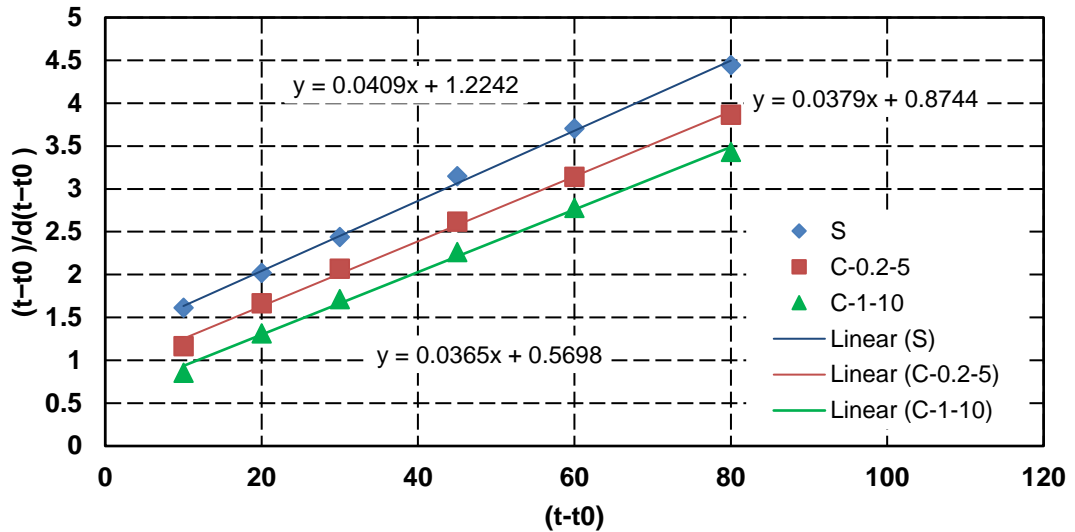
Figure 5-26: Hyperbolic relations proposed by Ross (S, C-0.2-10 and C–1–10)

From Higgins et al. (2013) data it can be seen that the beam under sustained loading, again, is unlikely to have the same deflection as the beam under a repeating load.

However, the difference between the ultimate deflection of REP-B-19 and SUS-B-19 is higher than that of Higgins et al. (2013) beams (i.e. S and C-0.2-5). As the difference is due to the loss of tension stiffening, it indicates that the loss of tension stiffening is higher in our case than Higgins et al. (2013) case. This is because of the creep and the shrinkage strain, which are 1.48 and 410 µε respectively, whereas Higgines et al (2013) long-term material properties, i.e. creep and shrinkage, are 1.1 and 250 µε respectively. It is believed that developing microcracks at the steel concrete interface, due to restraint to shrinkage, leads to decreasing in the tension stiffening (Wu, 2010).

In our case, the shrinkage is almost 40% higher than Higgins et al. (2013). Thus the loss of tension stiffening in REP-B-19 is higher than that in beam C-0.2-5.

5.8 Summary

The current chapter aims to highlight the impact on the loading characteristics on the evaluation (focusing particularly on the long-term deflection) of the deformation of realized reinforced concrete beams, namely the tension stiffening code provisions (i.e. within the Eurocode 2) are reviewed with a clear intention to reassess their operational value and predicted capacity. From above, it can conclude the following:

1. Eurocode 2 (2004) equations to predict the shrinkage overestimate the shrinkage at early ages and underestimate the shrinkage at 90 days, whereas Model Code (2010) overestimates the shrinkage.

2. Both Eurocode 2 (2004) and Model code (2010) equations accurately predict the creep coefficient.

3. The Eurocode 2 (2004) suggested equation to predict the long-term deflection overestimates the deflection in the early ages, especially when the reinforced concrete beams are subjected to a moment close to the crack moment.

4. Under long-term loading, the load factor β is not constant over time (i.e. $\beta=0.5$), and better prediction occurs when β starts with 0.75 and reduces gradually to 0.5.

5. There is a linear relationship between number of cracks and the shrinkage deflection, that is beams which have more cracks develop more deflection due to shrinkage.

6. Beams subjected to repeated loads are unlikely to have the same long-term deflection as beams under sustained loads, i.e. more factors are required for the Eurocode 2 (2004) suggested equation to predict the long-term deflection under repeated loading accurately.

7. In such cases (i.e. shrinkage strain high), low frequency could destroy all the bond between the reinforcement and the surrounding concrete.

Chapter 6 Finite Element Modelling

6.1 Introduction

This chapter provides details of the nonlinear analysis of reinforced concrete beams under sustained and repeated loading, using a commercial finite element software, i.e Midas FEA. Firstly, the nonlinear analysis was based on the evaluation on the material proprieties (creep and shrinkage). To prove the accuracy of the nonlinear finite element software, the result was compared with experimental data presented in Chapter 4. The concrete was modelled as a 3D solid box. For the long-term behaviour, "construction stages" must be defined in analysis of the beam, to reflect the effect of evolving in material properties with time (creep and shrinkage displacements). Thus, concrete is considered as an isotropic elastic material to enable (creep/shrinkage) functions to be included. According to CEB-FIP Model Code (1990), for elastic analysis of concrete, a reduced modulus of elasticity should be used to reflect the initial plastic strain, thus the modulus of elasticity of concrete was multiplied by 0.85. It is important to activate the weight density of the concrete in the long-term analysis, as the dead load should be considered.

Midas FEA allows the input of creep and shrinkage values, along with the strength parameters of concrete, to conduct the analysis. However, Midas FEA is flexible about the code used (CEB-FIP 1990, ACI, PCA, Combined ACI, PCA and AASHTO), when it comes to defining shrinkage strain and creep coefficient. In this study, the experimental creep and shrinkage data relied only on direct input.

6.2 Element Types and Used Mesh

Solid elements are generally used to model 3-D solid structures such as concrete and are suitable for both linear and nonlinear analysis. Midas FEA solid elements are:

Linear elements, such as 4 node tetrahedron, 6 node pentahedron or 8 node hexahedron (brick element).

Quadratic elements, like 10 node tetrahedron, 15 node pentahedron or 20 node hexahedron quadratic elements are shown in Figure 6-1.

Tetrahedron

Pentahedron

Hexahedron

Linear elements   Quadratic elements
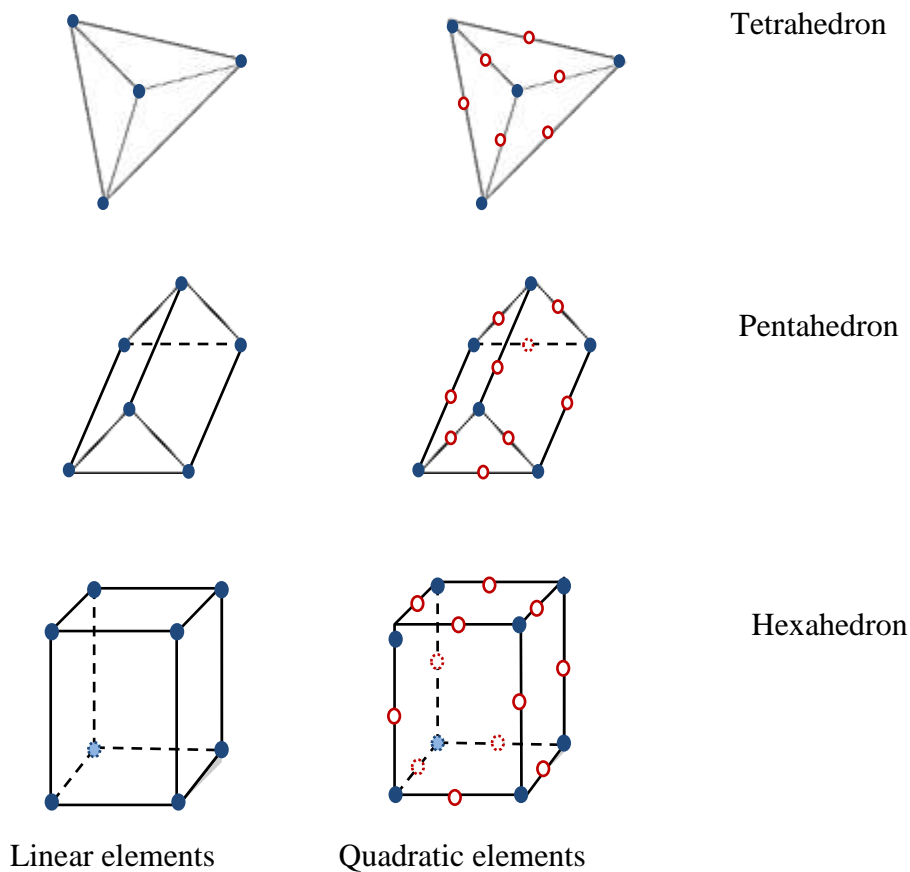
Figure 6-1: Midas FEA solid elements type

Linear hexahedron, or quadratic, elements are suggested by the Midas FEA company to give an accurate output when detailed analysis results are

required. In this chapter, an element sensitivity study was undertaken to conclude the best element for the analysis.

For the steel reinforcement, Midas FEA provides a bar reinforcement element, in which the steel properties can be defined. As the reinforcement is embedded inside the concrete, the bar section is necessary to define where the reinforcement and their concrete mother elements (i.e. elements in the solid section) are assumed to be perfectly bonded.

Figure 6-2 illustrates the general process that Midas FEA follows to generate 3D mesh of any solid section. Firstly, 1D mesh is created on the boundary edges, followed by 2D mesh on the surfaces of the selected section. After generating 1D and 2D mesh, Midas FEA creates 3D elements in the internal space. Mesh sensitivity was studied to find the most appropriate mesh for the concrete model. Auto-Mesh Edge was used, as it is the only provided way to mesh the reinforcement. The software suggested that the reinforcement element size should be the same as the concrete element size.
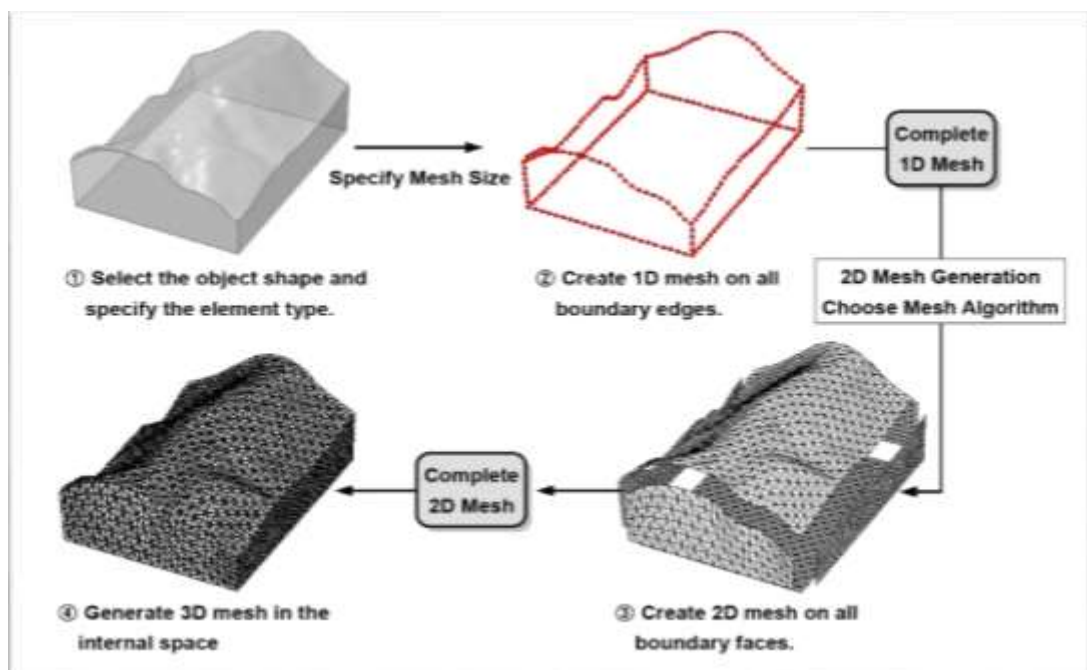
Figure 6-2: General process for mesh generation

6.3 Construction Stages

Midas FEA allows time affects to take place in the analysis by defining construction stages. Firstly, a base model was developed by assigning elements, loads and boundary conditions in order to define the construction stages. The next stages were defined based on the constitution order. Midas FEA allows the user to start with a duration of 0 days and a possibility of changing boundary conditions and loading in each stage. The unlimited number of stages during the analyses makes the result more accurate. The illustration of the construction stages concept is shown in Figure 6-3.
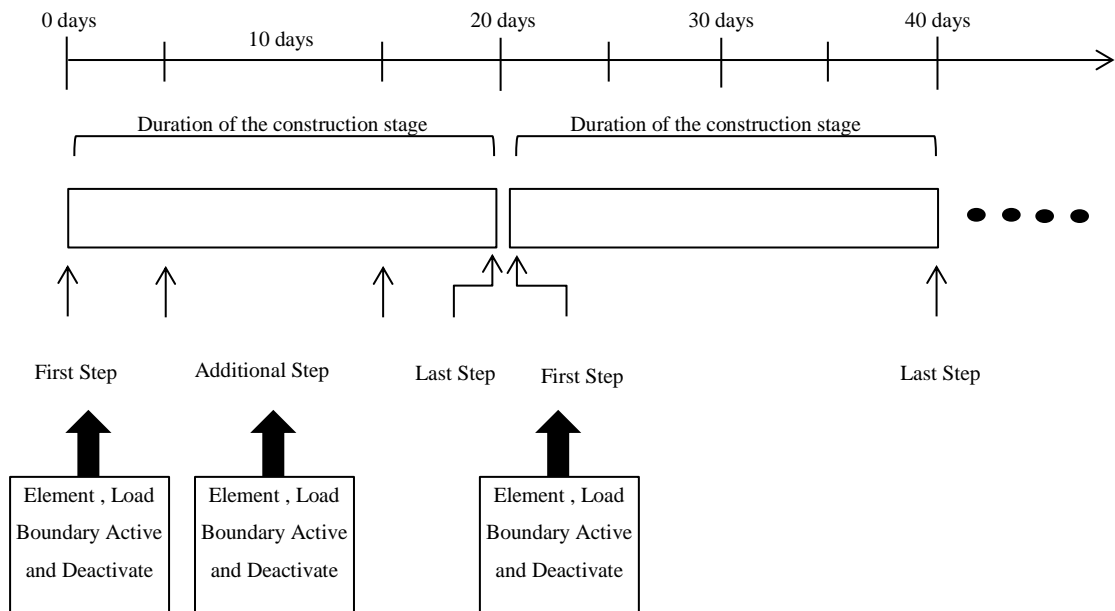
Figure 6-3: Concept of composing construction stages

In this study, 9 construction stages were defined, with recordings taken every 10 days, similar to the experimental data gathered. The elements used, the loads and the boundary conditions were activated in the first stage, i.e t = 0 to get the elastic deflection, at an element age of 28 days. Though it is not necessary to activate elements, loads and boundary conditions in the next stages, or the element age in the following stages, as they were activated in the first stage, it is necessary to allocate the duration of each stage.

6.4 Sensitivity Study

6.4.1 Effect of Element Type and Mesh Size on the Deflection

There are two mesh types Midas FEA provides to use: map mesh, for structured mesh and auto mesh, for unstructured mesh, as shown in Figure 6-4.

Structured mesh   Unstructured mesh
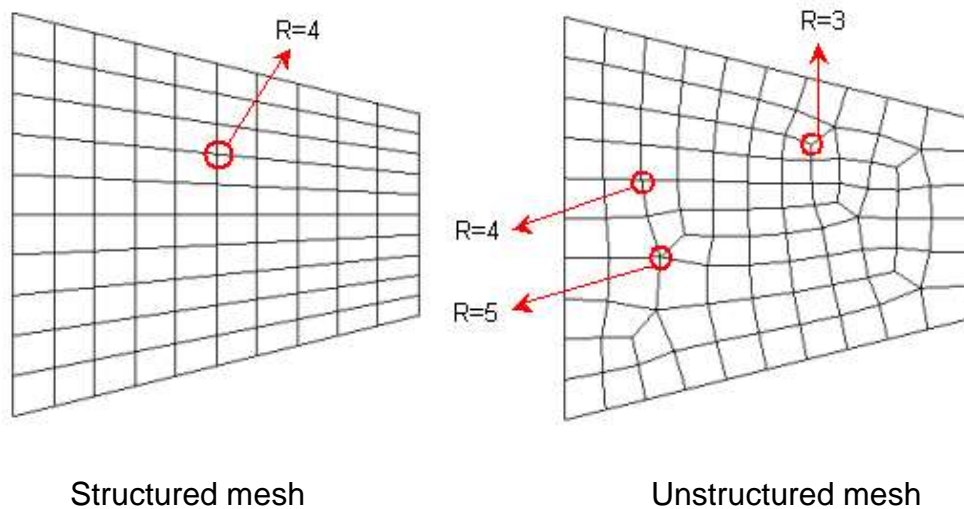
Figure 6-4: Midas FEA mesh types

The effect of the element types and mesh size of the reinforced concrete beams under long-term sustained loads was tested by changing the element types and mesh size, and plotting the corresponding time-deflection behaviour. SUS-B19 was simulated, as the concrete between cracks were elastic and no more cracks developed during the test. Figure 6-5 and Figure 6-6 illustrate the convergence of the result for each element type and mesh size, respectively.

Figure 6-5 shows, map mesh element type (linear or quadratic) does not affect the analysis, while in auto mesh, quadratic elements gave better estimation than linear elements. However, both linear and quadratic elements underestimate the long-term developed deflection. Therefore, the mesh size was carried on linear map mesh, as shown in Figure 6-6.

138

Four mesh sizes (i.e. 100 mm, 50 mm, 25 mm and 10 mm) were used to find the adequate mesh size. Although concrete was modelled as an elastic material, Figure 6-6 shows that the lower mesh size, the better behaviour. The model with 10 mm element size (189000 elements) took 28 hours to give the final results. Thus, in this study 25 mm linear map mesh was used in the analysis to give better estimates and to save time.
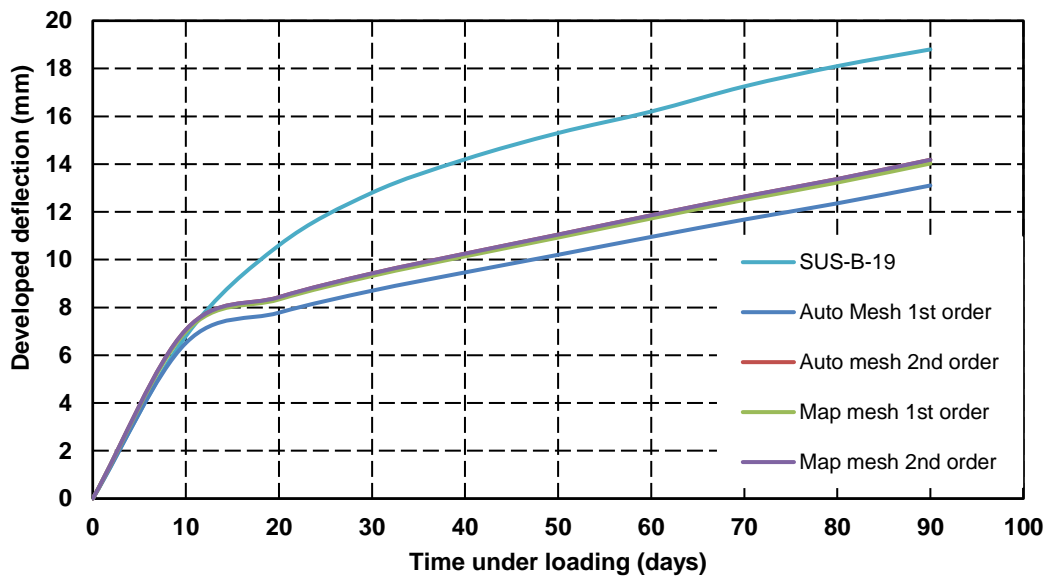
Figure 6-5: Effect of mesh types on the long-term deflection (mesh size 25 mm)
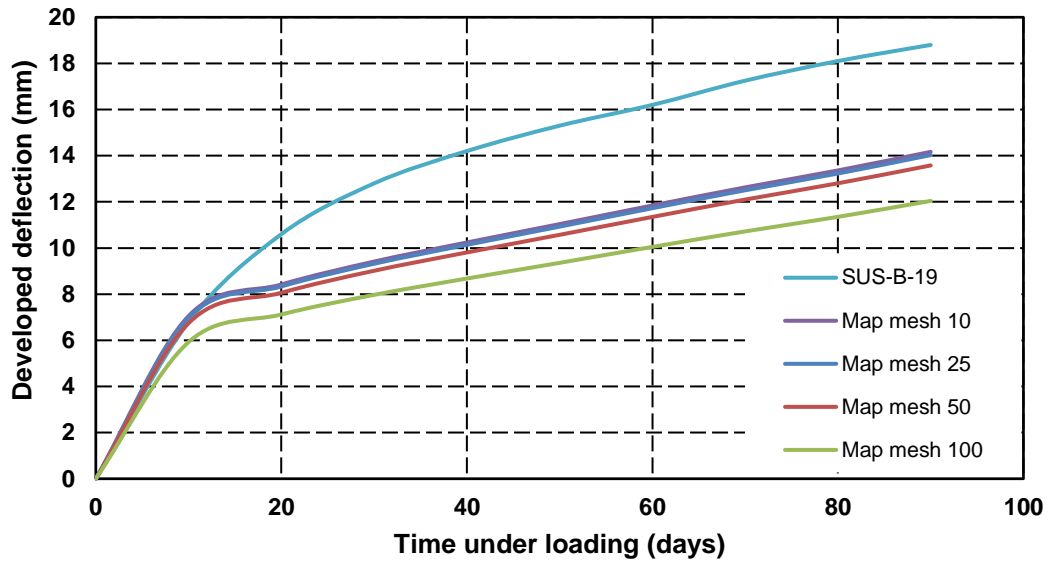
Figure 6-6: Effect of mesh size on the long-term deflection

6.5 Predicting the Long-Term Deflection Using Midas FEA

6.5.1 Beams under Sustained Loading

In Midas FEA, the total long-term curvature results from the summation of the individually calculated creep and shrinkage curvatures; the total long-term deflection can, therefore, be separated into creep and shrinkage deflection. Figures 6-7a, 6-7b and 6-7c show the graphical comparison of the experimental and numerical-developed mid-span deflection of the selected reinforced concrete beams under 19 kN, 5 kN and 3 kN of sustained loads, respectively.

The software underestimates the long-term developed mid-span deflection in all cases, likely from the creep or shrinkage deflection (as Midas FEA ignores the tension stiffening effect). Midas FEA separates shrinkage and creep deflections, making it possible to examine which deflection is underestimated (i.e. creep deflection or shrinkage deflection). Figures 6-7a, 6-7b and 6-7c

show that the creep deflection is a function of the sustained load, i.e. the creep deflection in Figure 6-7a is higher than that in Figures 6-7b and 6-7c and the creep deflection in Figure 6-7b is higher than that in Figure 6-7c. This indicates that the underestimation is in the shrinkage deflection. In same figures, it can be seen that the shrinkage deflection in all cases, irrespective of load level, is the same. This contradicts the published literature (Mu et al., 2008) and the previous assessment of long-term deflection being due to creep and shrinkage equally. Previously, it was found that the deflection due to creep and shrinkage depended on the cracking level (Marí et al., 2010). Daud et al. (2015) attributed the inability of Midas FEA to correctly predict the long-term deflections to the section geometry, pointing out that the reinforced concrete beam, which was modelled as elastic, does not have uniformly distributed shrinkage applied throughout its cross-section.

Time Under Load (days)
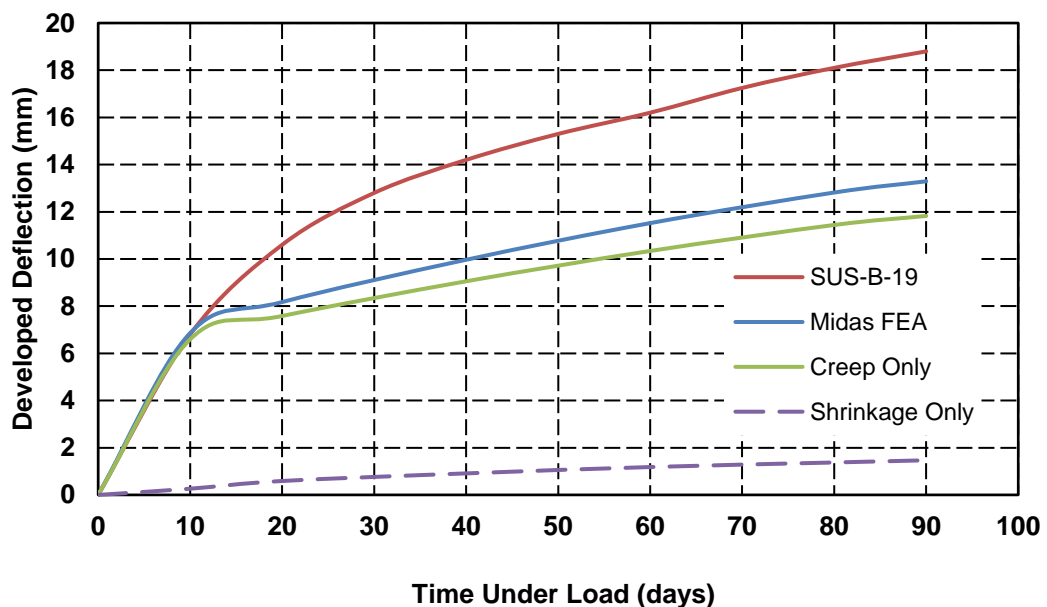
(a)
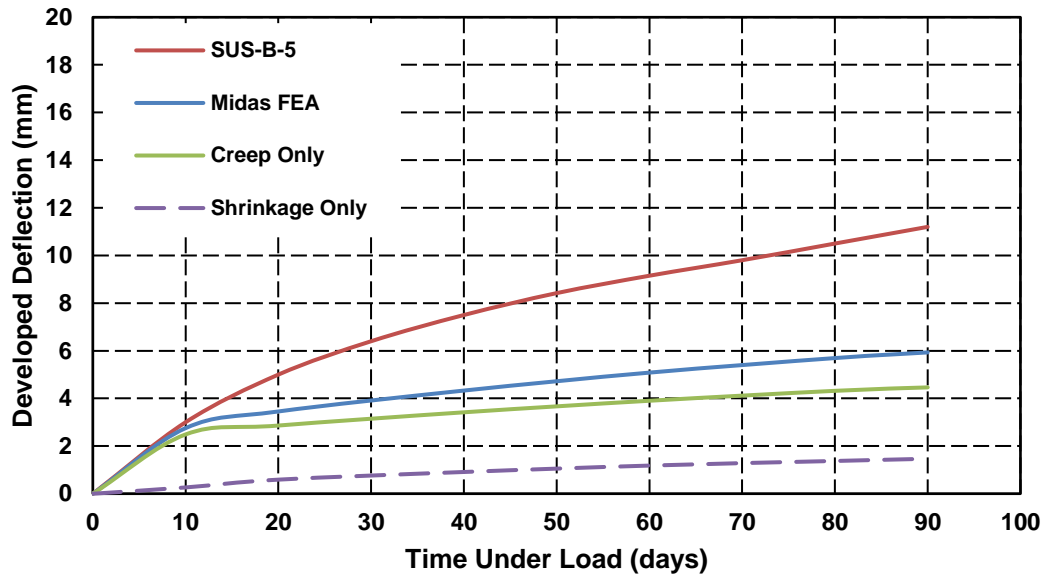
(b)
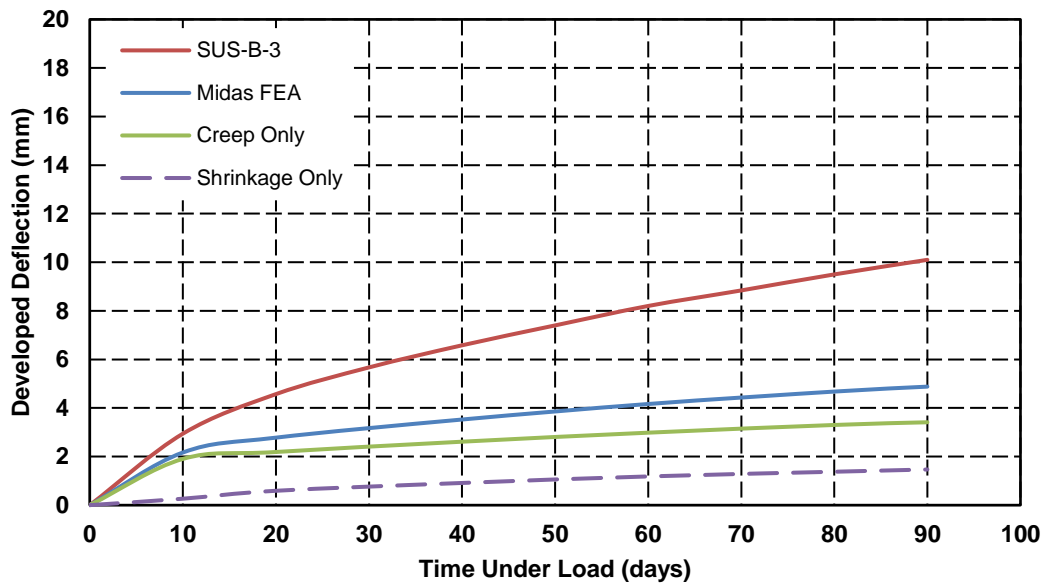
(c)

Figure 6-7: Mid-span developed deflection with time (a) SUS-B-19
(b) SUS-B-5 (c) SUS-B-3

Moreover, the limited capability of the software does not allow for simulation of repeated/cycled loadings when it comes to simulating beams under repeated loading. For these reasons, and in order to address this limitation, the beam segment was divided into two sections (i.e., compression and tension section), as indicated in Figure 6-8.
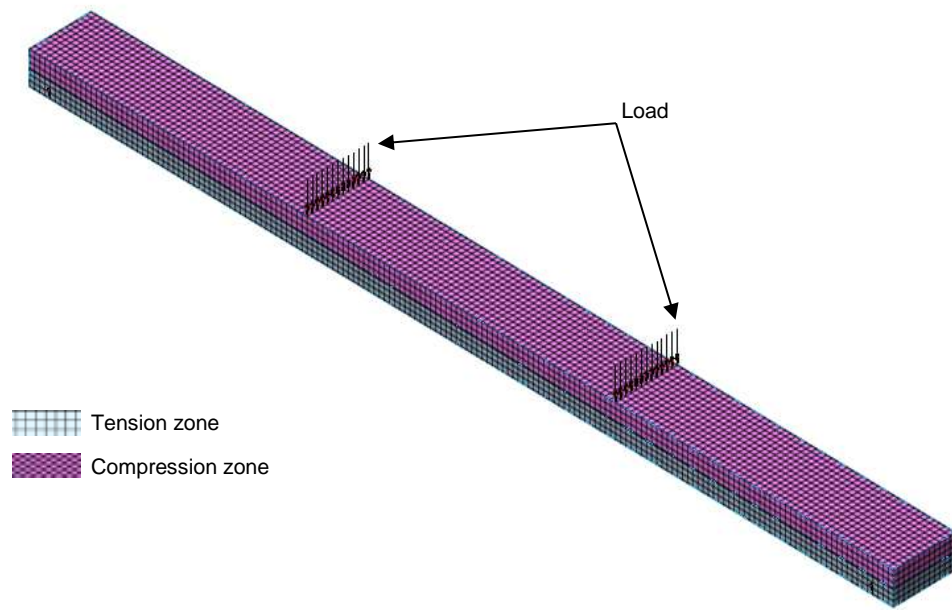
Figure 6-8: Beam model - Midas FEA

In the compression zone (red), all the shrinkage provision was applied as expected, however in the tension zone, different percentages of shrinkage were parametrically applied until an appropriate amount of shrinkage satisfied the experimental deflection, and the surface strain matched the experimental results. The lesser amount of shrinkage in the tension zone represents the shrinkage percentage in the cracked section, as the total curvature results from the cracked and uncracked section. The tension section depth was selected to be twice the cover depth, as the neutral axis depends on the loading amount. In this study, the comparison between the experimental and finite elements will be on the developed deflection, as cracks developed with time on beams SUS-

B-5 and SUS-B-3 and Midas FEA assumes the concrete is elastic in order to activate creep and shrinkage functions. However, for the case of stabilized crack patterns, the concrete between cracks is elastic, as long as no secondary cracks develop.

For the first beams (i.e. SUS-B-19), Figure 6-9 shows the developed mid-span deflection with time. Three different values of relatively low shrinkage percentages were applied in the tension zone (i.e. 0%, 10% and 20%). The 0% shrinkage was the first attempt to give an indication on the long-term behaviour where there is no shrinkage effect in the tension zone. The 0% shrinkage in the tension zone overestimated the developed deflection (still with a good estimation at less than 20% difference). Thus two more values were applied to find the most appropriate value of shrinkage in tension zone. Figure 6-9 shows these different values of shrinkage, bringing the overall long-term mid-span developed deflection behaviour close to the experimental observations, allowing the software to predict its development with time.
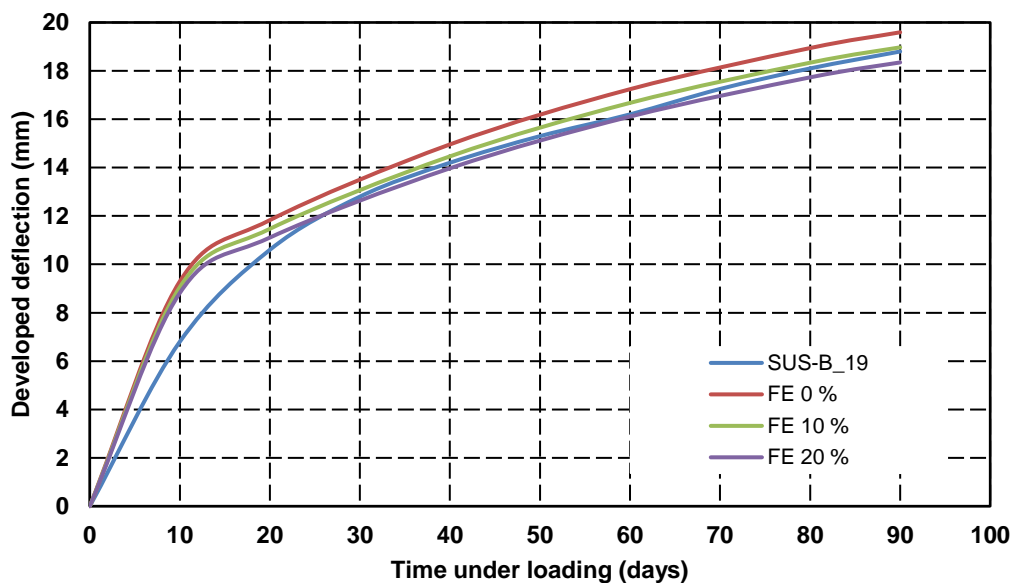
Figure 6-9: Mid-span developed deflection vs. time under load (SUS-B-19 and Midas FEA)

Also, regardless of the fraction of shrinkage applied, the evolving displacement renders a very close match to experiments at 90 days, which evidently sets the question of which value would be best to choose. For this reason, Table 6-1 compares further the experimental mid-span deflection and surface strain outputs against that produced by the numerical model in order to recover the optimum value of the shrinkage to be used in the tension zone. Namely it identifies that the mid-span deflection is getting relatively closer to the test measurements when the shrinkage in the tension zone is considered equal to 10% of the shrinkage in the compression zone.

Table 6-1: Numerical mid-span deflection development results for SUS-B-19

Deformation	Experiment	FE 0% shrinkage	Exp/FE	FE 10% shrinkage	Exp/FE	FE 20% shrinkage	Exp/FE
Deflection (mm)	18.8	19.6	1.04	18.9	1	18.3	0.94

Similarly, different values of shrinkage in the tension zone were applied for the other two beams (i.e. SUS.B.5 and SUS-B-3). For SUS-B-5 the shrinkage percentages in the tension zone were 15%, 20% and 25%. Figure 6-11 illustrates the behaviour of the simulated SUS-B-5 after applying the modification. Figure 6-11 and Table 6-2 show that 15% shrinkage in the tension zone gives the most accurate production.
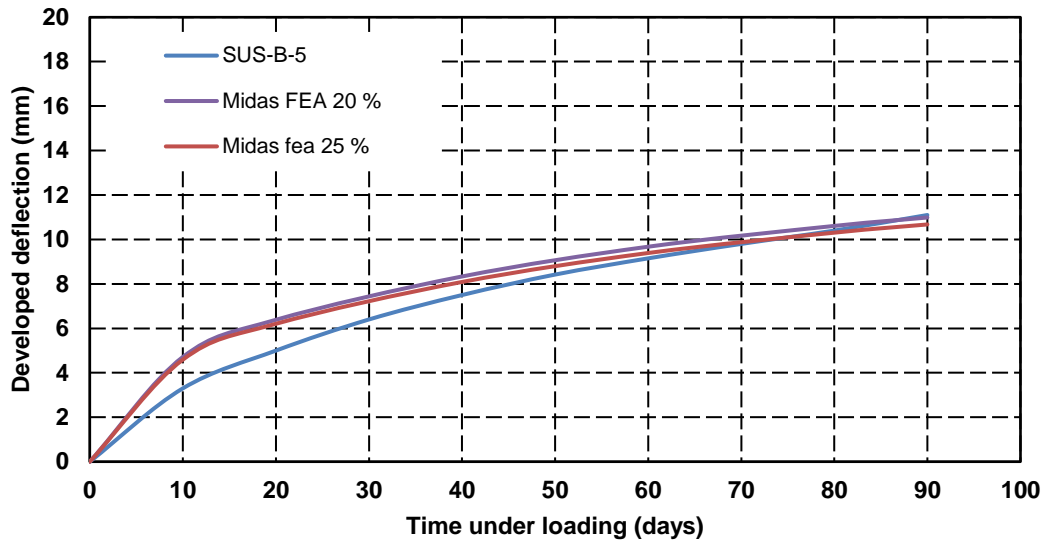
Figure 6-10: Mid-span developed deflection vs. time under load (SUS-B-5 and Midas FEA

Table 6-2: Numerical mid-span deflection development results for SUS-B-5

Deformation	Experiment	FE 15 % shrinkage	Exp/FE	FE 20 % shrinkage	Exp/FE	FE 25 % shrinkage	Exp/FE
Deflection (mm)	11.1	11.3	1.01	10.9	0.98	10.6	0.95

Twenty percent, 25% and 30% were the shrinkage percentages that were applied in the tension zone for the third beam, i.e. SUS-B-3 . Figure 6-12 and Table 6-3 compare the developed deflection predicted by Midas FEA when the shrinkage is not uniform all over the section with that found from the experiment. Both Figure 6-12 and Table 6-3 show good agreement between the experimental and Midas FEA after the modification. However, 25% shrinkage in the tension zone is the best value applied to the tension zone to make Midas FEA predict the deflection accurately.
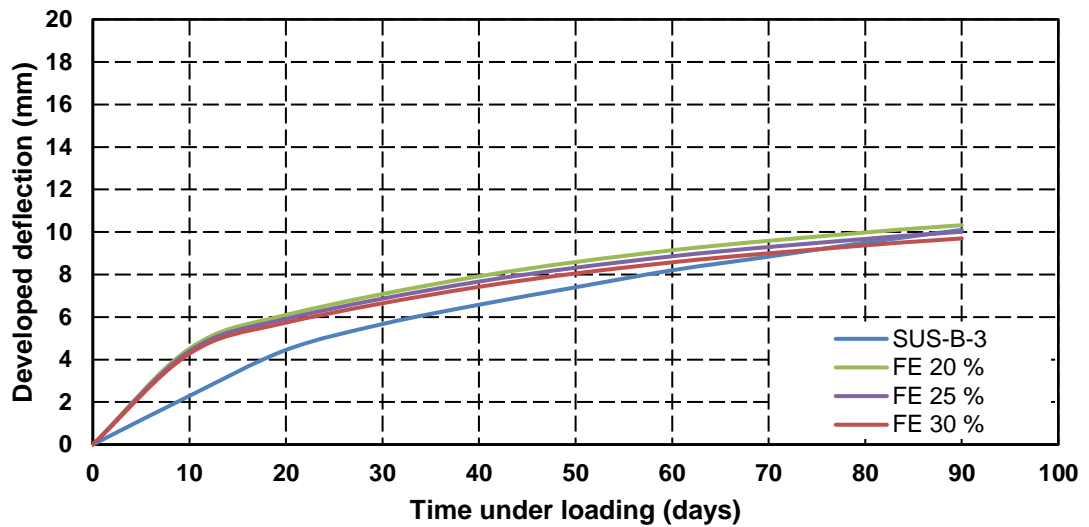
Figure 6-11: Mid-span developed deflection vs. time under load (SUS-B-3 and Midas FE

Table 6-3: Numerical mid-span deflection development results for SUS-B-3

Deformation	Experiment	FE 20% shrinkage	Exp/FE	FE 25% shrinkage	Exp/FE	FE 30% shrinkage	Exp/FE
Deflection (mm)	10.1	10.3	1.02	10.01	0.99	9.7	0.96

From this section, the data indicates that, as the cracks developed from one crack to stabilized crack patterns, the shrinkage percentages in the tension zone were varied from 15% to 25%. This shows that shrinkage percentages in the tension zone depend on the number of cracks, i.e. beams having higher number of cracks are expected to have less shrinkage percentage in the tension zone. This agrees with the outcome of section 5.6, i.e. shrinkage curvature depends on the number of cracks in tension zone.

In addition, it can be seen from Figure 6-11 and Figure 6-12 that in the early ages the software Midas FEA developed more deflection than the tested beams. This higher deflection in the early ages results from the neutral axis position. In this study the tension zone was 72 mm. However, the neutral axis position is not constant, as it depends on the amount of the applied moment and the shrinkage strain in concrete (Forth et al., 2014). In addition, Midas FEA uses the Eurocode 2 (2004) equations to predict the deflection and the Eurocode 2 (2004) overestimates the deflection in the early stages, as shown previously in section 5.5.1. Additionally the software overestimates the deflection in the beams SUS-B-5 and SUS-B-3 because the software assumes the concrete is elastic, while in these two beams more cracks developed during the test. In contrast, in the case of stabilized crack patterns, the concrete between cracks is elastic, as long as no secondary cracks develop. This means that the shrinkage percentage in the tension zone is affected by the number of cracks.

Figure 6-13 shows the effect of the number of cracks on the percentage of the shrinkage in the tension zone. Once the first cracks develop and the concrete transforms from uncracked into cracked status, the shrinkage percentage drops from the full amount (i.e. 100%) to 25% and reaches 10% when the reinforced concrete beams reach stabilized crack pattern. This variation in the shrinkage percentages in the tension zone explains the effect of cracks on long-term deflection of cracked members. That could explain the findings of El-Badry (1988), i.e. the long-term deflection in reinforced concrete beams is more significant in cracked members (Nie and Chie 2000).
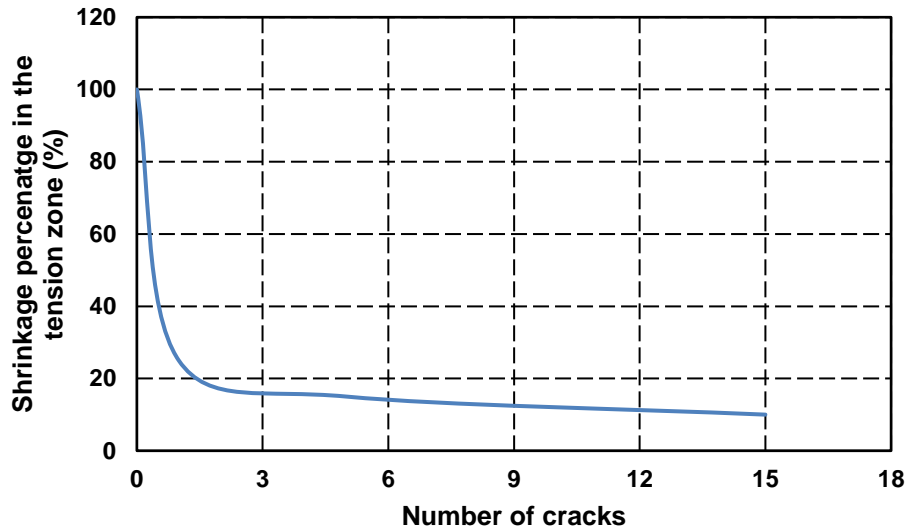
Figure 6-12: shrinkage percentage in tension zone vs number of cracks

6.5.2 Beams under Repeated Loading

For the second case (i.e debonded beams), the standard numerical FE idealisation could not predict accurately the time-dependant behaviour for either the mid-span deflection or the surface strain. Thus, the same approximate technique was adopted in the simulation of debonded beams (whereby reducing the shrinkage in tension zone yields a better match to experiments). The shrinkage percentage parametric variation in this case was taken as 40%, 50% and 60%, which is more than that in the case of a fully bonded beam. This is due to the number of cracks (i.e. nominally inhibiting shrinkage deflection) being higher in the fully bonded beam than in the debonded beam. Along these lines, it was previously found that once cracking has developed, the modulus of elasticity of the concrete surrounding the reinforcement is reduced (Forth et al., 2014). In such a case and with the reinforcement fully debonded from the concrete mass, the modulus of elasticity of the tension zone is 10% that of the normal concrete.
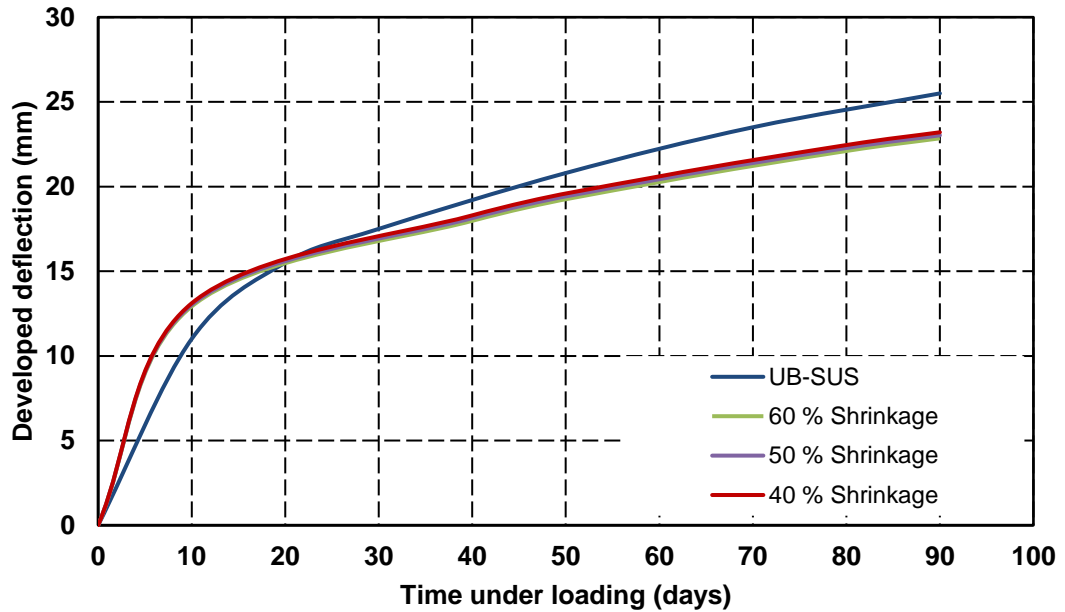
Figure 6-13: Mid-span developed deflection vs. time under load (SUS-UB-19 and Midas FEA)

In Figure 6-14, combining experimental and numerical model findings, it can be seen that for the relatively early beam ages (below 10 days), both the mid-span deflection and surface strain in the tension zone are over-predicted by the FE solutions. Such an overshoot can be justified when the creep contribution is considered the same for both compression and tension, while Forth (2015) stated that the rate of creep in compression is higher than that in tension creep.

After 20 days, there is better agreement between the experimental results with those predicted by the Midas FEA for both the monitored behaviour variables. Table 6-4 compares the mid-span deflections of the tested beams with the finite element models. It can be seen that 50% shrinkage in the tension zone gives the best prediction.

Table 6-4: Numerical mid-span deflection and surface strain development results for SUS-UB-19 beams

Deformation	Experiment	40% shrinkage	Exp/FE	50% shrinkage	Exp/FE	60% shrinkage	Exp/FE
Deflection (mm)	25.5	23.2	110 %	23.02	110 %	22.8	112 %

6.6 Verification of the Numerical Model

Two other cases will be used to verify this model and will confirm that the procedure used in this chapter, i.e. the shrinkage, is not uniform over the entire section and that this method is not only used for a specific geometry.

In the first case, a reinforced concrete beam of dimensions 4200 mm long with a cross section of 300 X 150 mm and the same materials properties was used. The main difference with this beam is its reinforcement condition, at a symmetrical reinforcement of 3 Ø 16 mm in both compression and tension zone.

The second case is Mias et al. (2013) reinforced concrete beams. Their reinforced concrete beams have different geometry, material properties and reinforcement conditions. They tested two beams for 250 days (N_L1_S10 and N-L2_S10) and the other two beams for 700 days (H_L1_S10 and H_L2_S10).

The first case, i.e. SUS-SYB-19, was simulated by applying 10% shrinkage in the tension zone, as this beam was subjected to the stabilized crack patterns and the same number of cracks developed. Figure 6-15 indicated that Midas FEA predicted the developed deflection accurately after applying the necessary modification. However, Midas FEA overestimates the deflection by 8%, which is still acceptable. This 8% overestimation in Midas FEA developed

deflection might result in the neutral axis position (i.e. tension zone), whereas for cases of symmetrical reinforcement, the tension zone will be higher than 72 mm.
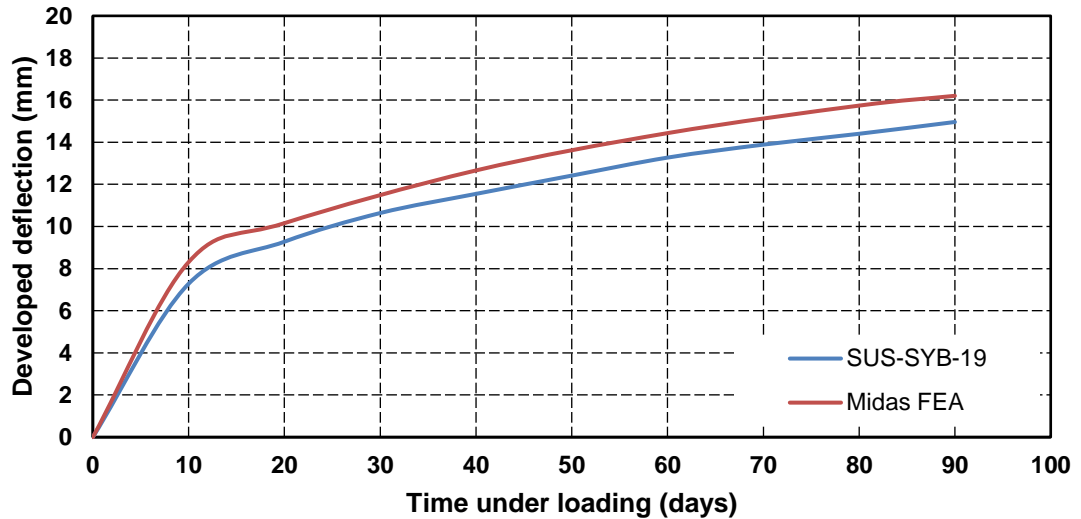
Figure 6-14: Mid-span developed deflection vs. time under load (SUS-SYB-19 and Midas FEA

For the second case, four reinforced concrete beams were simulated (i.e. N_L1_S10, N-L2_S10, H_L1_S10 and H_L2_S10). Figures 6-16, 6-17, 6-18 and 6-19 compare the mid-span developed deflection of Mias et al. (2013) with that predicted by Midas FEA. Midas FEA predicts the development accurately with good agreement, after the shrinkage is reduced in the tension zone.
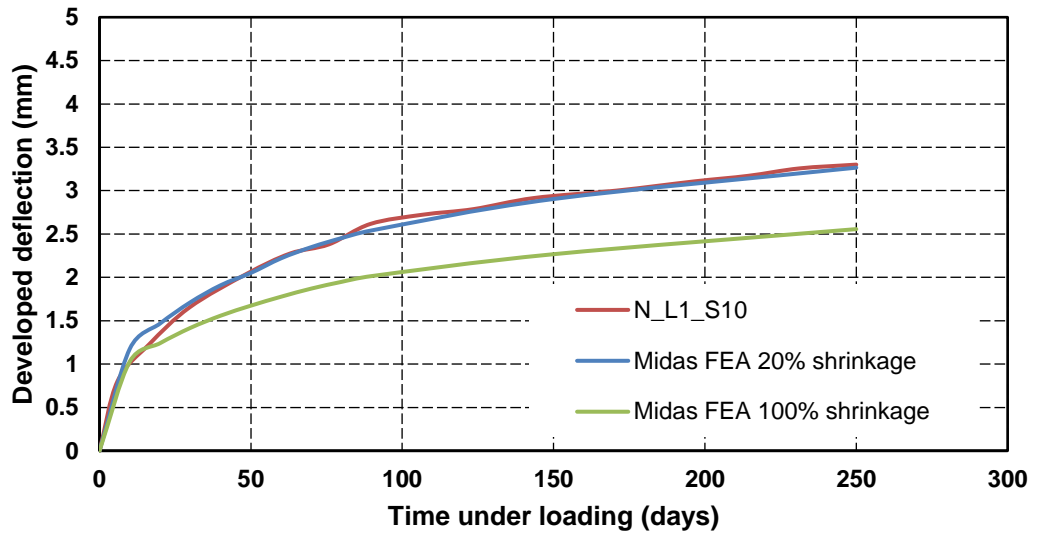
Figure 6-15: Mid-span developed deflection vs. time under load (N_L1_S10 and Midas FEA
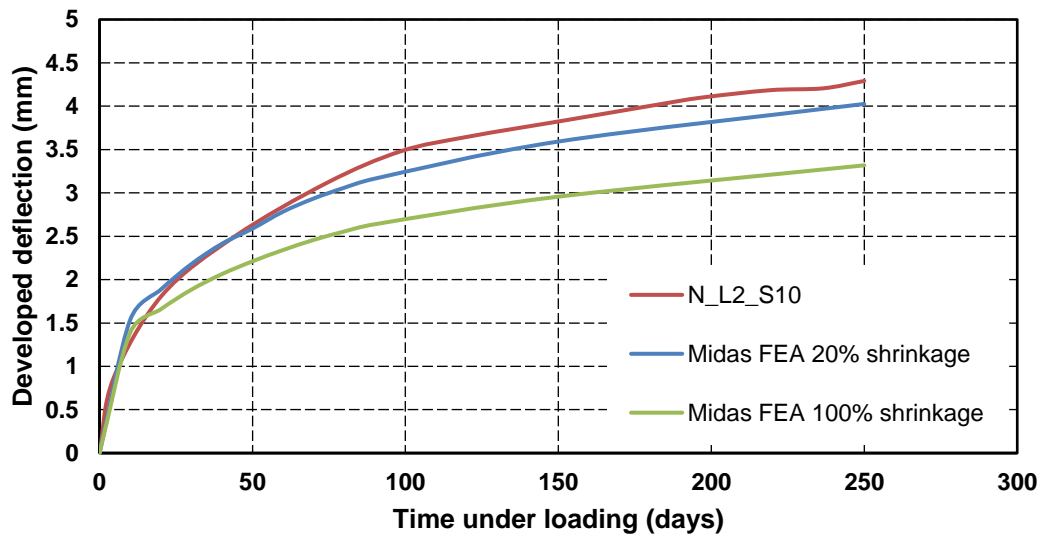
Figure 6-16: Mid-span developed deflection vs. time under load (N_L2_S10 and Midas FEA
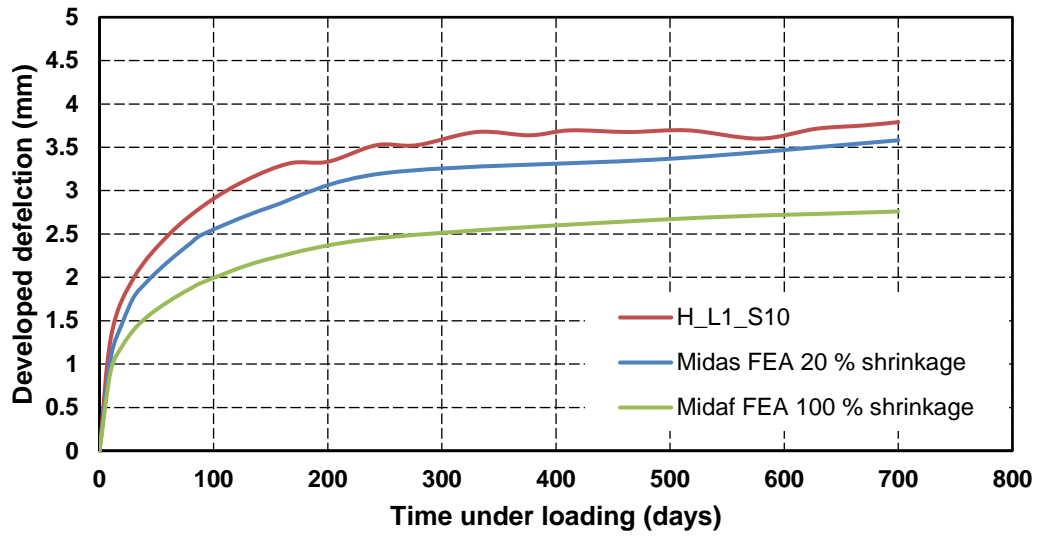
Figure 6-17: Mid-span developed deflection vs. time under load (H_L1_S10 and Midas FEA
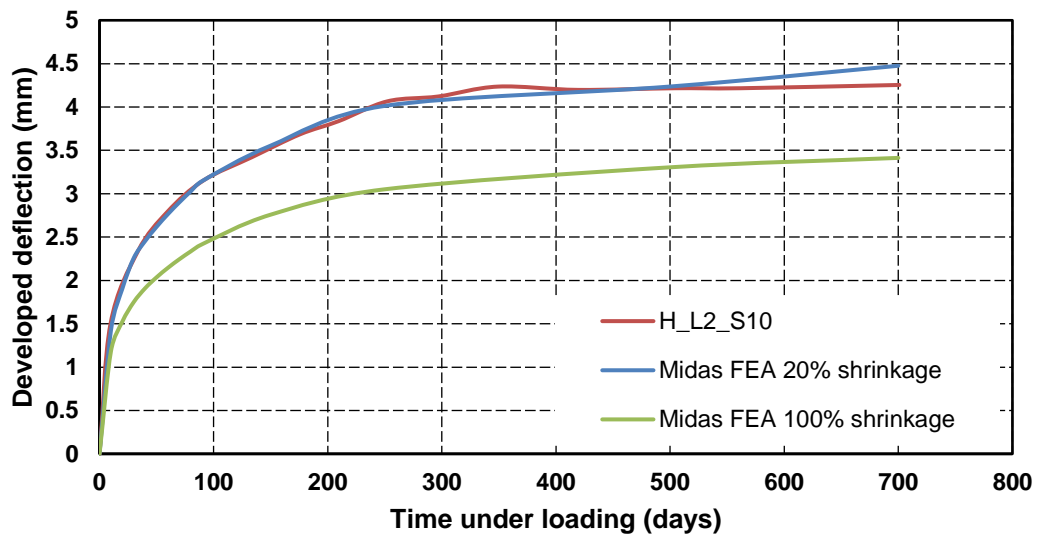
Figure 6-18: Mid-span developed deflection vs. time under load (H_L2_S10 and Midas FEA

6.7 Numerical Elimination of Shrinkage Curvature

The change of material behaviour over time (i.e. creep, shrinkage and tension stiffening) was considered in the analysis above to find the holistic long-term behaviour of the reinforced concrete beams. However, to eliminate the shrinkage effect from the analysis, the shrinkage contribution was artificially nullified so that the long-term mid-span deflection predictions are solely due to creep and tension stiffening. Relevant to this, Figure 6-19 illustrates the mid-span deflection due to creep and tension stiffening for the distinct cases of sustained and repeated loads on identical beams. There is a much more rapid initial increase in the mid-span deflection in the case of repeated loading. Namely, after 10 days the beam under repeated load has 4.2 mm mid-span deflection more than the one with the sustained load. In this sense, the results are in good agreement with Higgins et al. (2013), where the additional deformations in both tension and compression zones caused by repeated loading mostly occur within the first 10 days. After this period, both beams presented approximately the same deflection development rate.

As the shrinkage was eliminated for SUS-B-19 and REP-B-19 beams, Figure 6-19 shows the long-term deflection of these two beams due to the loss of tension stiffening. The difference of the long-term deflection of these two beams is 4.2 mm, which is the tension stiffening contribution on the overall deflection, i.e. 10% from the overall deflection; the overall deflection for the fully bonded reinforcement beam under sustained loading was 43.8 mm at the end of the test.
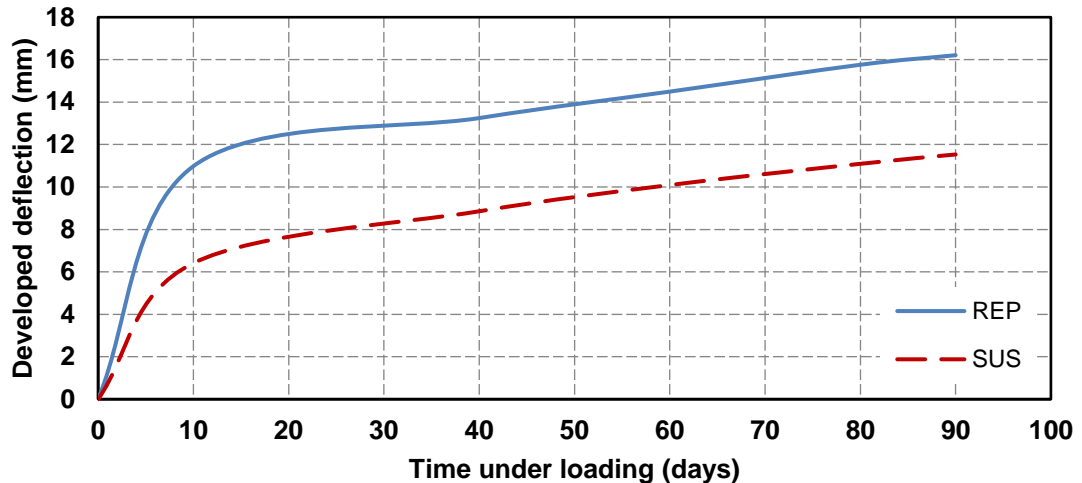
Figure 6-19: Mid-span deflection due to lose of tension stiffening

6.8 Summary

In this chapter, a nonlinear finite element software was employed to simulate the long-term deflection of reinforced concrete beams under sustained and repeated loads. Firstly, the way of shrinkage distribution over the cross section does not allow the software to predict the long-term deflection accurately. A necessary modification to the shrinkage distribution was applied. After the modification, the following conclusions can be drawn:

1. In the stabilised crack stage, concrete between cracks acts elastically.
2. Shrinkage curvature is a function of the number of cracks, i.e. beams having higher number of cracks develop more deflection.
3. For beams under sustained loading, Midas FEA needs to adopt only 10% of the shrinkage in the tension zone in the case of fully cracked sections, while it is 15% and 25% when the section has one crack and 5 cracks, respectively.
4. For the case of repeated loading, 50% shrinkage in the tension zone and the modulus of the elasticity should be reduced.

5. 4.2 mm is the deflection due to loss of tension stiffening, which is about 10% from the overall deflection.

Chapter 7 Conclusions and Recommendations for Future Works

7.1 Introduction

The current thesis aims to investigate the long-term behaviour of reinforced concrete beams under sustained and repeated loading and the factors effecting it, such as creep, shrinkage and tension stiffening. Both experimental and finite element simulation were used to achieve these goals. Throughout this study, it is possible to assist the Eurocode 2 (2004) suggested equation to predict the long-term deflection. Based on the aforementioned idea, the following sections provide the detailed conclusions obtained from this work.

7.2 Conclusions.

From each part of this investigation, the following conclusions can be drawn.

7.2.1 Experimental Conclusions

1. There was about 94% bond strength lost when the reinforcement ribs were ground away.
2. The bond between concrete and steel in reinforced concrete beams subjected to a repeating load can be significantly damaged due to the loading, even though the frequency is relatively low (i.e. 0.2 H_z).
3. The additional deformation caused by repeated loads have shown to occur within 10 to 20 days, depending on the material properties.
4. For the case of cyclic repeated loading, more coefficients should be involved in the Eurocode 2 (2004) equation to reflect the repeated loading effects in long-term loading.

5. The behaviour of fully bonded reinforced concrete beams under a small amount of amplitude and frequency repeated loading was almost the same as reinforced concrete beams with debonded reinforcement.

6. Beams having a high amount of compression reinforcement have less developed deflection with time.

7. Compression reinforcement does not have significant effect on the number of cracks nor the surface strain development in the tension zone.

8. The long-term mid-span developed deflection of the artificially debonded beams subjected to sustained loading is higher than that for fully bonded beams by 36%.

9. The long-term deflection starts only a single day after the sustained loading has been applied.

10. In the case of stabilized crack patterns, the concrete between the cracks acts elastically.

11. As expected, creep and dry shrinkage induced cracks are a function of the sustained applied moment. For higher sustained moments (i.e. closer to the stabilized crack pattern), fewer cracks will develop after initial loading.

7.2.2 Theoretical Conclusions

1. Eurocode 2 (2004) equations to predict the shrinkage overestimate the shrinkage at early ages and underestimate the shrinkage at 90 days, whereas Model Code (2010) overestimates the shrinkage.

2. Eurocode 2 (2004) and Model Code (2010) predict creep coefficient accurately.

3. The Eurocode 2 (2004) equation to predict the long-term deflection overestimates the deflection in the first ages, especially when the reinforced concrete beams are subjected to a moment close to the cracking moment.

4. Under long-term loading, the load factor β is not constant at all times (i.e. β=0.5). Better predictions are made when β starts with 0.75 and reduces gradually to 0.5.

5. There is a linear relationship between number of cracks and the shrinkage deflection; beams with more cracks develop more deflection due to shrinkage.

6. Beams subjected to repeated loads are unlikely to have the same deflection as beams under sustained loads, i.e. more factors should be applied to the Eurocode 2 (2004) equation to predict the long-term deflection under repeated loading.

7. In such cases (i.e. shrinkage strain high), low frequency destroys all the bond between the reinforcement and the surrounding concrete.

7.2.3 Numerical Conclusions

1. In the stabilised crack stage, concrete between cracks acts elastically.

2. Shrinkage curvature is a function of the number of cracks, i.e. beams having higher number of cracks develop more deflection.

3. For beams under sustained loading, Midas FEA needs to adopt only 10% of the shrinkage in the tension zone in the case of fully cracked sections, while it is 15% and 25% when the section has one crack and 5 cracks, respectively.

4. For the case of repeated loading, 50% shrinkage in the tension zone and the modulus of the elasticity should be reduced.

5. 4.2 mm is the deflection due to loss of tension stiffening, which is about 10% from the overall deflection.

7.3 Recommendations and Future Works

Based on the experimental work carried out in this thesis and the simulation results, the following future investigations are proposed:

1. More experimental tests can be conducted to investigate the influence of material properties (i.e. weight concrete, ultra-high strength concrete) on the long-term deflection of debonded reinforced concrete beams.

2. Further to the current research, a study of the long-term behaviour of reinforced concrete slabs under cyclic loading is recommended, as in real conditions, slabs are more likely subjected to cyclic loads.

3. Flexural behaviour of fully cracked steel fibre reinforced concrete beams under long-term loading need to be investigated in order to study the effect of adding steel fibre on the loss of tension stiffening.

4. Further research is required to understand the bond behaviour of corroded reinforcement.

References

ABRISHAMI, H. H. & MITCHELL, D. 1996. Analysis of Bond Stress Distributions in Pullout Specimens. *Journal of Structural Engineering,* 122**,** 255-261.

ACI COMMITTEE. 2014. Building code requirements for structural concrete (ACI 318-14) and commentary. *ACI, Farmington Hills, United States.*

AHMED , K. T. A. A. 2013. *Long Term Deflection of High Performance Reinforced Concrete Beam.* PhD Thesis, Univeristy of Leeds.

ALMUSALLAM, A. A., AL-GAHTANI, A. S. & AZIZ, A. R. 1996. Effect of reinforcement corrosion on bond strength. *Construction and building materials,* 10**,** 123-129.

BAKOSS, S. L., GILBERT, R. I., FAULKES, K. A. & PULMANO, V. A. 1982. Long-Term Deflections of Reinforced Concrete Beams. *Magazine of Concrete Research,* 34**,** 203-212.

BAZANT, Z. P. 1972. Prediction of Concrete Creep Effects Using Age-Adjusted Effective Modulus Method. *ACI journal,* 69**,** 212-217.

BAZANT, Z. P. 1975. Theory of Creep and Shrinkage in Concrete Structures: A Precis of Recent Developments. *Mechanics Today,* 2**,** 1-93.

BAZANT, Z. P. & OH, B. H. 1983. Spacing of Cracks in Reinforced Concrete. *Journal of structural Engineering,* 109**,** 2066-2085.

BEEBY, A. & SCOTT, R. 2004a. Tension Stiffening of Concrete, Behaviour of Tension Zones in Reinforced Concrete including Time Dependent Effects. Supplementary Information, The Concrete Society. Camberley, Technical Report 59.

BEEBY, A. W. & SCOTT, R. H. 2004b. Insights into the Cracking and Tension Stiffening Behaviour of Reinforced Concrete Tension Members Revealed by Computer Modelling. *Magazine of concrete research,* 56**,** 179-190.

BENTUR, A., IGARASHI, S.-I. & KOVLER, K. 2001. Prevention of Autogenous Shrinkage in High-Strength Concrete by Internal Curing Using Wet Lightweight Aggregates. *Cement and Concrete Research,* 31**,** 1587-1591.

BHATTACHARYA, S. 2014. Challenges in Design of Foundations for Offshore Wind Turbines. *Engineering & Technology Reference,* 1.

BROOKS, J. 2003. *Elasticity, shrinkage, creep and thermal movement, Advanced Concrete Technology: Concrete Properties*, Butterworth-Heinemann.

BS EN 197-1: 2011. Cement. Composition, specifications and conformity criteria for common cements. *British Standerds Institution*

BS EN 206: 2013+A1:2016. Concrete. Specification, performance, production and conformity. *British Standerds Institution.*

BS EN 1008: 2002. Mixing water for concrete. Specification for sampling, testing and assessing the suitability of water, including water recovered from processes in the concrete industry, as mixing water for concrete. *British Standerds Institution.*

BS EN 12350-2 2009. Testing fresh concrete. Slump-test. British Standard Institute, London.

BS EN 12390-3: 2009. Testing hardened concrete. Compressive strength of test specimens. *British Standerds Institution*

References

BS EN 12390-5: 2009. Testing hardened concrete. Flexural strength of test specimens. *British Standerds Institution*

BS EN 12620: 2002 +A1:2008. Aggregates for concrete. *British standered Institution*

BUETTNER, D. R. & HOLLRAH, R. L. Creep recovery of plain concrete. Journal Proceedings, 1968. 452-461.

CABRERA, J. & GHODDOUSSI, P. The Effect of Reinforcement Corrosion on the Strength of the Steel/Concrete Bond. Int. Conf., Bond in Concrete—from Res. to Pract, 1992. 10.11-10.24.

CARLSON, R. W. Drying Shrinkage of Large Concrete Members. Journal Proceedings, 1937. 327-336.

CEB-FIP 1990. *CEB-FIP Model Code 1990 : Design Code, Comite Euro-International du Béton*, T. Telford.

CHEN, G. & BAKER, G. 2003. Influence of Bond Slip on Crack Spacing in Numerical Modeling of Reinforced Concrete. *Journal of Structural Engineering,* 129**,** 1514-1521.

CHONG, K. T., FOSTER, S. J. & GILBERT, R. I. 2008. Time-Dependent Modelling of RC Structures Using The Cracked Membrane Model and Solidification Theory. *Computers & Structures,* 86**,** 1305-1317.

CLARKE, G., SCHOLZ, H. & ALEXANDER, M. 1988. New Method to Predict the Creep Deflection of Cracked Reinforced Concrete Flexural Members. *ACI Materials Journal*.

CORLEY, W. G. & SOZEN, M. A. Time-Dependent Deflections Reinforced Concrete Beams. Aci Journal Proceedings, 1966. 373-386.

COUNTO, U. J. 1964. The effect of the elastic modulus of the aggregate on the elastic modulus, creep and creep recovery of concrete. *Magazine of Concrete Research,* 16**,** 129-138.

DAUD, S., FORTH, J. P. & NIKITAS, N. Time-Dependent Behaviour of Reinforced Concrete Beams under Sustained and Repeated Loading. World Academy of Science, Engineering and Technology, 2015.

DAUD, S., FORTH, J. P. & NIKITAS, N. 2016. Time-Dependent Behavior of Reinforced Concrete Beams under Sustained Loading. *Environment, Efficiency and Economic Challenges for Concrete.* Dundee, Scotland

DEMIS, S., PILAKOUTAS, K. & APOSTOLOPOULOS, C. 2010. Effect of corrosion on bond strength of steel and non-metallic reinforcement. *Materials and corrosion,* 61**,** 328-331.

DEZI, L., IANNI, C. & TARANTINO, A. M. 1993. Simplified Creep Analysis of Composite Beams with Flexible Connectors. *Journal of Structural Engineering,* 119**,** 1484-1497.

EDWARDS, A. & YANNOPOULOS, P. Local Bond-Stress to Slip Relationships for Hot Rolled Deformed Bars and Mild Steel Plain Bars. Journal Proceedings, 1979. 405-420.

EL-BADRY, M. M. 1988. *Serviceability of reinforced concrete structures*, Civil Engineering, University of Calgary.

References

EL-ZAROUG, O. R. 2008. *Flexural Behaviour of Concrete Slabs Reinforced with GFRP Rebar Subjected to Varying Temperature Histories.* PhD Thesis University of Leeds.

EL MAADDAWY, T., SOUDKI, K. & TOPPER, T. 2005. Long-Term Performance of Corrosion-Damaged Reinforced Concrete Beams. *ACI Structural Journal,* 102**,** 649.

ESPION, B. & HALLEUX, P. 1990. Long-Term Deflections of Reinforced Concrete Beams: Reconsideration of Their Validity. *Structural Journal,* 87**,** 232-236.

EUROCODE 2 2004. *Design of Concrete Structures / British Standards Institution: Part 1-1: General Rules and Rules for Buildings,* London, British Standards Institution.

EYRE, J. & NOKHASTEH, M. 1992. Strength assessment of corrosion damaged reinforced concrete slabs and beams. *Proceedings of the Institution of Civil Engineers-Structures and Buildings,* 94**,** 197-203.

FABER, O. Plastic Yield, Shrinkage, and Other Problems of Concrete, and their Effect on Design. Minutes of the Proceedings, 1928. Thomas Telford, 27-73.

FANG, C., LUNDGREN, K., CHEN, L. & ZHU, C. 2004. Corrosion Influence on Bond in Reinforced Concrete. *Cement and Concrete Research,* 34**,** 2159-2167.

FELDMAN, L. R. & BARTLETT, F. M. 2007. Bond Stresses Along Plain Steel Reinforcing Bars in Pullout Specimens. *ACI Structural Journal,* 104**,** 685.

FELDMAN, L. R. & BARTLETT, F. M. 2008. Bond in Flexural Members with Plain Steel Reinforcement. *ACI Structural Journal,* 105**,** 552.

FORTH, J. P. 2015. Predicting The Tensile Creep of Concrete. *Cement and Concrete Composites,* 55**,** 70-80.

FORTH, J. P. & BEEBY, A. W. 2014. Study of Composite Behavior of Reinforcement and Concrete in Tension. *ACI Structural Journal,* 111**,** 397-406.

FORTH, J. P., BROOKS, J. J. & BINGEL, P. R. 2003. Movement in a Seven Storey Reinforced Concrete Frame. *Proceedings of the Institution of Civil Engineers-Structures and Buildings,* 156**,** 131-140.

FORTH, J. P., MU, R., SCOTT, R. H., JONES, A. E. & BEEBY, A. W. 2014. Verification of Cracked Section Shrinkage Curvature Models. *Proceedings of the ICE-Structures and Buildings,* 167**,** 274-284.

GAMBHIR, M. L. 2013. *Concrete technology: theory and practice*, Tata McGraw-Hill Education.

GARCIA-TAENGUA, E., MARTÍ-VARGAS, J. & SERNA, P. 2016. Bond of reinforcing bars to steel fiber reinforced concrete. *Construction and Building Materials,* 105**,** 275-284.

GERGELY, P. & LUTZ, L. A. 1968. Maximum crack width in reinforced concrete flexural members. *ACI , SP-20***,** pp 87-117.

GHALI, A. 1993. Deflection of Reinforced Concrete Members: A Critical Review. *ACI Structural Journal,* 90**,** 364-373.

GILBERT, R. 2001. Shrinkage Cracking and Deflection The Serviceability of Concrete Structures. *Electronic Journal of Structural Engineering,* 1**,** 2-14.

GILBERT, R. 2002. Creep and shrinkage models for high strength concrete–proposals for inclusion in AS3600. *Australian Journal of Structural Engineering,* 4**,** 95-106.

References

GILBERT, R. I. 1988. *Time Effects in Concrete Structures,* Amsterdam, Elsevier.

GILBERT, R. I. 1999. Deflection calculation for reinforced concrete structures—why we sometimes get it wrong. *Structural Journal,* 96**,** 1027-1032.

GILBERT, R. I. Calculation of Long-Term Deflection. CIA Seminar. Brisbane, 2008.

GILBERT, R. I. & RANZI, G. 2010. *Time-Dependent Behaviour of Concrete Structures*, CRC Press.

GILKEY, H. & ERNST, G. Report of Project Committee on Use of High Elastic Limit Steel as Reinforcement for Concr~ te, Sustained Loading Tests on Slender Concrete Beams Reinforced with High Elastic Limit Steel. Proceedings, 1935. 81.

GOTO, Y. 1971. Cracks formed in concrete around deformed tension bars. *ACI,* 68**,** 244-251.

GRIBNIAK, V., BACINSKAS, D., KACIANAUSKAS, R., KAKLAUSKAS, G. & TORRES, L. 2013. Long-Term Deflections of Reinforced Concrete Elements: Accuracy Analysis of Predictions by Different Methods. *Mechanics of Time-Dependent Materials,* 17**,** 297-313.

GRIBNIAK, V., KAKLAUSKAS, G. & BACINSKAS, D. 2008. Shrinkage in reinforced concrete structures: A computational aspect. *Journal of Civil Engineering and Management,* 14**,** 49-60.

HALL, T. & GHALI, A. 2000. Long-term deflection prediction of concrete members reinforced with glass fibre reinforced polymer bars. *Canadian Journal of Civil Engineering,* 27**,** 890-898.

HAMAD, B. S. 1979. *Effect of Casting Position on Development of Anchored Reinforcement.* Doctoral dissertation, Graduate School of the University of Texas at Austin.

HANSEN, T. C. & MATTOCK, A. H. Influence of Size and Shape of Member on the Shrinkage and Creep of Concrete. Journal Proceedings, 1966. 267-290.

HARANKI, B. 2009. *Strength, Modulus of Elasticity, Creep and Shrinkage of Concrete Used in Florida.* M.Sc, University of Florida.

HAWKINS, N. M., LIN, I. & JEANG, F. 1982. Local Bond Strength of Concrete for Cyclic Reversed Loadings. *Bond in concrete***,** 151-161.

HIGGINS, L., FORTH, J. P., NEVILLE, A., JONES, R. & HODGSON, T. 2013. Behaviour of Cracked Reinforced Concrete Beams under Repeated and Sustained Load Types. *Engineering Structures,* 56**,** 457-465.

HOBBS, D. 1982. Shrinkage and Load Induced Curvature of Reinforced Concrete Beams. *Fundamental Research on Creep and Shrinkage of Concrete.* Springer.

HOLT, E. E. 2001. *Early Age Autogenous Shrinkage of Concrete*, Technical Research Centre of Finland.

JAYASINGHE, T. 2011. *Prediction of Time-dependent Deformations in Post-tensioned Concrete Suspended Beams and Slabs in Tall Buildings.* Ph.D, RMIT University.

JNAID, F. & ABOUTAHA, R. 2015. Nonlinear Finite Element Modeling of Unbonded Steel Reinforced Concrete Beams. *World Academy of Science, Engineering and Technology,* 2**,** 6.

JNAID, F. & ABOUTAHA, R. S. 2014. Residual Flexural Strength of RC Beams with Unbonded Reinforcement. *ACI Structural Journal,* 111.

References

JONES, M. R., FORTH, J. P., THISTLETHWAITE, C. & HIGGINS, L. 2012. Reducing the Variability of Predicting the Longevity of Reinforced Concrete Marine Structures Subjected to Physical and Chemical Degradation. *Concrete in the low carbon era, proceedings of the International Conference.* Dundee, Scotland.

KIM, Y., SIM, J. & PARK, C. 2012. Mechanical properties of recycled aggregate concrete with deformed steel re-bar. *Journal of marine science and technology,* 20**,** 274-280.

KIMURA, H. & JIRSA, J. O. 1992. *Effects of bar deformation and concrete strength on bond of reinforcing steel to Concrete*, Phil M. Ferguson Structural Engineering Laboratory, University of Texas at Austin.

KOHNO, K., OKAMOTO, T., ISIKAWA, Y., SIBATA, T. & MORI, H. 1999. Effects of Artificial Lightweight Aggregate on Autogenous Shrinkage of Concrete. *Cement and Concrete Research,* 29**,** 611-614.

KRISHNAKUMAR, S., SAM, A., JAYASREE, S. & THOMAS, J. 2013. Bond strength of concrete containing crushed concrete aggregate (CCA). *Am. J. Eng. Res***,** 1-6.

LAM, J. P. 2002. *Evaluation of Concrete Shrinkage and creep Prediction Models.* M.Sc, San Jose State University.

LI, Y., BAO, J. & GUO, Y. 2010. The Relationship Between Autogenous Shrinkage and Pore Structure of Cement Paste With Mineral Admixtures. *Construction and Building Materials,* 24**,** 1855-1860.

LIU, Y. 2007. *Strength, Modulus of Elasticity, Shrinkage and Creep of Concrete.* Phd, University of Florida.

LORMAN, W. R. 1940. Theory of Concrete Creep. *Proc. Am. Soc. Test. Mater,* 40**,** 1082-1102.

MALUMBELA, G., ALEXANDER, M. & MOYO, P. 2009. Steel Corrosion on RC Structures Under Sustained Service Loads—A Critical Review. *Engineering Structures,* 31**,** 2518-2525.

MANGAT, P. & ELGARF, M. 1999. Bond Characteristics of Corrding Reinforcement in Concrete Beams. *Materials and Structures,* 32**,** 89-97.

MARÍ, A. R., BAIRÁN, J. M. & DUARTE, N. 2010. Long-Term Deflections in Cracked Reinforced Concrete Flexural Members. *Engineering Structures,* 32**,** 829-842.

MIAS, C., TORRES, L., TURON, A. & SHARAKY, I. 2013. Effect of Material Properties on Long-Term Deflections of GFRP Reinforced Concrete Beams. *Construction and Building Materials,* 41**,** 99-108.

MO, Y. & CHAN, J. 1996. Bond and slip of plain rebars in concrete. *Journal of materials in Civil Engineering,* 8**,** 208-211.

MODEL CODE 2010. fib Model Code for Concrete Structures 2010:First complete draft – volume 1. BERLIN 55: ERNST & SOHN.

MOHAMMED, T. U., OTSUKI, N., HISADA, M. & SHIBATA, T. 2001. Effect of Crack Width and Bar Types on Corrosionof Steel in Concrete. *Journal of Materials in Civil Engineering,* 13**,** 194-201.

MU, R., FORTH, J. P., BEEBY, A. W. & SCOTT, R. 2008. Modelling of Shrinkage Induced Curvature of Cracked Concrete Beams. *Tailor Made Concrete Solutions (Walraven JC and Steelhurst D (eds)). Taylor & Francis, Abingdon, UK***,** 573-578.

References

NEILD, S., WILLIAMS, M. & MCFADDEN, P. 2002. Non-Linear Behaviour of Reinforced Concrete Beams Under Low-Amplitude Cyclic and Vibration Loads. *Engineering Structures,* 24**,** 707-718.

NEVILLE, A. M. & BROOKS, J. J. 2010. *Concrete Technology,* Harlow, Eggland, Prentice Hall.

NEVILLE, A. M., DILGER, W. H. & BROOKS, J. J. 1983. *Creep of Plain and Structural Concrete*, Construction press.

NEVILLE, A. M. & HIRST, G. A. 1978. Mechanism of Cyclic Creep of Concrete. *ACI Special Publication,* 55.

NIE, J. & CAI, C. S. 2000. Deflection of Cracked RC Beams Under Sustained Loading. *Journal of Structural Engineering,* 126**,** 708-716.

NILSON, A. H. 1985. Design Implications of Current Research on High-Strength Concrete. *Special Publication,* 87**,** 85-118.

NURNBERGEROVA, T., KRIZMA, M. & HAJEK, J. 2000. Long-Term Deflections of Reinforced Concrete Beams. *Indian Journal of Engineering and Materials Sciences* 7**,** 29-34.

PAULSON, K. A., NILSON, A. H. & HOVER, K. C. 1991. Long-Term Deflection of High-Strength Concrete Beams. *ACI Materials Journal,* 88**,** 197-206.

PICKETT, G. 1956. *Effect of Aggregate on Shrinkage of Concrete and Hypothesis Concerning Shrinkage*, Portland Cement Association.

PILLAI, U. & MENON, D. 2003. *Reinforced Concrete Design*, New Delhi: Tata McGraw-Hill.

RAOOF, M. & LIN, Z. 1997. Structural Characteristics of RC Beams With Exposed Steel. *Proceedings of the ICE-Structures and Buildings,* 122**,** 35-51.

RAPHAEL, J. M. Tensile strength of concrete. Journal Proceedings, 1984. 158-165.

REHM, G. & ELIGEHAUSEN, R. 1979. Bond of ribbed bars under high cycle repeated loads. *ACI Journal,* 76 (2)**,** 297–313.

ROSS, A. 1937. Concrete Creep Data. *Structural Engineer,* 15**,** 314-326.

SAMRA, R. M. 1997. Time-Dependent Deflections of Reinforced Concrete Beams Revisited. *Journal of Structural Engineering,* 123**,** 823-830.

SAVOIA, M. 2011. *Time-Dependent Behaviour of Reinfoced Concrete Slabs.* M.Sc, The University of Sydney.

SCANLON, A. & BISCHOFF, P. H. 2008. Shrinkage restraint and loading history effects on deflections of flexural members. *ACI Structural Journal,* 105**,** 498.

SCOTT, R. H. & BEEBY, A. W. 2005. Long-Term Tension-Stiffening Effects in Concrete. *ACI Structural Journal,* 102**,** 31-39.

SHARAF, H. & SOUDKI, K. Strength Assessment of Reinforced Concrete Beams With Debonded Reinforcement and Confinement with CFRP Wraps. Proceedings of 4th Structural Speciality Conference of the Canadian Society for Civil Engineering, Montreal, Quebec, Canada, 2002. 10.

SOROUSHIAN, P. & RAVANBAKHSH, S. 1998. Control of Plastic Shrinkage Cracking With Specialty Cellulose Fibers. *Materials Journal,* 95**,** 429-435.

TAMTSIA, B. T. & BEAUDOIN, J. J. 2000. Basic Creep of Hardened Cement Paste a Re-Examination of The Role of Water. *Cement and Concrete Research,* 30**,** 1465-1475.

References

TANG, W., CUI, H. & WU, M. 2014. Creep and Creep Recovery Properties of Polystyrene Aggregate Concrete. *Construction and Building Materials,* 51**,** 338-343.

TAZAWA, E.-I. & MIYAZAWA, S. 1995a. Experimental Study on Mechanism of Autogenous Shrinkage of Concrete. *Cement and Concrete Research,* 25**,** 1633-1638.

TAZAWA, E.-I. & MIYAZAWA, S. 1995b. Influence of cement and admixture on autogenous shrinkage of cement paste. *Cement and Concrete Research,* 25**,** 281-287.

TROST, H. 1967. Auswirkungen des Superpositionsprinzips auf Kriech-und Relaxationsprobleme bei Beton und Spannbeton. *Beton-und Stahlbetonbau,* 62**,** 230-238.

TROXELL, G., RAPHAEL, J. & DAVIS, R. Long-Time Creep and Shrinkage Tests of Plain and Reinforced Concrete. ASTM Proceedings, 1958. 1-20.

VAKHSHOURI, B. & NEJADI, S. Limitations and Uncertainties in the Long-Term Deflection Calculation of Concrete Structures. Vulnerability, Uncertainty, and Risk: Quantification, Mitigation, and Management, 2014a. ASCE, 535-546.

VAKHSHOURI, B. & NEJADI, S. Limitations and Uncertainties in the Long-Term Deflection Calculation of Concrete Structures. Second International Conference on Vulnerability and Risk Analysis and Management (ICVRAM) and the Sixth International Symposium on Uncertainty, Modeling, and Analysis (ISUMA), 2014b.

VANDEWALLE, L. 2000. Concrete creep and shrinkage at cyclic ambient conditions. *Cement and Concrete Composites,* 22**,** 201-208.

VOLLUM, R. 2009. Comparison of Deflection Calculations and Span-to-Depth Ratios in BS 8110 and Eurocode 2. *Magazine of Concrete Research,* 61**,** 465-476.

VOLLUM, R. & AFSHAR, N. 2009. Influence of Construction Loading on Deflections in Reinforced Concrete Slabs. *Magazine of Concrete Research,* 61**,** 3-14.

VOLLUM, R. L. 2002. Influences of Shrinkage and Construction Loading on Loss of Tension Stiffening in Slabs. *Magazine of Concrete Research* [Online], 54. Available: http://www.icevirtuallibrary.com/content/article/10.1680/macr.2002.54.4.273.

WALLO, E. M. & KESLER, C. E. 1968. Prediction of creep in structural concrete. *University of Illinois. Engineering Experiment Station. Bulletin; no. 498*.

WANG, X.-H., GAO, X.-H., LI, B. & DENG, B.-R. 2011. Effect of Bond and Corrosion Within Partial Length on Shear Behaviour and Load Capacity of RC Beam. *Construction and Building Materials,* 25**,** 1812-1823.

WASHA, G. & FLUCK, P. 1952. Effect of Compressive Reinforcement on the Plastic Flow of Reinforced Concrete Beams. *ACI Journal,* 49.

WASHA, G. W. Plastic flow of thin reinforced concrete slabs. Journal Proceedings, 1947. 237-260.

WASHA, G. W. & FLUCK, P. Plastic flow (creep*) of reinforced concrete continuous beams. Journal Proceedings, 1956. 549-561.

WEATHERSBY, J. H. 2003. *Investigation of Bond Slip Between Concrete and Steel Reinforcement under Dynamic Loading Conditions.* Mississippi State University.

References

WU, M. H. Q. 2010. *TENSION STIFFENING IN REINFORCED CONCRETE–INSTANTANEOUS AND TIME-DEPENDENT BEHAVIOUR.* PhD thesis UNIVERSITY OF NEW SOUTH WALES, SYDNEY.

ZANUY, C., DE LA FUENTE, P. & ALBAJAR, L. 2010. Estimation of Parameters Defining Negative Tension Stiffening. *Engineering Structures,* 32**,** 3355-3362.

ZANUY, C., MAYA, L. F., ALBAJAR, L. & DE LA FUENTE, P. 2011. Transverse Fatigue Behaviour of Lightly Reinforced Concrete Bridge Decks. *Engineering Structures,* 33**,** 2839-2849.

ZHANG, Q., LE ROY, R., VANDAMME, M. & ZUBER, B. 2014. Long-Term Creep Properties of Cementitious Materials: Comparing Microindentation Testing With Macroscopic Uniaxial Compressive Testing. *Cement and Concrete Research,* 58**,** 89-98.

ZHOU, H., LU, J., XV, X., DONG, B. & XING, F. 2015. Effects of Stirrup Corrosion on Bond–Slip Performance of Reinforcing Steel in Concrete: An Experimental Study. *Construction and Building Materials,* 93**,** 257-266.